

LA-UR-11-3072
June 2011
EP2011-0152

Hydrologic Testing Report for Consolidated Unit 16-021(c)-99


Prepared by the Environmental Programs Directorate

Los Alamos National Laboratory, operated by Los Alamos National Security, LLC, for the U.S. Department of Energy under Contract No. DE-AC52-06NA25396, has prepared this document pursuant to the Compliance Order on Consent, signed March 1, 2005. The Compliance Order on Consent contains requirements for the investigation and cleanup, including corrective action, of contamination at Los Alamos National Laboratory. The U.S. government has rights to use, reproduce, and distribute this document. The public may copy and use this document without charge, provided that this notice and any statement of authorship are reproduced on all copies.


Hydrologic Testing Report for Consolidated Unit 16-021(c)-99

June 2011

Responsible project manager:

John P. McCann		Project Manager	Environmental Programs	6-6-2011
Printed Name	Signature	Title	Organization	Date

Responsible LANS representative:

Michael J. Graham		Associate Director	Environmental Programs	7 June 11
Printed Name	Signature	Title	Organization	Date

Responsible DOE representative:

George J. Rael		Manager	DOE-LASO	6-8-2011
Printed Name	Signature	Title	Organization	Date

EXECUTIVE SUMMARY

This report describes the results of hydrologic testing conducted on deep-perched intermediate groundwater in the vadose zone beneath Technical Area 16, near Consolidated Unit 16-021(c)-99. The primary objective of the testing was to obtain field-scale measurements of hydrogeologic properties and aquifer parameters for the deep-perched intermediate groundwater system. Two long-term (10-d) pumping tests were conducted on both screens of CdV-16-4ip, completed in variably saturated Puye Formation sediments. A 24-h pumping test was conducted on R-25b, completed in the Otowi Formation of the Bandelier Tuff. Multiple screens in five nearby monitoring wells (R-25, R-25b, CdV-16-1i, CdV-16-2ir, and R-63), completed in deep-perched intermediate and regional groundwater, were monitored for drawdown responses during the pumping tests.

The static water level observed in screen 1 of CdV-16-4ip was substantially higher (281 ft) than that in screen 2, showing a strong downward hydraulic gradient, highly resistive sediments separating the two screened zones, and little hydraulic connection between the screens. The aquifer testing confirmed this finding, showing no drawdown in either zone as a result of pumping the other zone.

Test data showed that CdV-16-4ip screen 1 is located in a laterally limited pocket or channel of highly transmissive sediments, surrounded by material with lower transmissivity. The data indicate screen 1 is completed in a zone with an estimated lower-bound transmissivity of 4000 to 7000 gallons per day (gpd)/ft, corresponding to a lower-bound hydraulic conductivity on the order of 13 ft/d. Large initial pumping rates quickly dewatered those sediments, reflecting a much lower effective transmissivity (about 130 gpd/ft) for the broader perched zone, suggesting limited water production potential. The perched zone appeared to recharge at a rate of about 4.8 gallons per minute (gpm) from laterally adjacent sediments during the 10-d pumping period and during the recovery period. The only monitored location that showed a response to pumping CdV-16-4ip screen 1 was R-25 screen 2, located 430.4 ft away. The drawdown response was muted, suggesting an indirect hydraulic connection between these zones. The pumping test data collected at CdV-16-4ip screen 2 in the lower perched zone indicated this zone is spatially extensive and has a transmissivity of approximately 660 gpd/ft, with an average hydraulic conductivity of 2.0 ft/d. The 10 d of pumping screen 2 showed no measurable drawdown at any of the nearby monitoring locations.

Based on the pumping test data from both screens of CdV-16-4ip, the two deep-perched intermediate groundwater zones do not appear to be hydraulically connected, and the lower perched zone does not appear to be hydraulically connected with the regional aquifer. The test data indicate the long-term pumping rates that can be effectively sustained by both screens at CdV-16-4ip are less than 5 gpm for each screen. The total mass of RDX (hexahydro-1,3,5-trinitro-1,3,5 triazine) removed during the two 10-d pumping tests at CdV-16-4ip was less than 0.4 lb.

The pumping test conducted at R-25b induced slight responses in R-25 screens 1 and 2 (located 55 ft away), demonstrating the perched zones in the Bandelier Tuff and Puye Formation within the upper perched horizon are hydraulically connected and should be treated hydrologically as one perched zone. The test data from R-25b indicate a formation hydraulic conductivity of around 0.3 ft/d.

CONTENTS

1.0 INTRODUCTION 1

 1.1 Historical Background..... 1

 1.2 Regulatory Context..... 2

 1.3 Overview of Report..... 2

2.0 CONCEPTUALIZATION OF GROUNDWATER FLOW CONDITIONS 3

 2.1 Vadose Zone Perched Groundwater 3

 2.2 Regional Aquifer 5

3.0 DESCRIPTION OF PUMPING TESTS 5

 3.1 CdV-16-4ip Pumping Tests 5

 3.2 R-25b Pumping Test..... 6

4.0 THEORETICAL METHODS FOR ANALYSIS..... 6

 4.1 Barometric Corrections 6

 4.2 Time-Drawdown Methods..... 7

5.0 INTERPRETATION OF PUMPING TEST DATA..... 7

 5.1 CdV-16-4ip Pumping Tests 7

 5.2 R-25b Pumping Test..... 8

6.0 SUMMARY AND CONCLUSIONS 8

7.0 REFERENCES..... 9

Figures

Figure 1.0-1 Location of TA-16 with respect to Laboratory technical areas and surrounding landholdings..... 13

Figure 1.0-2 Location of Consolidated Unit 16-021(c)-99 and associated features..... 14

Figure 1.2-1 Monitoring wells in the vicinity and downgradient of TA-16 and approximate boundaries of contaminated deep-perched zone 15

Figure 1.2-2 Well completion diagram of CdV-16-4ip 16

Figure 1.2-3 Well completion diagram of R-25b..... 17

Figure 2.1.1 Formation microimager logs showing lithologies hosting perched groundwater at wells CdV-16-4ip and CdV-16-1(i) 18

Figure 2.1-2 Cross-section of vadose zone and regional hydrostratigraphy near R-25 and CdV-16-4ip 19

Figure 2.1-3 Screen elevations versus piezometric water levels along R-25 (in blue) and CdV-16-4ip (in red)..... 20

Figure 3.1-1 RDX concentration during development and pumping tests in the upper and lower CdV-16-4ip screens..... 21

Table

Table 6.0-1 Estimated Hydraulic Parameters for CdV-16-4ip and R-25b Aquifer Pump Tests 23

Appendixes

Appendix A Drawdown Data (on CD included with this document)
Appendix B CdV-16-4ip Pump Test Analysis
Appendix C Well R-25b Pump Test Analysis
Appendix D Groundwater Treatment

Acronyms and Abbreviations

amsl	above mean sea level
bgs	below ground surface
CME	corrective measures evaluation
EPA	Environmental Protection Agency (U.S.)
GAC	granular activated carbon
gpd	gallons per day
gpm	gallons per minute
HE	high explosives
IM	interim measure
LANL	Los Alamos National Laboratory
NMED	New Mexico Environment Department
NOD	notice of disapproval
NPDES	National Pollutant Discharge Elimination System
RDX	hexahydro-1,3,5-trinitro-1,3,5-triazine
RPF	Records Processing Facility
TA	technical area
WES-EDA	Waste and Environmental Services Division–Environmental Data and Analysis

1.0 INTRODUCTION

This report describes hydrologic testing at wells CdV-16-4ip and R-25b completed to collect additional data on aquifer properties of deep-perched groundwater below Consolidated Unit 16-021(c)-99 (the 260 Outfall). The 260 Outfall is located in Technical Area 16 (TA-16) in the southwest corner of Los Alamos National Laboratory (LANL or the Laboratory). Figure 1.0-1 shows the location of TA-16 with respect to Laboratory technical areas, while Figure 1.0-2 shows the location of Consolidated Unit 16-021(c)-99 and associated features.

CdV-16-4ip was installed at the direction of the New Mexico Environment Department (NMED) to provide field-scale estimates of aquifer parameters for the deep-perched groundwater zone at the 260 Outfall and ultimately to assess the potential for pumping and treatment of contaminated perched groundwater.

This document provides detailed results of aquifer testing conducted at borehole CdV-16-4ip and well R-25b. This report was developed to meet the requirements of NMED's "Approval with Modifications: Supplemental Investigation Work Plan for Intermediate and Regional Groundwater at Consolidated Unit 16-021(c)-99" (NMED 2009, 104973). A description of the test plan is provided in the "Hydrologic Testing Work Plan for Consolidated Unit 16-021(c)-99" (LANL 2010, 108534).

The aquifer pumping test data and analyses will be used in the alternative selection process in the revised corrective measures evaluation (CME) for Consolidated Unit 16-021(c)-99, the schedule for which will be negotiated with NMED following submittal of the TA-16 well network evaluation in December 2012.

1.1 Historical Background

Building 16-260, located on the north side of TA-16 (shown as TA-16-260 in Figure 1.0-2), has been used for processing and machining high explosives (HE) since 1951. Because water was used to machine the HE (which is slightly water-soluble), wastewater from machining operations contained dissolved HE and may have contained entrained HE cuttings. Historical wastewater treatment at building 16-260 consisted of routing the water to 13 settling sumps to recover any entrained HE cuttings. From 1951 to 1996, the water from these sumps was discharged to the 260 Outfall that drained into Cañon de Valle. In 1994, outfall discharge volumes were measured at several million gallons per year. The discharge volumes were probably higher during the 1950s when HE production output from the 260 Outfall was substantially greater than it was in the 1990s (LANL 1994, 076858). In the past, barium was a constituent of certain HE formulations and inert components and was present in the outfall wastewater.

During the late 1970s, the 260 Outfall was permitted by the U.S. Environmental Protection Agency (EPA) to operate as EPA Outfall No. 05A056 under the Laboratory's National Pollutant Discharge Elimination System (NPDES) permit (EPA 1990, 012454). The last NPDES-permitting effort for the 260 Outfall occurred in 1994. The NPDES-permitted 260 Outfall was deactivated in November 1996, and EPA officially removed it from the Laboratory's NPDES permit in January 1998. This waste stream is currently managed by pumping the sumps and treating the water at the TA-16 HE wastewater treatment plant.

Solid Waste Management Unit 16-021(c) consists of two portions: an upper drainage channel and former settling pond, and a lower drainage channel leading to Cañon de Valle. The entire length of the channel from the 260 Outfall to Cañon de Valle is approximately 600 ft. The former settling pond, which was removed during a 2000–2001 interim measure (IM) cleanup (LANL 2002, 073706), was approximately 50 ft long x 20 ft wide and was located approximately 45 ft below the 260 Outfall. The upper drainage channel continues approximately 350 ft northeast from the former settling pond to a 15-ft, near-vertical cliff that marks the break between the upper and lower drainage channels. Beyond this cliff, the lower

channel runs another 200 ft to Cañon de Valle. The IM cleanup removed more than 1300 yd³ of contaminated soil from the settling pond and channel. Approximately 90% of HE in the Consolidated Unit 16-021(c)-99 source area was removed (LANL 2002, 073706).

A second phase of cleanup directed by the “Corrective Measures Implementation Plan for Consolidated Unit 16-021(c)-99, Revision 1” (LANL 2007, 098192) was conducted in 2009 to remove residual soil exceeding risk-based media cleanup standards, to remove the building 16-260 concrete outfall trough, and to inject grout in a contaminated surge bed beneath the former HE settling pond. This cleanup resulted in the removal of approximately 30 yd³ of concrete outfall trough debris, 10 yd³ of contaminated soils from beneath the trough, and 20 yd³ of contaminated soil from the 16-260 drainage.

1.2 Regulatory Context

The Laboratory completed an initial CME report for contaminated deep-perched and regional groundwater associated with Consolidated Unit 16-021(c)-99 in July 2007 and recommended a phased remediation strategy consisting of monitored natural attenuation for both the deep-perched and regional aquifers and assessment of the feasibility of groundwater recovery and treatment (the pump-and-treat alternative) based on a proposed aquifer pumping test.

NMED subsequently issued a notice of disapproval (NOD) on the CME report (NMED 2008, 101311) and requested a supplemental investigation work plan to collect sufficient data to evaluate the feasibility of the remedial alternatives proposed in the CME. In response to NMED’s NOD, the Laboratory developed the “Supplemental Investigation Work Plan for Intermediate and Regional Groundwater at Consolidated Unit 16-021(c)-99” (LANL 2008, 103165), proposing additional characterization activities to reduce or eliminate uncertainties in the hydrogeologic conceptual model at TA-16. These activities included installing an additional monitoring well, conducting additional groundwater sampling, and conducting single-well aquifer pumping tests and a multiwell aquifer pumping test to further characterize deep-perched and regional groundwater. In February 2010, the “Hydrologic Testing Work Plan for Consolidated Unit 16-021(c)-99” (LANL 2010, 108534) was submitted, and this document was subsequently approved by NMED on May 20, 2010 (NMED 2010, 109689). In a letter dated June 14, 2010 (LANL 2010, 109766), the Laboratory requested that implementation of any tracer test be deferred until after the pump tests were completed. NMED approved this request in a letter dated June 25, 2010 (NMED 2010, 110435).

Previous activities completed under the supplemental investigation work plan include (1) the installation of new monitoring wells R-25b, R-25c (a dry well), R-47i, R-48, and R-63; (2) quarterly characterization sampling of R-25b, R-47i, and R-48; and (3) completion of single-well, short-duration pumping tests in R-47i, R-48, and R-63. Figure 1.2-1 shows the location of wells in the vicinity and downgradient of TA-16.

Activities addressed in this report include performance of hydrologic tests at wells CdV-16-4ip and R-25b (shown in Figure 1.2-1). Well completion diagrams for CdV-16-4ip and R-25b are shown in Figures 1.2-2 and 1.2-3; the well completion reports for R-25b and CdV-16-4ip (LANL 2008, 105018; LANL 2011, 111608) provide additional information on installation of these wells.

1.3 Overview of Report

Section 2 of this report presents a hydrologic conceptual model for the test area and summarizes available hydrologic data for the site. Section 3 provides the details of the aquifer testing, including the location and design of the test wells and a description of the aquifer testing conducted. Data analysis methods are discussed in section 4, and interpretation of the results is provided in section 5. Section 6 summarizes the findings and presents the conclusions of this analysis. The references cited in this report are listed in section 7. Appendix A presents drawdown, pumping rate and RDX (hexahydro-1,3,5-trinitro-

1,3,5 triazine) concentration data (on CD included with this report). Appendixes B and C present detailed pump test analyses for CdV-16-4ip and R-25b, respectively. Appendix D describes the treatment of the water pumped during the CdV-14-4ip test.

2.0 CONCEPTUALIZATION OF GROUNDWATER FLOW CONDITIONS

Based on the results of previous investigations, a conceptual site model has been developed for groundwater flow and contaminant transport in the vadose zone and the underlying regional aquifer at TA-16. An important component of the conceptual model is that the perched saturated horizons are within the vadose zone. Preliminary calculations conducted during the CME (LANL 2007, 098734) suggest that groundwater in the perched horizons contains the largest inventory of HE in the environment on a mass basis; estimates range from as low as ~700 kg of RDX to as high as ~8000 kg of RDX. Investigations of vadose zone and regional groundwater at TA-16 have been conducted during the past several years, and the results of these investigations are discussed in several reports (e.g., Longmire 2005, 088510; LANL 2006, 093798; LANL 2007, 096003; LANL 2007, 095787). The conceptual models for the saturated vadose zone horizons and regional aquifer are summarized below.

2.1 Vadose Zone Perched Groundwater

The vadose zone beneath TA-16 extends from the ground surface to the top of the regional aquifer. It is about 1200 ft thick and includes zones with different groundwater saturation levels. R-25 contains a multiport Westbay system that provides information on both deep perched and regional groundwater. Formation microimager logs showing lithologies hosting perched groundwater at wells CdV-16-4ip and CdV-16-1(i) are shown in Figure 2.1-1. The upper section of the vadose zone surrounding R-25 and CdV-16-4ip is within Bandelier Tuff units and is predominantly unsaturated (Figure 2.1-2). The deep vadose zone surrounding R-25 and CdV-16-4ip is predominantly within Puye Formation sediments and includes two perched saturated horizons located between ~750 ft and 1200 ft below ground surface (bgs). Deep vadose zone saturation also exists within the Otowi Member of the Bandelier Tuff (Figure 2.1-2). Water-level head difference of 281 ft and dry well screens at R-25 (screen 3) and R-25c indicate the two perched zones are separated by a 100 to 150 ft of Puye sediments that are under variable intermittent saturation.

Geochemical data suggest the upper and lower zones of saturation underlying TA-16 such as that observed at R-25 represent separate groundwater systems (Robinson et al. 2005, 091682). Two hydrologic systems are presented that would produce the distinctly separate perched water conditions observed in the vadose zone underlying Cañon de Valle. Groundwater infiltrating along deeply penetrating fractures would intercept and spread laterally into permeable nonwelded tuffs and stratified volcanoclastic deposits, forming the perched zones. Localized heterogeneities, such as the clay-rich alteration zones in the Puye Formation combined with high recharge, result in complex flow structures that contain mounding, partly connected saturated zones, and locally confined conditions.

Relatively thin (<5 ft) silt- and clay-rich beds appear to be the primary stratigraphic control for perching layers that underlie the saturated zones within the deep vadose zone. Additionally, a widespread 1-ft-thick soil occurs on top of the Puye Formation that may act as a local partial confining layer for saturation in the Otowi Member. In the Puye Formation, rocks hosting saturation in the two perched zones consist of layered stacks of Puye boulder, gravel, and sand deposits (Figure 2.1-1). The Puye Formation is a proximal alluvial fan deposit, and its hydraulic properties are anticipated to be highly heterogeneous, an assumption confirmed by the borehole video and geophysical logs and by pumping tests conducted at CdV-16-4ip (section 5 and Appendix B). Borehole video and formation microimager logs at CdV-16-1i and R-25 screen 1 indicate that the saturation in the Otowi Member is controlled at least in part by high-angle open fractures (Figure 2.1-1).

The perched groundwater horizons are believed to extend from west to east for more than 6500 ft and from north to south for approximately 3280 ft. The perched horizons have been detected at R-26 screen 1; R-25b, R-25 screens 1, 2, 4; CdV-16-1i; CdV-16-2ir; and R-47i (Figure 1.2-1). The perched zone was not observed at R-18 and R-48, limiting its north-south extent (Figure 1.2-1). The low-permeability Tschicoma dacite observed in R-48 (~2000 ft south of Cañon de Valle) may impede the southward flow of water in the deep-perched system (Figure 1.2-1).

Vadose zone groundwater is recharged by mountain-front precipitation and subsequent infiltration both along the Pajarito fault zone located just to the east of TA-16 and along canyon bottoms (e.g., infiltration along upper Cañon de Valle) and discharged to the underlying regional aquifer. The degree of hydraulic connection between the perched horizons and the regional aquifer is not certain.

Water-level data indicate groundwater within the perched horizons generally flows from west to east. There is some evidence of a southerly component of flow within the Otowi Member of the Bandelier Tuff in the vicinity of R-25, possibly from recharge along Cañon de Valle.

Water-level data from multiple screens in R-25 and CdV-16-4ip indicate hydraulic pressures within the deep vadose zone tend to decline with depth at slope close to 1:1, which defines unit vertical hydraulic gradients (Figure 2.1-3).

In systems where groundwater heads are near atmospheric pressure, (i.e., little head rise above the well screen), steep vertical gradients may indicate unsaturated conditions, whereas modest vertical gradients may indicate predominantly saturated flow. For idealized conditions in which the vertical hydraulic conductivity is spatially constant and uniform, the following conditions would apply theoretically.

Vertical hydraulic gradients greater than 1 would tend to indicate predominantly unsaturated zone flow; in this case, groundwater movement in the vadose zone is predominantly controlled by the retention properties of the flow media. Vertical hydraulic gradients greater than 1 are observed between screens 2 and 4 at R-25, signifying the groundwater is unsaturated; the unsaturated flow conditions between screens 2 and 4 are confirmed by R-25 screen 3, which is dry (Figure 2.1-3).

Vertical hydraulic gradients less than 1 are likely to indicate predominantly saturated conditions. Such gradients are observed between R-25 screens 1 and 2 in the vadose zone and between screen 5 and screens 6, 7, and 8 in the regional aquifer (Figure 2.1-3). This suggests the likelihood of continuous saturation from screen 1 to screen 2 and throughout the zone spanned by screens 6, 7, and 8.

Vertical hydraulic gradients equal to 1 represent a borderline condition. For perfectly constant and spatially uniform vertical hydraulic conductivity, a gradient of 1 would suggest vertical, fully saturated vadose-zone flow; in this case, the groundwater (Darcy) velocity is equal to fully saturated vertical hydraulic conductivity. It is important to note that although the groundwater is fully saturated in the flow medium, the hydraulic pressure is near atmospheric pressure, and therefore, the water is on the cusp of being under "unsaturated" or "vadose zone" conditions. (If a screen is placed within this zone, it may be dry even though the flow medium is fully saturated.)

In practice, however, geologic media are heterogeneous and exhibit variable vertical hydraulic conductivity with depth. The natural strata will include layers with relatively greater hydraulic conductivity and those with correspondingly lower hydraulic conductivity. This nonuniformity guarantees that both saturated and unsaturated conditions will exist when the hydraulic gradient is near or equal to 1. (Full saturation will occur immediately above the tighter layers, with unsaturated conditions prevailing elsewhere.)

Vertical hydraulic gradients close to 1 are observed between R-25 screens 4 and 5 and CdV-16-4ip screens 1 and 2 (Figure 2.1-3). Given the inevitable stratification and/or heterogeneity of the sediments, alternating saturated and unsaturated conditions are expected to occur within these intervals.

Examination of the water levels in the vicinity of CdV-16-4ip suggests that unsaturated to fully saturated groundwater flow under vadose zone conditions is expected to occur between the perched zones and between the lower perched zone and the regional aquifer. The groundwater flow direction should be predominantly vertical and controlled by gravity and hydrogeological properties of the medium; the lateral component of the groundwater flow is also expected because of medium anisotropy; the dip of the layering of the hydrostratigraphic units is expected to be predominantly to the east. The flux of the downward groundwater flow through the vadose zone is expected to be temporally and spatially variable and impacted by spatial heterogeneity of the flow medium and temporal/spatial distribution of the infiltration recharge of the vadose zone.

2.2 Regional Aquifer

The regional aquifer in the vicinity of northern TA-16 is predominantly unconfined, with the water table located within the Puye Formation (Figure 2.1-1) at a depth of approximately 1000–1300 ft bgs. Most regional wells near TA-16 have screens installed near the regional water table; exceptions include R-26 where the regional screen (screen 2) is placed deep (~319 ft) in the regional aquifer and R-25 where several screens (6, 7, and 8) are located at depth within the regional aquifer. Water levels in regional wells near TA-16 show little influence from transient effects of deeper water-supply pumping (LANL 2006, 091450).

A water-table map of the regional aquifer near and downgradient of TA-16 is presented in Figure 1.2-1. The water-table contours indicate that groundwater generally flows from west to east, with some perturbation near R-25, perhaps reflecting local recharge. Downgradient (east) of R-25, the regional groundwater flow direction incorporates a northerly component of flow, near R-18 and R-17. This may be a result of aquifer heterogeneity/anisotropy.

3.0 DESCRIPTION OF PUMPING TESTS

Pumping tests were conducted to better understand the hydrogeological settings of the area, to quantify the aquifer properties, and ultimately to assess the potential for pumping and treatment of contaminated perched groundwater beneath the northern portion of TA-16. The tests were conducted by pumping wells CdV-16-4ip and R-25b. During the tests, water levels were recorded in all nearby wells.

3.1 CdV-16-4ip Pumping Tests

Well CdV-16-4ip was completed with two screens. Screen 1 (the upper screen) is 63.6 ft long and extends from 815.6 ft to 879.2 ft bgs, whereas screen 2 (the lower screen) is 31.1 ft long and extends from 1110.0 to 1141.1 ft bgs (Figure 1.2-2) and both well screens are located in the Puye Formation. The static water level at the upper screen is around 809 ft bgs (i.e. about 7 ft above the top of upper screen). The static water elevation at screen 2 is around 1098 ft bgs, 12 ft above the top of screen.

Pump tests were performed on both of the screens of CdV-16-4ip. Testing of each zone included a brief step-drawdown test followed by a 10-d pump test. Each step-drawdown test was followed by recovery data collection overnight. Each 10-d test was started the morning after the step-drawdown test and was followed by a minimum of 12 d of monitored recovery. Detailed information regarding the pump tests conducted at the two screens of CdV-16-4ip is provided in Appendix B. The water-level and pumping-rate data collected during the pump tests are provided in Appendix A (on CD).

During the pumping tests at CdV-16-4ip, water levels were recorded in several nearby wells. The wells and screen zones included in the monitoring effort along with their horizontal distances from CdV-16-4ip were R-25 screens 1, 2, 4, 5, 6, 7, and 8 (430.4 ft); R-25b (477.1 ft); CdV-16-1i (554.2 ft); CdV-16-2ir (1086.4 ft); and R-63 (1064.3 ft). During the pumping events at screen 1, water-level responses were observed only at the monitoring location R-25 (screen 2). Pumping at screen 2 of CdV-16-4ip resulted in no water-level responses at any of the nearby monitoring locations.

Activated carbon treatment was used successfully during the pumping test to treat groundwater from both screens in well CdV-16-4ip. Figure 3.1-1 presents the RDX concentration during development as well as during pumping tests. The RDX concentrations measured before activated carbon treatment were relatively steady, with a slightly increasing trend during the two 10-d pumping tests. The RDX concentration averaged 185 µg/L during the testing of the upper screen. At an average flow rate of just under 10 gallons per minute (gpm), approximately 0.3 lb of RDX was removed. The influent concentration of RDX in the lower screen averaged just 24 µg/L. The average flow rate was just over 6 gpm; over 10 d, an additional 0.02 lb of RDX was removed. The relatively steady RDX concentrations during the pumping tests suggest the concentrations are spatially uniform in the perched zones near the pumped screens. Detailed information about RDX concentrations and groundwater treatment during the pump tests is provided in Appendix D.

3.2 R-25b Pumping Test

R-25b lies within the Otowi Member of the Bandelier Tuff, above the Puye Formation (Figure 2.1-1). The well screen is 20.8 ft long, extending from 750.0 to 770.8 ft bgs. Several wells and screen intervals were monitored during the R-25b pumping test; however, only R-25 screens 1 and 2 showed a response to pumping R-25b. R-25 screen 1 is 20.8 ft long and is located within the Otowi Member of the Bandelier Tuff; R-25 screen 2 is 10.8 ft long and lies within the Puye Formation.

Because of the drawdown response observed in R-25 screens 1 and 2 during the R-25b pumping test, it was assumed in the hydraulic analysis described below that the three screened intervals were within the same hydrologic unit. The zone of saturation was considered to extend from the R-25 screen 1 static water level (6779.3 ft above mean sea level [amsl]) to the base of R-25 screen 2 (6622.7 ft amsl), a span of 156.6 ft. R-25b was tested by operating a dedicated Bennett pump for 24 h at a constant discharge rate averaged 0.60 gpm. Following shutdown of the pump test, recovery data were recorded for a little more than 2 d.

Detailed information about the pump test conducted at R-25b is provided in Appendix C. The water-level and pumping-rate data collected during the pumping tests are provided in Appendix A (on CD). R-25b test waters were containerized and will be disposed of off-site following waste characterization.

4.0 THEORETICAL METHODS FOR ANALYSIS

This section describes various theoretical methods adopted for analyzing the data obtained from the CdV-16-4ip and R-25b pumping tests.

4.1 Barometric Corrections

The background water-level data collected in conjunction the pumping tests allow the analyst to see what water-level fluctuations occur naturally in the aquifer and help distinguish between water-level changes caused by conducting the pumping test and changes associated with other causes. The collected water level data often require correction for effects of barometric pressure and Earth tide; this was done using

BETCO (barometric and Earth tide correction) software (Toll and Rasmussen 2007, 104799) to modify the data. The corrected barometric pressure data reflecting pressure conditions at the water table were compared with the water-level hydrograph to discern the correlation between the two and to determine whether water-level corrections were needed before data analysis.

4.2 Time-Drawdown Methods

The transient variation of drawdowns during the pump test can be analyzed using a variety of methods. Among them is the Theis method (1934-1935, 098241). An alternative solution method applicable to time-drawdown data is the Cooper-Jacob method (1946, 098236), a simplification of the Theis equation that is mathematically equivalent to the Theis equation for most pumped well data. An exception occurs when the transmissivity of the aquifer is very low. In that case, some of the early pumped well drawdown data may not be well approximated by the Cooper-Jacob equation.

Because many of the monitoring wells completed on the Pajarito Plateau have well screens that only span a small section of the entire aquifer thickness (i.e., the wells are partially penetrating the aquifer), an alternate solution considered for assessing aquifer conditions is the Hantush (1961, 098237) solution for partially penetrating wells.

For unconfined aquifers, the commonly used solution of Neuman (1974, 085421) was adopted. The solution for confined aquifer can also be used for unconfined aquifers after correcting the observed drawdown values for dewatering effects using the relationships due to (Kruseman et al. 1991, 106681).

5.0 INTERPRETATION OF PUMPING TEST DATA

5.1 CdV-16-4ip Pumping Tests

Detailed description of the analyses of the CdV-16-4ip pumping tests is provided in Appendix B. The pumping test at CdV-16-4ip screen 1 demonstrated that the upper saturated perched zone at this screen is highly permeable, with lower-bound transmissivity values ranging from about 4000 to 7000 gallons per day (gpd)/ft. This corresponded to a lower-bound hydraulic conductivity on the order of 100 gpd/ft², or 13 ft/d, assuming saturated thickness equal to 69 ft (Appendix B). With extended pumping, however, drawdown increased dramatically, indicating the perched zone is limited in lateral extent. The brief (440 min) step-drawdown test showed pronounced boundary effects. The 10-d test at discharge rates ranging from 11.8 to 7.33 gpm effectively dewatered the bulk of the perched interval in the immediate vicinity of the pumped well. The perched zone appeared to be recharged at a rate of about 4.8 gpm from laterally adjacent sediments during the 10-d pumping period and much of the recovery period. This value probably represents the maximum sustainable yield that could realistically be obtained from screen 1 over time. The actual long-term yield may be less. The pumping test showed that screen 1 is installed in a moderately transmissive, but laterally limited, pocket of material surrounded by lower transmissivity material. The possible range of perched zone area is large because it relates to specific yield which can only be estimated. Assuming a specific yield of 0.05, the areal extent of the perched zone is on the order of 8900 ft². Late-time recovery data suggested an area-wide transmissivity of about 130 gpd/ft. Water levels were monitored in several wells during the screen 1 pumping test. Only R-25 screen 2 (430.4 ft away) showed a response to pumping. The hydraulic response at R-25 screen 2 was muted compared with what would be expected theoretically, suggesting a somewhat indirect hydraulic connection between CdV-16-4ip screen 1 and R-25 screen 2.

The pumping test at CdV-16-4ip screen 2 demonstrated the perched zone at the screen 2 level has moderate transmissivity. The transmissivity in the vicinity of the pumped screen is estimated at 660 gpd/ft, with an average hydraulic conductivity of 15.2 gpd/ft², or 2.0 ft/d assuming a thickness of 43.3 ft, equivalent to the distance from the static water level to the bottom of the screen. The specific capacity of screen 2 after pumping 5 gpm for 10 d was 0.253 gpm/ft. Late-time pumping test data suggest the perched zone might be recharged from the vadose zone above (delayed yield under phreatic conditions). Late-time pumping test behavior might also result from lateral or vertical heterogeneities (vertical stratification or lateral facies boundaries with different transmissivity).

5.2 R-25b Pumping Test

A detailed description of the analyses of the R-25b pumping test is provided in Appendix C. The pumping test conducted at R-25b induced slight drawdown in both screens 1 and 2 in R-25, 55 ft away. The perched aquifer was interpreted as consisting of a 156.6-ft thick interval extending from the static water level at R-25 screen 1 (6779.3 ft amsl) to the base of R-25 screen 2 (6622.7 ft amsl). Water levels in R-25b and R-25 screens 1 and 2 showed steep downward gradients suggesting significant vertical anisotropy. The anisotropy was judged to be more severe in the upper portion of the perched zone where heads between R-25b and R-25 screen 1 were substantially different although the elevation intervals spanned by the two screens overlap slightly. Storage effects and discharge rate variations precluded analysis of the pumping portion of the test. The late (post-storage) recovery data supported an analysis, yielding an estimated hydraulic conductivity of 0.29 ft/d. Analysis of the drawdown data from R-25 screen 2 produced hydraulic conductivity values averaging slightly more than 0.3 ft/d.

6.0 SUMMARY AND CONCLUSIONS

A series of pump tests were conducted in two saturated perched zones above the regional aquifer in the vadose zone beneath TA-16. The primary objective of the analysis was to evaluate hydrogeological properties of the perched zones and ultimately the potential to use pump-and-treat to clean up the contaminated perch groundwater beneath northern TA-16. The field tests were conducted by pumping CdV-16-4ip (screens 1 and 2) and R-25b. All the nearby monitoring wells (regional and intermediate screens) were monitored for potential drawdown responses. Table 6.0-1 summarizes the estimated hydraulic parameters for each aquifer pumping test.

The pumping tests demonstrated that the upper perched zone is highly heterogeneous. Test data showed that CdV-16-4ip screen 1 is located in a laterally limited pocket or channel of highly transmissive sediments (lower-bound transmissivity in the range of 4000 to 7000 gpd/ft). Large initial pumping rates quickly dewatered those sediments, reflecting a much lower effective transmissivity (about 130 gpd/ft) for the broader perched zone and suggesting limited water production potential. The only monitored location that showed response to pumping CdV-16-4ip screen 1 was R-25 screen 2. However, the response was muted, suggesting complicated spatial propagation of the pumping cone of depression through the saturated media and indicating a somewhat indirect hydraulic connection between these zones.

The pumping test conducted at R-25b induced slight responses in R-25 screens 1 and 2, demonstrating the perched zones in the Bandelier Tuff and Puye Formation within the upper perched horizon are hydraulically connected and should be treated hydrogeologically as one perched zone. This conclusion is also supported by vertical hydraulic gradient data (Figure 2.1-3).

The interpretation of the pumping test data collected at CdV-16-4ip screen 2 in the lower perched zone suggested that the flow medium has low to moderate permeability and is spatially extensive. Pumping in this zone did not cause measurable drawdown at any of the nearby monitoring locations.

Based on the pumping test data, the two perched zones above the regional aquifer in the vadose zone beneath the northern portion of TA-16 do not appear to be hydraulically connected. There is also no apparent indication the lower perched zone is hydraulically connected with the regional aquifer.

The borehole geophysical investigations conducted in CdV-16-2ir (Kleinfelder 2005, 093665) indicate that the vadose zones (1) between the perched zones and (2) between the lower perched zone and the regional aquifer appear to have relatively high saturation. Nevertheless, the steep vertical gradients imply vadose conditions in these zones. Such localized saturations further confirm the complexity and heterogeneity of the vadose zone beneath northern TA-16.

The observed partial hydraulic connection of perched zones is consistent with the groundwater pathway conceptual model presented by Robinson et al. (2005, 091682) that describes when groundwater reaches a deep perched zone, it rapidly percolates laterally along high-permeability pathways until the perching horizon pinches out or is breached by high-permeability features such as fractures or lateral changes in lithology, which serve as vertical conduits for water migration so groundwater migrates in a stair-step fashion from one perching horizon to another. Once groundwater reaches a deep perched zone, it rapidly percolates laterally along high-permeability pathways until the perching horizon pinches out or is breached by high-permeability features such as fractures or lateral changes in lithology.

The two perched zones screened by R-25b and CdV-16-4ip do not appear to be highly transmissive. The long-term pumping rates that can be effectively sustained by these zones at CdV-16-4ip are less than 5 gpm for each screen. The total mass of RDX removed during the two 10-d pumping events at well CdV-16-4ip is less than 0.4 lb.

Originally, a tracer test was included in this hydrologic testing project to provide additional data for the conceptual model of groundwater flow at the site and to provide information on the connectivity within discrete perched horizons. However, this tracer test would provide limited additional information for the conceptual model, given the extensive data collected from the successfully completed aquifer tests conducted on both screens of CdV-16-4ip and on R-25b, and this tracer test is no longer recommended.

The results of the hydrologic pumping tests at CdV-16-4ip and R-25b will be used to explore the viability of the pump and treat remedial alternative for groundwater in the upcoming CME report.

7.0 REFERENCES

The following list includes all documents cited in this report. Parenthetical information following each reference provides the author(s), publication date, and ER ID. This information is also included in text citations. ER IDs are assigned by the Environmental Programs Directorate's Records Processing Facility (RPF) and are used to locate the document at the RPF and, where applicable, in the master reference set.

Copies of the master reference set are maintained at the NMED Hazardous Waste Bureau and the Directorate. The set was developed to ensure that the administrative authority has all material needed to review this document, and it is updated with every document submitted to the administrative authority. Documents previously submitted to the administrative authority are not included.

Cooper, H.H., Jr., and C.E. Jacob, August 1946. "A Generalized Graphical Method for Evaluating Formation Constants and Summarizing Well-Field History," *American Geophysical Union Transactions*, Vol. 27, No. 4, pp. 526-534. (Cooper and Jacob 1946, 098236)

- EPA (U.S. Environmental Protection Agency), 1990. "NPDES Authorization to Discharge Waters of the United States," Water Management Division, EPA Region 6, Dallas, Texas. (EPA 1990, 012454)
- Hantush, M.S., July 1961. "Drawdown around a Partially Penetrating Well," *Journal of the Hydraulics Division, Proceedings of the American Society of Civil Engineers*, Vol. 87, No. HY 4, pp. 83-98. (Hantush 1961, 098237)
- Kleinfelder, November 2005. "Final Completion Report, Characterization Well CdV-16-2(i)r," report prepared for Los Alamos National Laboratory, Project No. 49436, Albuquerque, New Mexico. (Kleinfelder 2005, 093665)
- Kruseman, G.P., N.A. de Ridder, and J.M. Verweij, 1991. Excerpted page from *Analysis and Evaluation of Pumping Test Data*, International Institute for Land Reclamation and Improvement, Netherlands. (Kruseman et al. 1991, 106681)
- LANL (Los Alamos National Laboratory), May 9, 1994. "Process Flow Reductions from Waste Minimization for Value Engineering Study," Los Alamos National Laboratory, Los Alamos, New Mexico. (LANL 1994, 076858)
- LANL (Los Alamos National Laboratory), July 2002. "Interim Measure Report for Potential Release Site 16-021(c)-99," Los Alamos National Laboratory document LA-UR-02-4229, Los Alamos, New Mexico. (LANL 2002, 073706)
- LANL (Los Alamos National Laboratory), January 2006. "Investigation Report for the TA-16-340 Complex [Consolidated Units 13-003(a)-99 and 16-003(n)-99 and Solid Waste Management Units 16-003(o), 16-026(j2), and 16-029(f)]," Los Alamos National Laboratory document LA-UR-06-0153, Los Alamos, New Mexico. (LANL 2006, 091450)
- LANL (Los Alamos National Laboratory), August 2006. "Investigation Report for Intermediate and Regional Groundwater, Consolidated Unit 16-021(c)-99," Los Alamos National Laboratory document LA-UR-06-5510, Los Alamos, New Mexico. (LANL 2006, 093798)
- LANL (Los Alamos National Laboratory), April 2007. "Evaluation of the Suitability of Wells Near Technical Area 16 for Monitoring Contaminant Releases from Consolidated Unit 16-021(c)-99," Los Alamos National Laboratory document LA-UR-07-2370, Los Alamos, New Mexico. (LANL 2007, 095787)
- LANL (Los Alamos National Laboratory), May 2007. "Corrective Measures Implementation Plan for Consolidated Unit 16-021(c)-99," Los Alamos National Laboratory document LA-UR-07-2019, Los Alamos, New Mexico. (LANL 2007, 096003)
- LANL (Los Alamos National Laboratory), July 2007. "Corrective Measures Implementation Plan for Consolidated Unit 16-021(c)-99, Revision 1," Los Alamos National Laboratory document LA-UR-07-4715, Los Alamos, New Mexico. (LANL 2007, 098192)
- LANL (Los Alamos National Laboratory), August 2007. "Corrective Measures Evaluation Report, Intermediate and Regional Groundwater, Consolidated Unit 16-021(c)-99," Los Alamos National Laboratory document LA-UR-07-5426, Los Alamos, New Mexico. (LANL 2007, 098734)
- LANL (Los Alamos National Laboratory), June 2008. "Supplemental Investigation Work Plan for Intermediate and Regional Groundwater at Consolidated Unit 16-021(c)-99," Los Alamos National Laboratory document LA-UR-08-3991, Los Alamos, New Mexico. (LANL 2008, 103165)

- LANL (Los Alamos National Laboratory), December 2008. "Completion Report for Well R-25b, Revision 1," Los Alamos National Laboratory document LA-UR-08-7831, Los Alamos, New Mexico. (LANL 2008, 105018)
- LANL (Los Alamos National Laboratory), February 2010. "Hydrologic Testing Work Plan for Consolidated Unit 16-021(c)-99," Los Alamos National Laboratory document LA-UR-10-0404, Los Alamos, New Mexico. (LANL 2010, 108534)
- LANL (Los Alamos National Laboratory), June 14, 2010. "Submittal of the Response to the Approval with Modifications for the Hydrologic Testing Work Plan for Consolidated Unit 16-021(c)-99," Los Alamos National Laboratory letter (EP2010-0274) to J.P. Bearzi (NMED-HWB) from M. Graham (LANL) and D. Gregory (DOE-LASO), Los Alamos, New Mexico. (LANL 2010, 109766)
- LANL (Los Alamos National Laboratory), January 2011. "Completion Report for Intermediate Well CdV-16-4ip," Los Alamos National Laboratory document LA-UR-11-0187, Los Alamos, New Mexico. (LANL 2011, 111608)
- Longmire, P., May 2005. "Characterization Well R-25 Geochemistry Report," Los Alamos National Laboratory report LA-14198-MS, Los Alamos, New Mexico. (Longmire 2005, 088510)
- Neuman, S.P., April 1974. "Effect of Partial Penetration on Flow in Unconfined Aquifers Considering Delayed Gravity Response," *Water Resources Research*, Vol. 10, No. 2, pp. 303-312. (Neuman 1974, 085421)
- NMED (New Mexico Environment Department), April 22, 2008. "Notice of Disapproval Corrective Measures Evaluation Report, Intermediate and Regional Groundwater Consolidated Unit 16-021(c)-99," New Mexico Environment Department letter to D. Gregory (DOE-LASO) and D. McInroy (LANL) from J.P. Bearzi (NMED-HWB), Santa Fe, New Mexico. (NMED 2008, 101311)
- NMED (New Mexico Environment Department), January 26, 2009. "Approval with Modifications, Supplemental Investigation Work Plan for Intermediate and Regional Groundwater at TA-16 (Consolidated Unit 16-021(c)-99)," New Mexico Environment Department letter to D. Gregory (DOE-LASO) and D. McInroy (LANL) from J.P. Bearzi (NMED-HWB), Santa Fe, New Mexico. (NMED 2009, 104973)
- NMED (New Mexico Environment Department), May 20, 2010. "Approval with Modifications, Hydrologic Testing Work Plan, Consolidated Unit 16-021(c)-99," New Mexico Environment Department letter to G.J. Rael (DOE-LASO) and M. Graham (LANL) from J.P. Bearzi (NMED-HWB), Santa Fe, New Mexico. (NMED 2010, 109689)
- NMED (New Mexico Environment Department), June 25, 2010. "Approval, Revised Schedule, R-25b and CdV-16-4ip Pumping Tests and Tracer Test, Hydrologic Testing Work Plan for Consolidated Unit 16-021(c)-99," New Mexico Environment Department letter to G.J. Rael (DOE-LASO) and M. Graham (LANL) from J.P. Bearzi (NMED-HWB), Santa Fe, New Mexico. (NMED 2010, 110435)
- Robinson, B.A., D.E. Broxton, and D.T. Vaniman, 2005. "Observations and Modeling of Deep Perched Water beneath the Pajarito Plateau," *Vadose Zone Journal*, Vol. 4, pp. 637-652. (Robinson et al. 2005, 091682)

Theis, C.V., 1934-1935. "The Relation Between the Lowering of the Piezometric Surface and the Rate and Duration of Discharge of a Well Using Ground-Water Storage," *American Geophysical Union Transactions*, Vol. 15-16, pp. 519-524. (Theis 1934-1935, 098241)

Toll, N.J., and T.C. Rasmussen, January–February 2007. "Removal of Barometric Pressure Effects and Earth Tides from Observed Water Levels," *Ground Water*, Vol. 45, No. 1, pp. 101–105. (Toll and Rasmussen 2007, 104799)

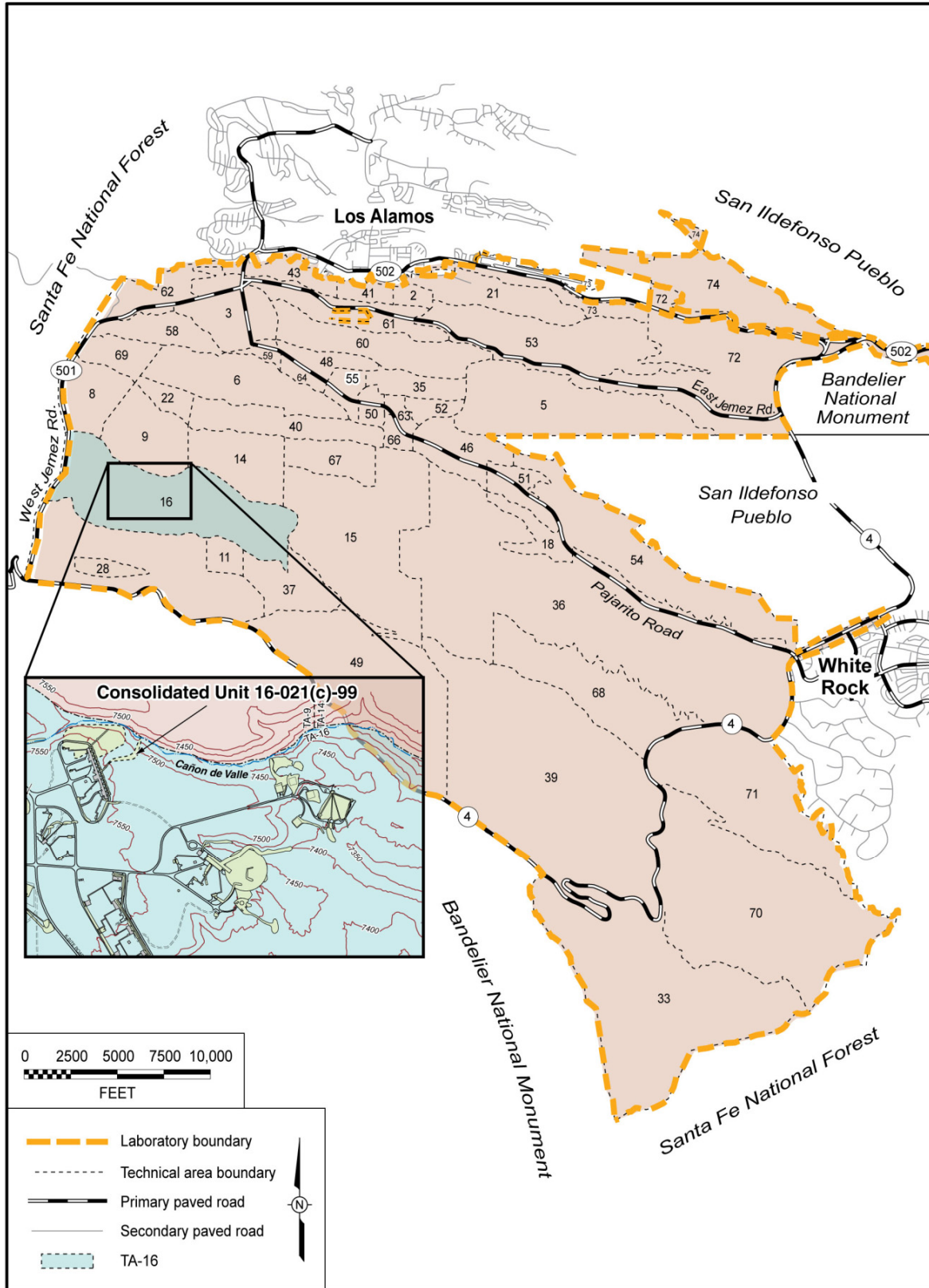


Figure 1.0-1 Location of TA-16 with respect to Laboratory technical areas and surrounding landholdings; Consolidated Unit 16-021(c)-99 is also shown.

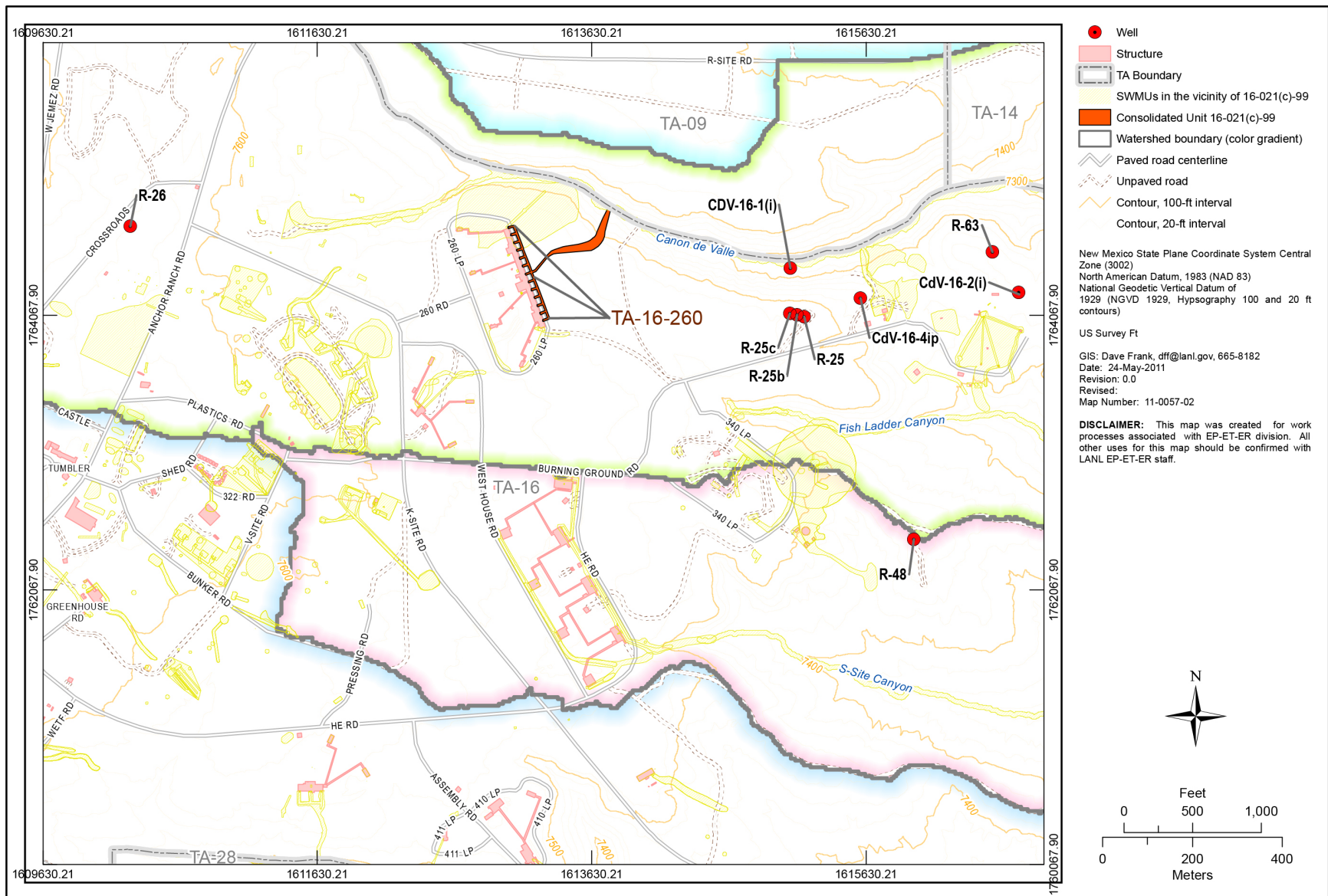


Figure 1.0-2 Location of Consolidated Unit 16-021(c)-99 and associated features

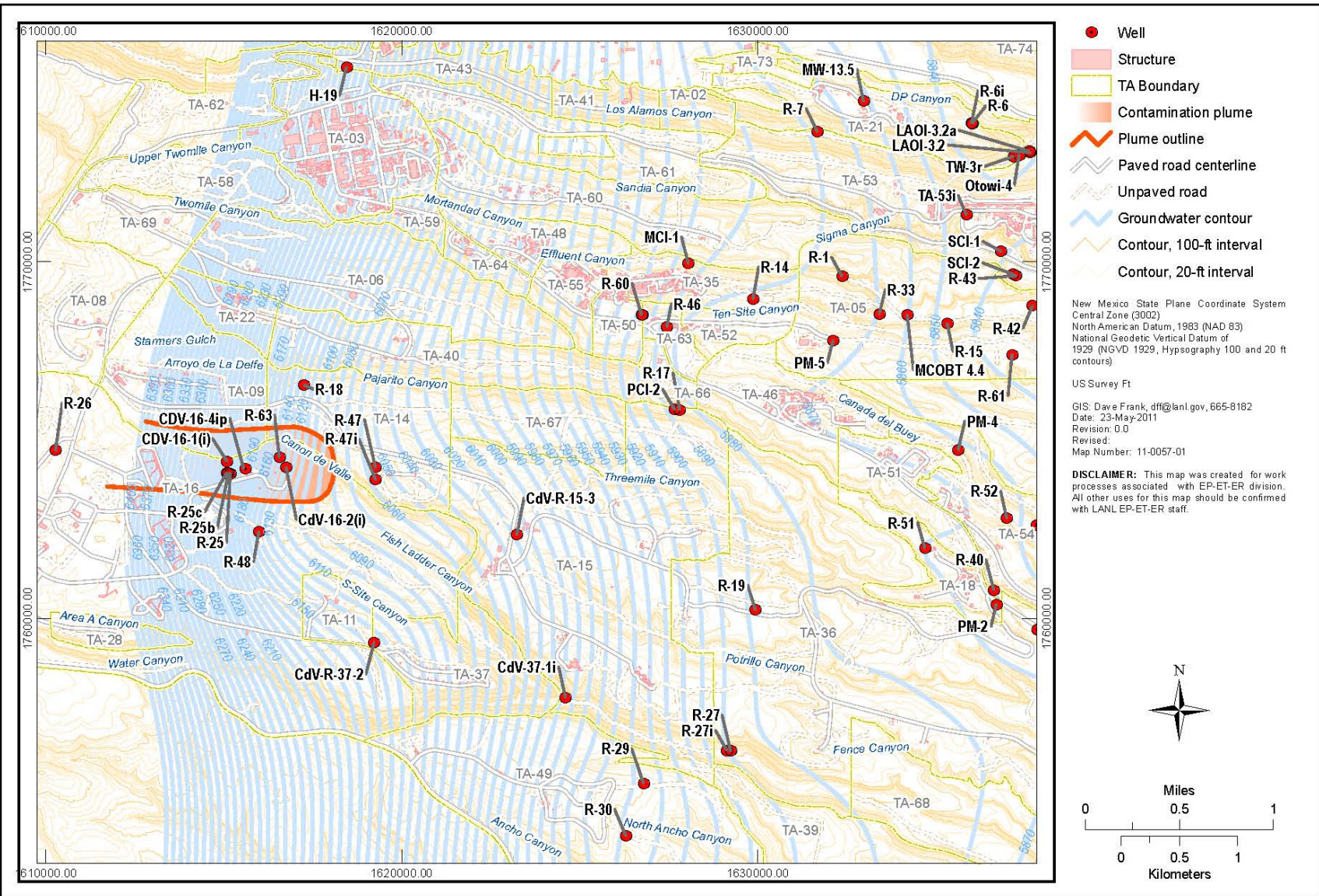


Figure 1.2-1 Monitoring wells in the vicinity and downgradient of TA-16 and approximate boundaries of contaminated deep-perched zone

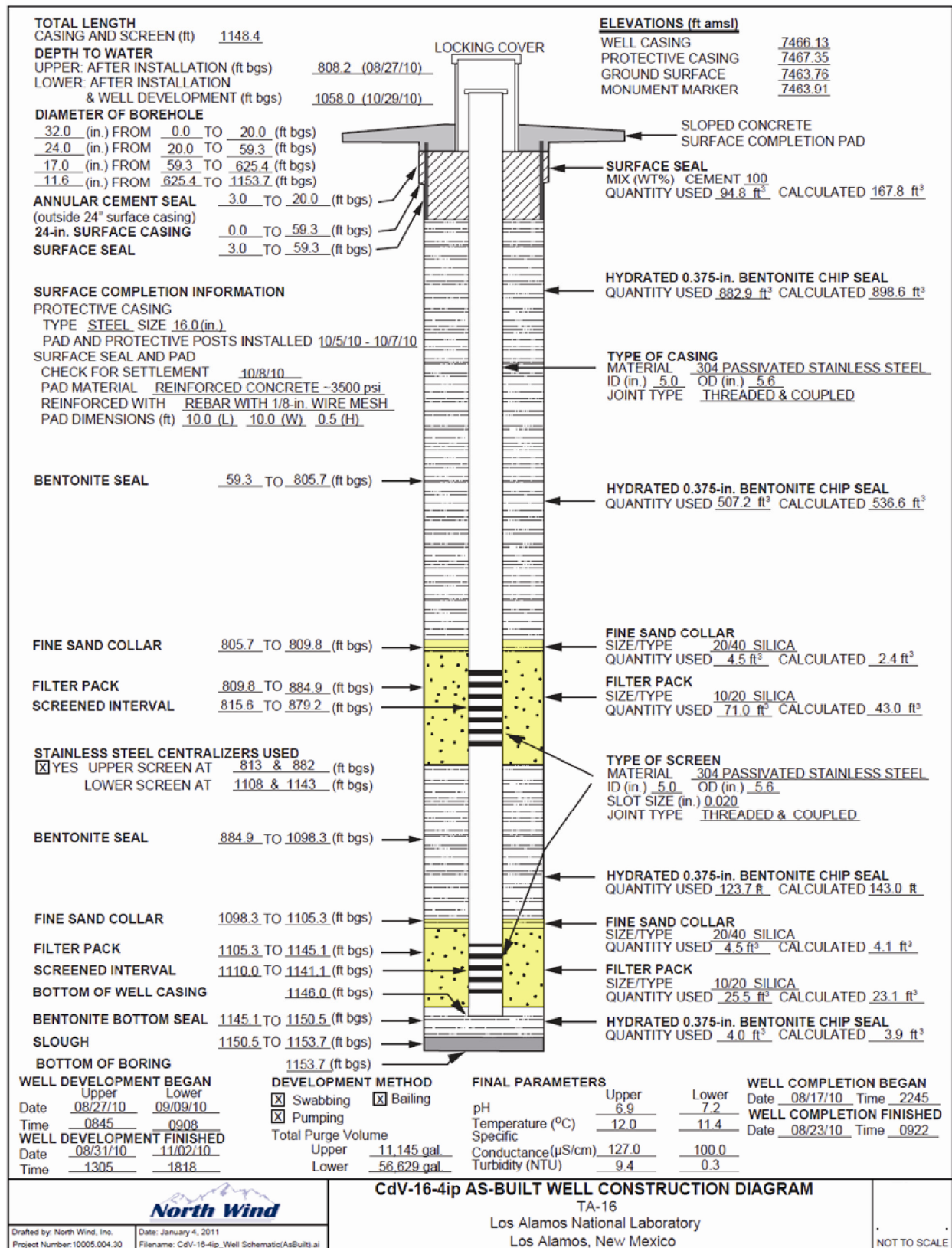


Figure 1.2-2 Well completion diagram of CdV-16-4ip

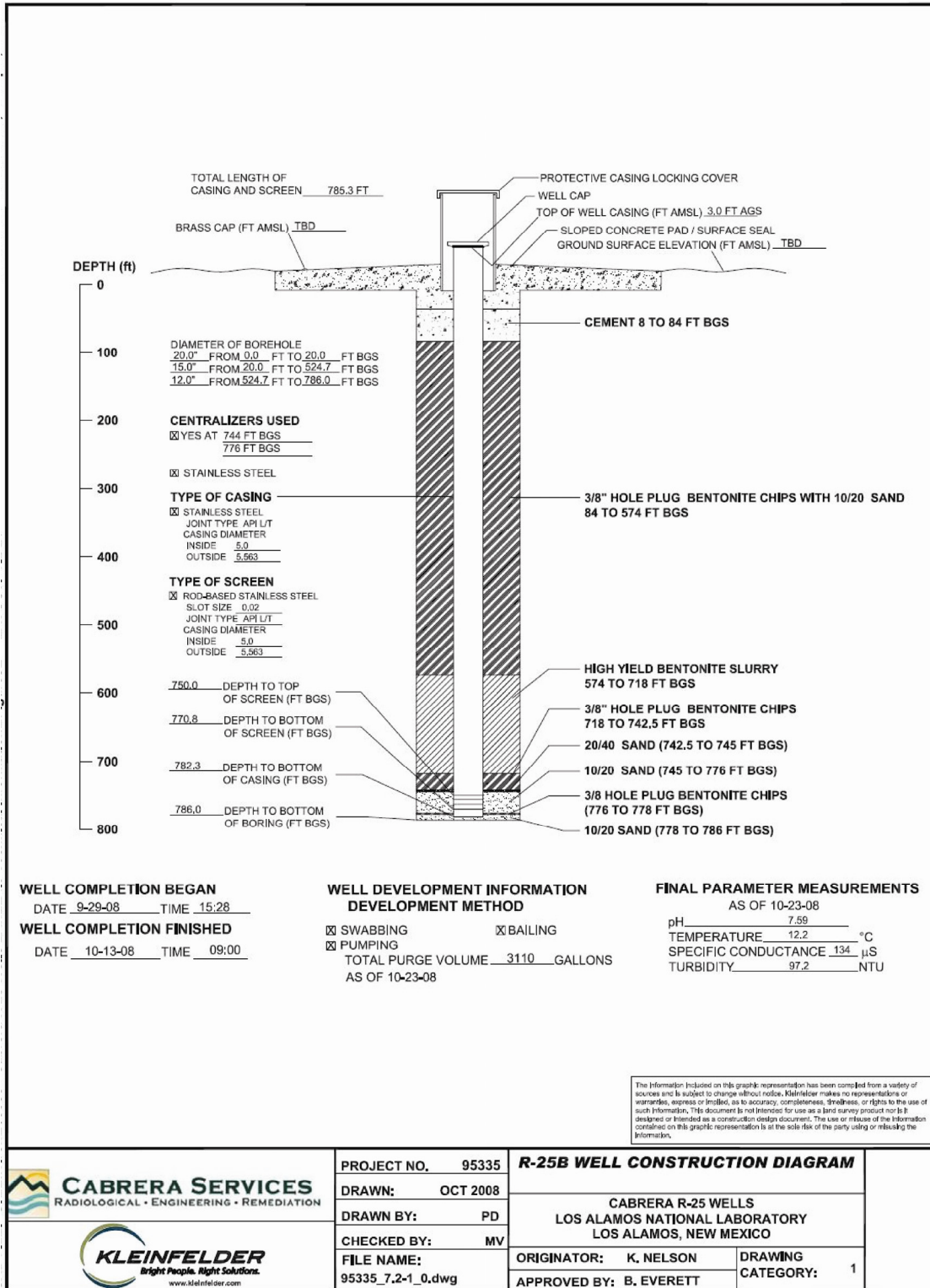
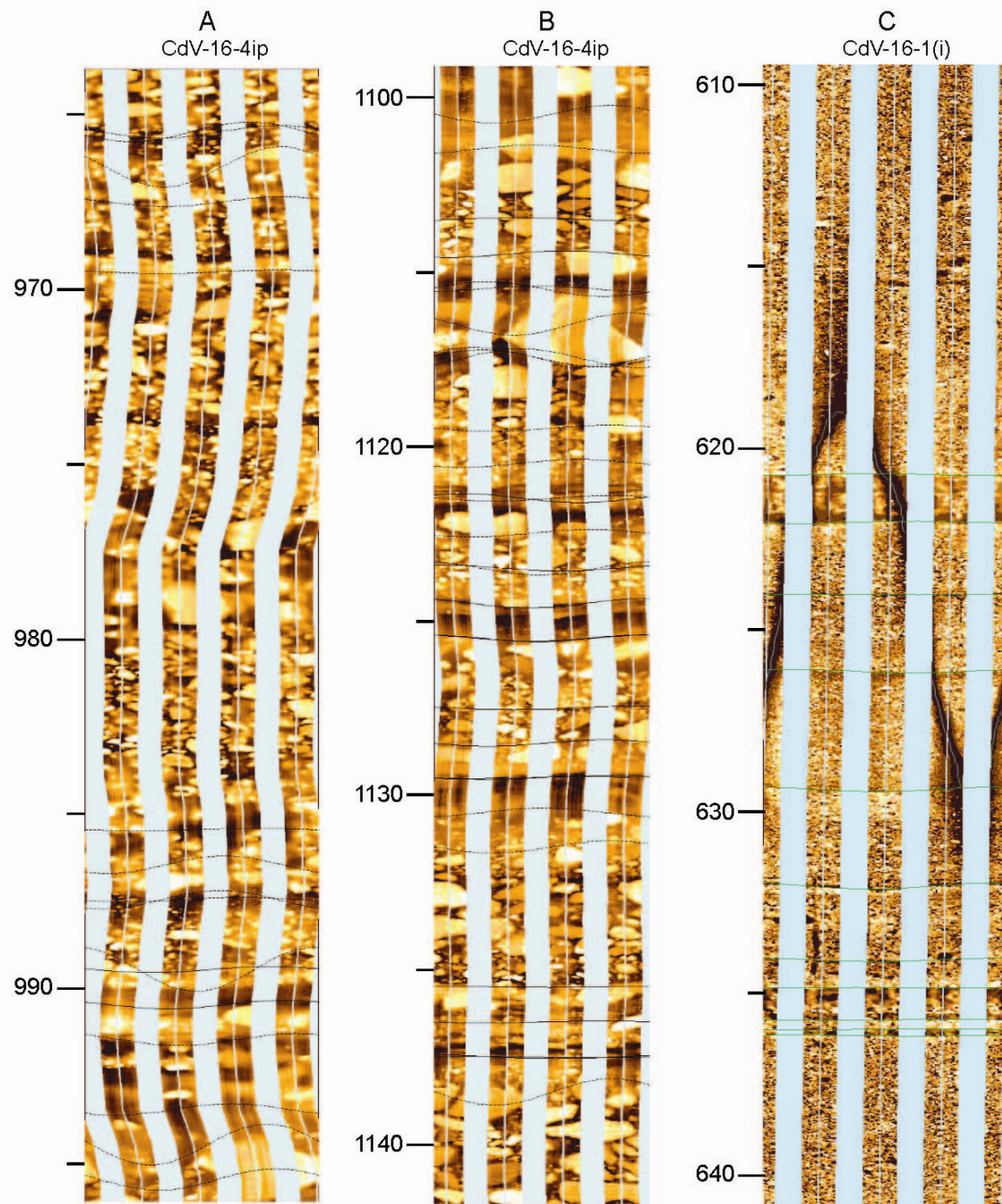
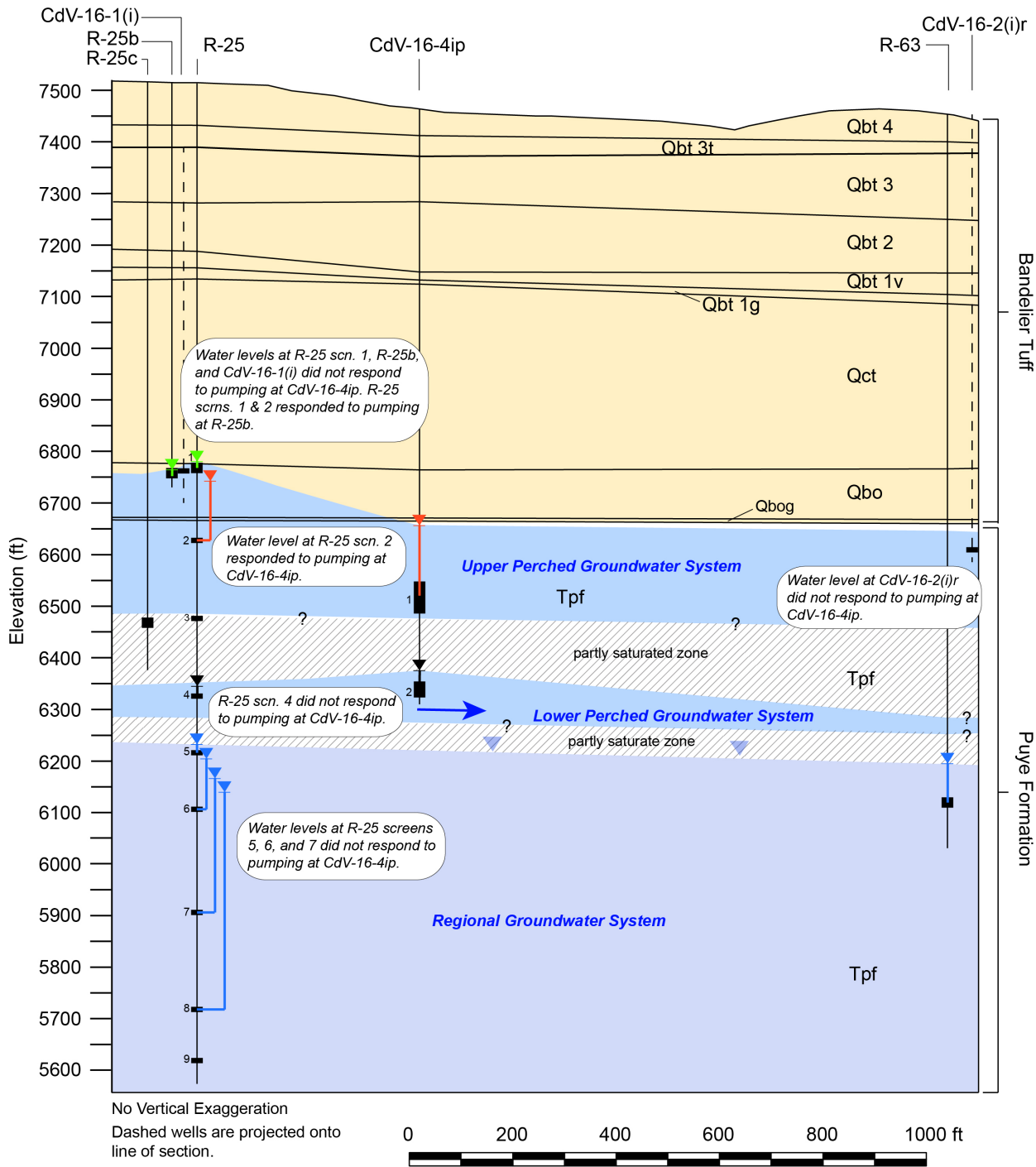


Figure 1.2-3 Well completion diagram of R-25b



Notes: A: Crudely stratified boulder-rich Puye deposits in the lower part of the upper perched zone. Silt beds in the interval 990–994 ft are believed to be the lower confining horizon for the upper perched zone. B: Stacks of boulder and gravel deposits separated by thin beds of sand and silt in the lower perched zone. C: Fractured Otowi Member ignimbrite deposits in the upper perched zone.

Figure 2.1.1 Formation microimager logs showing lithologies hosting perched groundwater at wells CdV-16-4ip and CdV-16-1(i)



Note: The blue, red, and green lines define hydraulic heads in the regional aquifer, upper perched Puye Formation (Tp) and upper perched Bandelier Tuff (Qbt and Qbo), respectively.

Figure 2.1-2 Cross-section of vadose zone and regional hydrostratigraphy near R-25 and CdV-16-4ip

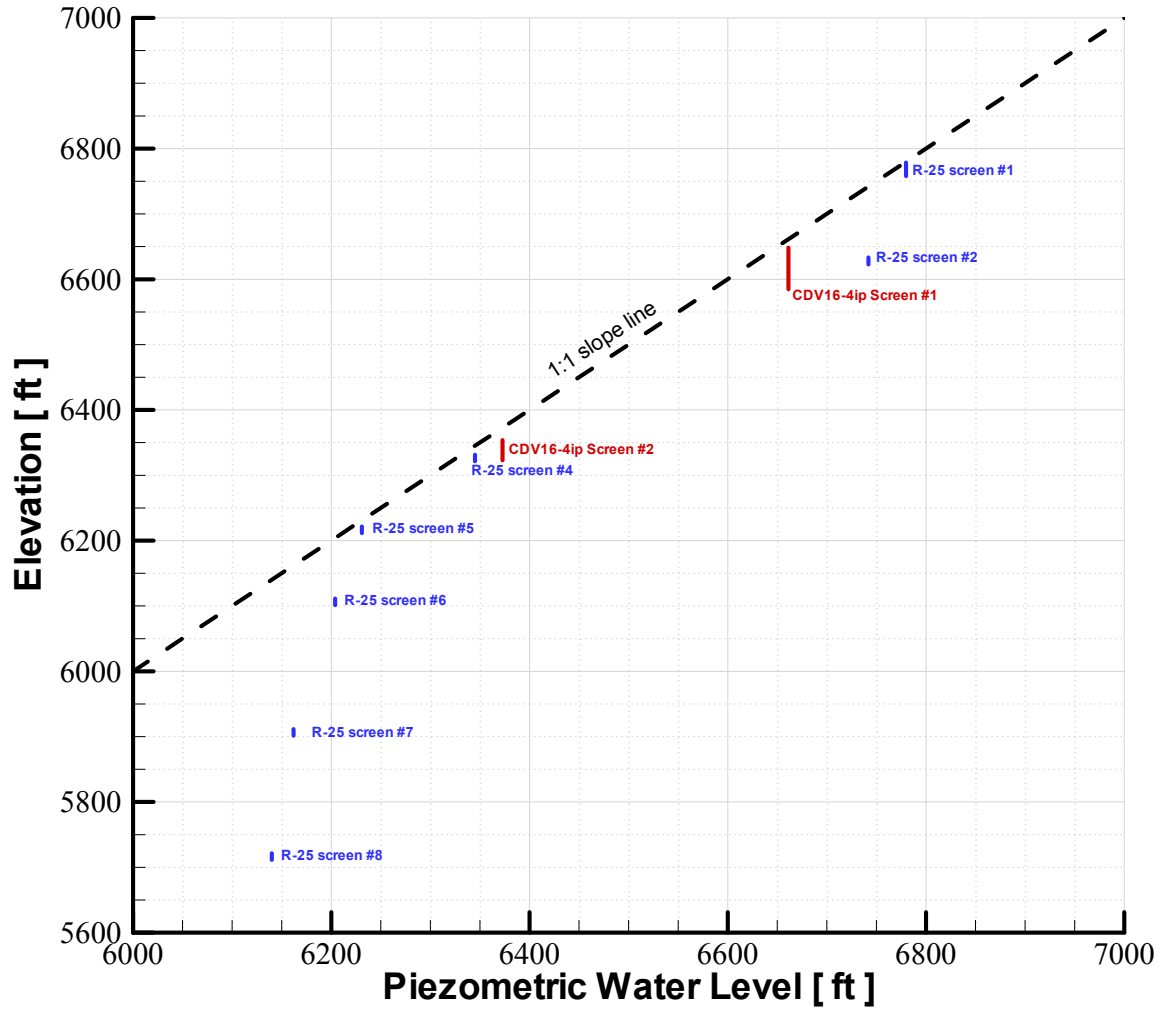


Figure 2.1-3 Screen elevations versus piezometric water levels along R-25 (in blue) and CdV-16-4ip (in red)

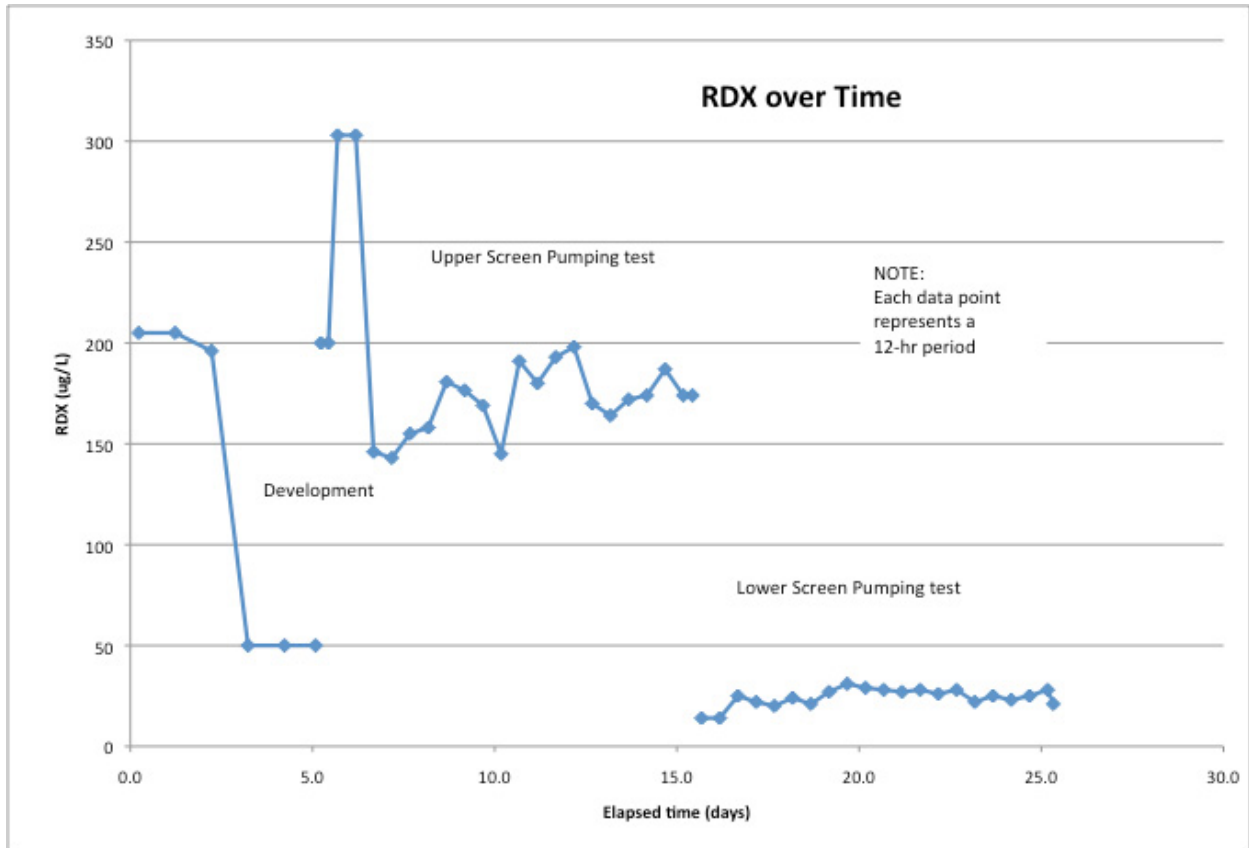


Figure 3.1-1 RDX concentration during development and pumping tests in the upper and lower CdV-16-4ip screens

Table 6.0-1
Estimated Hydraulic Parameters for CdV-16-4ip and R-25b Aquifer Pump Tests

Aquifer Properties	CdV-16-4ip Screen 1 (10-d test)	CdV-16-4ip Screen 2 (10-d test)	R-25b (1-d test)
Transmissivity	130 gpd/ft	660 gpd/ft	340 gpd/ft
Specific capacity	0.16 gpm/ft	0.25 gpm/ft	0.04 gpm/ft

Appendix A

Drawdown Data
(on CD included with this document)

Appendix B

CdV-16-4ip Pump Test Analysis

B-1.0 INTRODUCTION

This appendix describes the hydraulic analysis of pumping tests conducted from February to April 2011 at well CdV-16-4ip, a dual-screen perched-zone well located above Cañon de Valle within Technical Area 16 (TA-16). The tests on CdV-16-4ip were conducted to quantify the hydraulic properties of the two zones in which the well is screened, evaluate the hydraulic interconnection of the zones, and check for interference effects among neighboring wells.

Testing of each zone included a brief step-drawdown test followed by a 10-d pumping test. Each step-drawdown test was followed by recovery data collection overnight. Each 10-d test was started the morning after the step-drawdown test and was followed by a minimum of 12 d of recovery monitoring.

Unlike most of the pumping tests conducted on the Pajarito Plateau, no attempt was made to use an inflatable packer system in CdV-16-4ip to try to eliminate casing-storage effects in the test data. This is because pumping rates were maximized in an attempt to maximize drawdown effects in nearby wells; thus, dewatering of the well screens and filter packs and concomitant storage effects were inevitable and unavoidable.

During the pumping tests, water levels were recorded in several nearby wells. The wells and screened zones included in the monitoring effort, along with their horizontal distances from CdV-16-4ip, were R-25 screens 1, 2, 4, 5, 6, 7, and 8 (430.4 ft), R-25b (477.1 ft), CdV-16-1(i) (554.2 ft), CdV-16-2(i)r (1086.4 ft), and R-63 (1064.3 ft).

Conceptual Hydrogeology

Both screens in CdV-16-4ip lie within sands and gravels of the Puye Formation. Screen 1 is 63.6 ft long, extending from 815.6 to 879.2 ft below ground surface (bgs). Screen 2 is 31.1 ft long and set between the depths of 1110.0 and 1141.1 ft bgs.

The composite static water level measured on February 24, 2011, before testing was 811.0 ft bgs. The ground surface elevation at the well is 7463.9 ft above mean sea level (amsl), making the composite water-level elevation 6652.9 ft amsl.

During the screen 1 test effort, when the screened zones were isolated using an inflatable packer, the water level in screen 1 rose 0.9 ft, to a depth of 810.1 ft bgs and an elevation of 6653.8 ft amsl. (Complete equilibration had not yet occurred, so the true water level is likely a little higher.) At the same time, the water level in screen 2 declined 280.1 ft, making its depth to water 1091.1 ft bgs at an elevation of 6372.8 ft amsl. Thus, the water levels showed a large head difference of 281 ft, possibly greater.

The distance from the center of screen 1 (847.4 ft bgs) to the center of screen 2 (1125.55 ft bgs) is 278.15 ft. Thus, the computed vertical hydraulic gradient between the screened zones was greater than unity, indicative of perched conditions, severe vertical anisotropy, and low vertical permeability. This is consistent with observed water levels in the grouping of wells in this portion of Los Alamos National Laboratory, which show saturation above the regional water table with steep vertical gradients.

Inexplicably, during the screen 2 test effort, the initial static head over the known screen 2 transducer depth after packer inflation indicated a screen 2 water level of 1097.8 ft (elevation of 6366.1 ft amsl), in stark contradiction to the level measured during the screen 1 test effort after packer inflation, which was about 1091.1 ft bgs or 6372.8 ft amsl. The reason for the discrepancy could not be identified. Of note is that the screen 2 water level measured during the testing of screen 2 agreed with that measured months earlier during well development. At the end of the recovery period following the screen 2 tests, the water

level in screen 1 had recovered to a depth of 808.7 ft (elevation of 6655.2 ft amsl), while the screen 2 static water level was about 6364.9 ft. This made the measured head difference between the two zones 290.3 ft, again confirming a hydraulic gradient greater than unity.

CdV-16-4ip Screen 1 Testing

Screen 1 was tested from February 24 to March 20, 2011. After setting the pump and filling the drop pipe on February 24, a step-drawdown test was conducted on February 25. Following recovery overnight, the 10-d test was begun on February 26 and followed by recovery data collection from March 8 to 20.

Step-drawdown testing began at 7:00 a.m. on February 25 at an initial discharge rate of 4.1 gallons per minute (gpm). The rate was increased every 20 min at increments of around 1 gpm or less to a maximum rate of 20.7 gpm. During the final 20-min step, the rate was cut back to 10.6 gpm. The test was terminated at 2:20 p.m. after a total of 22 pumping steps had been conducted.

At 8:00 a.m. on February 26, the 10-d pumping test was initiated at a discharge rate of 11.8 gpm. Over time, as the drawdown in the well increased, the discharge rate declined gradually because of the increased pumping lift. By March 5, the rate had declined to 10.7 gpm. Because of concerns of drawing the pumping water level to the pump intake (causing cavitation), on March 5 the discharge rate was cut back to 7.9 gpm at 3:40 p.m. and then to 7.33 gpm at 3:50 p.m. where it remained for the balance of the pumping test.

The pump was shut off at 6:00 a.m. on March 8, and recovery data were collected until 7:08 a.m. Mountain Daylight Time (6:08 a.m. Mountain Standard Time) on March 20 when the packer was released and the pump was pulled from the well.

CdV-16-4ip Screen 2 Testing

Screen 2 was tested from March 20 to April 20, 2011. After setting the pump and filling the drop pipe on March 20, a step-drawdown test was conducted on March 21. Following recovery overnight, the 10-d test was begun on March 22 and followed by recovery data collection from April 1 to 20.

Step-drawdown testing began at 7:30 a.m. on March 21 at an initial discharge rate of 2.2 gpm. The rate was increased every 60 min at increments of around 2 to 3 gpm. When the rate reached 13.7 gpm, the pumping water level reached the pump intake, causing cavitation, so the test was terminated at that time.

At 12:00 p.m. on March 22, the 10-d pumping test was initiated at a discharge rate of 5 gpm. Over time, the rate remained fairly steady, ranging from about 4.9 gpm to a little more than 5.1 gpm.

The pump was shut off at 12:00 p.m. on April 1, and recovery data were collected until 7:40 a.m. on April 20 when brief pumping was performed in an attempt to collect water samples for radon analysis.

The pump was pulled from the well on April 21, when it was discovered that the transducer was missing from the transducer cage attached to the drop pipe. It was determined the transducer was dislodged from the cage at the moment that the packer separating screens 1 and 2 was deflated to allow pulling the pump. It was likely that the extreme hydraulic force caused by applying the screen 1 heads to the screen 2 zone was responsible. The transducer was subsequently fished out of the well on April 30.

B-2.0 BACKGROUND DATA

The background water-level data collected before the pumping tests help distinguish the naturally occurring water-level fluctuations from those caused by the pumping test.

Background water-level fluctuations have several causes, among them barometric pressure changes, operation of other wells in the aquifer, Earth tides, and long-term trends related to weather patterns. The background data hydrographs from the monitored wells were compared with barometric pressure data from the area to determine if a correlation existed.

Previous pumping tests on the plateau have demonstrated a barometric efficiency for most wells of between 90% and 100%. Barometric efficiency is defined as the ratio of water-level change divided by barometric pressure change, expressed as a percentage. In the initial pumping tests conducted on the early R-wells, downhole pressure was monitored using a vented pressure transducer. This equipment measures the difference between the total pressure applied to the transducer and the barometric pressure, with this difference being the true height of water above the transducer.

Subsequent pumping tests, including those at CdV-16-4ip, have utilized nonvented transducers. These devices simply record the total pressure on the transducer, that is, the sum of the water height plus the barometric pressure. This results in an attenuated “apparent” hydrograph in a barometrically efficient well. An example is a 90% barometrically efficient well. When monitored using a vented transducer, an increase in barometric pressure of 1 unit causes a decrease in recorded downhole pressure of 0.9 unit because the water level is forced downward 0.9 unit by the barometric pressure change. However, using a nonvented transducer, the total measured pressure increases by 0.1 unit (the combination of the barometric pressure increase and the water-level decrease). Thus, the resulting apparent hydrograph changes by a factor of 100 minus the barometric efficiency and changes in the same direction as the barometric pressure change, rather than in the opposite direction.

Barometric pressure data were obtained from the TA-54 tower site from the Waste and Environmental Services Division–Environmental Data and Analysis (WES-EDA) Group. The TA-54 measurement location is at an elevation of 6548 ft amsl, whereas the wellhead elevation is 7463.9 ft amsl. The static water level in CdV-16-4ip screen 1 was 810.1 ft bgs, making the water-level elevation 6652.9 ft amsl. The static water level in screen 2 was 1091.1 ft bgs at an elevation of 6372.8 ft amsl. Therefore, the measured barometric pressure data from TA-54 had to be adjusted to reflect the pressure at the elevation of the water table of each screen in CdV-16-4ip.

The following formula was used to adjust the measured barometric pressure data:

$$P_{WT} = P_{TA54} \exp \left[-\frac{g}{3.281R} \left(\frac{E_{4ip} - E_{TA54}}{T_{TA54}} + \frac{E_{WT} - E_{4ip}}{T_{WELL}} \right) \right] \quad \text{Equation B-1}$$

where P_{WT} = barometric pressure at the water table inside CdV-16-4ip

P_{TA54} = barometric pressure measured at TA-54

g = acceleration of gravity, in m/s² (9.80665 m/s²)

R = gas constant, in J/kg/degrees kelvin (287.04 J/kg/degrees kelvin)

E_{4ip} = land surface elevation at the CdV-16-4ip site, in feet (7463.9 ft)

E_{TA54} = elevation of barometric pressure measuring point at TA-54, in feet (6548 ft)

E_{WT} = elevation of the water level in CdV-16-4ip screens 1 and 2, in feet (6653.8/6372.8 ft)

T_{TA54} = air temperature near TA-54, in degrees kelvin (assigned a value of 43.3°F, or 279.4 K, for screen 1 and 50.5°F, or 283.4 K, for screen 2)

T_{WELL} = air temperature inside CdV-16-4ip, in degrees kelvin (assigned a value of 50.6°F or 283.5 K)

This formula is an adaptation of an equation WES-EDA provided. It can be derived from the ideal gas law and standard physics principles. An inherent assumption in the derivation of the equation is that the air temperature between TA-54 and the well is temporally and spatially constant, and that the temperature of the air column in the well is similarly constant.

The corrected barometric pressure data reflecting pressure conditions at the water table were compared with the water-level hydrograph to discern the correlation between the two and determine whether water-level corrections would be needed before data analysis.

B-3.0 IMPORTANCE OF EARLY DATA

When pumping or recovery first begins, the vertical extent of the cone of depression is limited to approximately the well screen length, the filter pack length, or the aquifer thickness in relatively thin permeable strata. For many pumping tests on the plateau, the early pumping period is the only time that the effective height of the cone of depression is known with certainty because, soon after startup, the cone of depression expands vertically through permeable materials above and/or below the screened interval. Thus, the early data often offer the best opportunity to obtain hydraulic conductivity information because conductivity would equal the earliest-time transmissivity divided by the well screen length.

Unfortunately, in many pumping tests (including those described here), casing-storage effects dominate the early-time data, potentially hindering the effort to determine the transmissivity of the screened interval. The duration of casing-storage effects can be estimated using the following equation (Schafer 1978, 098240).

$$t_c = \frac{0.6(D^2 - d^2)}{\frac{Q}{s}}$$

Equation B-2

where t_c = duration of casing-storage effect, in minutes

D = inside diameter of well casing, in inches

d = outside diameter of column pipe, in inches

Q = discharge rate, in gallons per minute

s = drawdown observed in pumped well at time t_c , in feet

The calculated casing-storage time is quite conservative. Often, the data show that significant effects of casing storage have dissipated after about half the computed time.

For wells screened across the water table or cases where the pumping water is pulled into the screen and filter pack, there can be an additional storage contribution from the filter pack around the screen. The following equation provides an estimate of the storage duration accounting for both casing and filter pack storage.

$$t_c = \frac{0.6[(D^2 - d^2) + S_y(D_B^2 - D_C^2)]}{\frac{Q}{s}} \quad \text{Equation B-3}$$

where S_y = short-term specific yield of filter media (typically 0.2)

D_B = diameter of borehole, in inches

D_C = outside diameter of well casing, in inches

This equation was derived from Equation B-2 on a proportional basis by increasing the computed time in direct proportion to the additional volume of water expected to drain from the filter pack. (To prove this, note that the left-hand term within the brackets is directly proportional to the annular area [and volume] between the casing and drop pipe while the right-hand term is proportional to the area [and volume] between the borehole and the casing, which is corrected for the drainable porosity of the filter pack. Thus, the summed term within the brackets accounts for all of the volume [casing water and drained filter pack water] appropriately.)

In some instances, it is possible to eliminate casing-storage effects by setting an inflatable packer above the tested screened interval before conducting the test. This approach was not applicable to the CdV-16-4ip pumping test effort because dewatering of the screens and filter packs was unavoidable.

B-4.0 TIME-DRAWDOWN METHODS

Time-drawdown data can be analyzed using a variety of methods. Among them is the Theis method (1934-1935, 098241). The Theis equation describes drawdown around a well as follows:

$$s = \frac{114.6Q}{T} W(u) \quad \text{Equation B-4}$$

where

$$W(u) = \int_u^{\infty} \frac{e^{-x}}{x} dx \quad \text{Equation B-5}$$

and

$$u = \frac{1.87r^2S}{Tt} \quad \text{Equation B-6}$$

and where s = drawdown, in feet

Q = discharge rate, in gallons per minute

T = transmissivity, in gallons per day per foot

S = storage coefficient (dimensionless)

t = pumping time, in days

r = distance from center of pumpage, in feet

To use the Theis method of analysis, the time-drawdown data are plotted on a log-log scale. Then, Theis curve matching is performed using the Theis type curve—a plot of the Theis well function $W(u)$ versus $1/u$. Curve matching is accomplished by overlaying the type curve on the data plot and, while keeping the coordinate axes of the two plots parallel, shifting the data plot to align with the type curve, effecting a matched position. An arbitrary point, referred to as the match point, is selected from the overlapping parts of the plots. Match-point coordinates are recorded from the two graphs, yielding four values: $W(u)$, $1/u$, s , and t . Using these match-point values, transmissivity and storage coefficient are computed as follows:

$$T = \frac{114.6Q}{s} W(u) \quad \text{Equation B-7}$$

$$S = \frac{Tut}{2693r^2} \quad \text{Equation B-8}$$

where T = transmissivity, in gallons per day per foot

S = storage coefficient (dimensionless)

Q = discharge rate, in gallons per minute

$W(u)$ = match-point value

s = match-point value, in feet

u = match-point value

t = match-point value, in minutes

An alternate solution method applicable to time-drawdown data is the Cooper-Jacob method (1946, 098236), a simplification of the Theis equation that is mathematically equivalent to the Theis equation for most pumped well data. The Cooper-Jacob equation describes drawdown around a pumping well as follows:

$$s = \frac{264Q}{T} \log \frac{0.3Tt}{r^2 S} \quad \text{Equation B-9}$$

The Cooper-Jacob equation is a simplified approximation of the Theis equation and is valid whenever the u value is less than about 0.05. For small radius values (e.g., corresponding to borehole radii), u is less than 0.05 at very early pumping times and therefore is less than 0.05 for most or all measured drawdown

values. Thus, for the pumped well, the Cooper-Jacob equation usually can be considered a valid approximation of the Theis equation. An exception occurs when the transmissivity of the aquifer is very low. In that case, some of the early pumped well drawdown data may not be well approximated by the Cooper-Jacob equation.

According to the Cooper-Jacob method, the time-drawdown data are plotted on a semilog graph, with time plotted on the logarithmic scale. Then a straight line of best fit is constructed through the data points and transmissivity is calculated using the following:

$$T = \frac{264Q}{\Delta s} \quad \text{Equation B-10}$$

where T = transmissivity, in gallons per day per foot

Q = discharge rate, in gallons per minute

Δs = change in head over one log cycle of the graph, in feet

Because many of the test wells completed on the plateau are severely partially penetrating, an alternate solution considered for assessing aquifer conditions is the Hantush equation for partially penetrating wells (Hantush 1961, 098237; Hantush 1961, 106003). The Hantush equation is as follows:

Equation B-11

$$s = \frac{Q}{4\pi T} \left[W(u) + \frac{2b^2}{\pi^2(l-d)(l'-d')} \sum_{n=1}^{\infty} \frac{1}{n^2} \left(\sin \frac{n\pi l}{b} - \sin \frac{n\pi d}{b} \right) \left(\sin \frac{n\pi l'}{b} - \sin \frac{n\pi d'}{b} \right) W \left(u, \sqrt{\frac{K_z}{K_r}} \frac{n\pi r}{b} \right) \right]$$

where s , Q , T , t , r , S , and u are as previously defined and

b = aquifer thickness

d = distance from top of aquifer to top of well screen in pumped well

l = distance from top of aquifer to bottom of well screen in pumped well

d' = distance from top of aquifer to top of well screen in observation well

l' = distance from top of aquifer to bottom of well screen in observation well

K_z = vertical hydraulic conductivity

K_r = horizontal hydraulic conductivity

with all terms expressed in consistent units.

In this equation, $W(u)$ is the Theis well function and $W(u,\beta)$ is the Hantush well function for leaky aquifers where:

$$\beta = \sqrt{\frac{K_z}{K_r}} \frac{n\pi r}{b} \quad \text{Equation B-12}$$

Note that for single-well tests, $d = d'$ and $l = l'$.

Unconfined Aquifer Drawdown Correction

For unconfined aquifers, the saturated aquifer thickness is reduced to below the original thickness during testing. This results in drawdown values that deviate from theoretical predictions, because well hydraulics formulas are based on 100% aquifer saturation. Before analysis, the actual drawdown values must be corrected for dewatering effects using the following formula (Kruseman et al. 1991, 106681):

$$s_c = s_a - \frac{s_a^2}{2b} \quad \text{Equation B-13}$$

where s_c = corrected drawdown, in feet

S_a = observed drawdown, in feet

b = saturated aquifer thickness, in feet

Assumptions required for validity of Equation B-13 are (1) homogeneous hydraulic conductivity, (2) full penetration of the producing zone by the well screen, and (3) no head loss associated with vertical flow. This last assumption is satisfied by one of two extremes—either zero permeability in the vertical direction so that there is no flow (and therefore no head loss) vertically, or infinite vertical permeability. Failure to meet any of these three assumptions leads to modest errors in application of the drawdown correction equation.

B-5.0 RECOVERY METHODS

Recovery data were analyzed using the Theis recovery method. This is a semilog analysis method similar to the Cooper-Jacob procedure.

In this method, residual drawdown is plotted on a semilog graph versus the ratio t/t' , where t is the time since pumping began, and t' is the time since pumping stopped. A straight line of best fit is constructed through the data points, and T is calculated from the slope of the line as follows:

$$T = \frac{264Q}{\Delta s} \quad \text{Equation B-14}$$

The recovery data are particularly useful compared with time-drawdown data. Because the pump is not running, spurious data responses associated with dynamic discharge rate fluctuations are eliminated. The result is that the data set is generally “smoother” and easier to analyze.

Recovery data also can be analyzed using the Hantush equation for partial penetration. This approach is generally applied to the early data in a plot of recovery versus recovery time.

B-6.0 SPECIFIC CAPACITY METHOD

The specific capacity of the pumped well can be used to obtain a lower-bound value of hydraulic conductivity. This helps frame the pumping test analysis, often helping the analyst reject spurious and contradictory computed aquifer parameter values.

The hydraulic conductivity is computed using formulas that are based on the assumption that the pumped well is 100% efficient. The resulting hydraulic conductivity is the value required to sustain the observed specific capacity. If the actual well is less than 100% efficient, it follows that the actual hydraulic conductivity would have to be greater than calculated to compensate for well inefficiency. Thus, because the efficiency is unknown, the computed hydraulic conductivity value represents a lower bound. The actual conductivity is known to be greater than or equal to the computed value.

For fully penetrating wells, the Cooper-Jacob equation can be iterated to solve for the lower-bound hydraulic conductivity. However, the Cooper-Jacob equation (assuming full penetration) ignores the contribution to well yield from permeable sediments above and below the screened interval. To account for this contribution, it is necessary to use a computation algorithm that includes the effects of partial penetration. One such approach was introduced by Brons and Marting (1961, 098235) and augmented by Bradbury and Rothschild (1985, 098234).

Brons and Marting introduced a dimensionless drawdown correction factor, s_p , approximated by Bradbury and Rothschild as follows:

$$s_p = \frac{1 - \frac{L}{b}}{\frac{L}{b}} \left[\ln \frac{b}{r_w} - 2.948 + 7.363 \frac{L}{b} - 11.447 \left(\frac{L}{b} \right)^2 + 4.675 \left(\frac{L}{b} \right)^3 \right] \quad \text{Equation B-15}$$

In this equation, L is the well screen length, in feet. When the dimensionless drawdown parameter is incorporated, the conductivity is obtained by iterating the following formula:

$$K = \frac{264Q}{sb} \left(\log \frac{0.3Tt}{r_w^2 S} + \frac{2s_p}{\ln 10} \right) \quad \text{Equation B-16}$$

The Brons and Marting procedure can be applied to both partially penetrating and fully penetrating wells.

To apply this procedure, a storage coefficient value must be assigned. Storage coefficient values generally range from 10^{-5} to 10^{-3} for confined aquifers and 0.01 to 0.25 for unconfined systems (Driscoll 1986, 104226). The perched nature of the screened zones and dewatering that occurred during testing suggested that the assumption of unconfined conditions was reasonable. The calculation result is not particularly sensitive to the choice of storage coefficient value, so a rough estimate is generally adequate to support the calculations.

The analysis also requires assigning a value for the saturated aquifer thickness, b . For screen 1, the well screen penetrated nearly the entire saturated zone. For simplicity, screen 1 was treated as fully penetrating. For screen 2, the saturated thickness was considered to be the distance from the static water level of 1097.8 ft bgs to the bottom of the well screen at a depth of 1141.1, a thickness of 43.3 ft.

B-7.0 BACKGROUND DATA ANALYSIS

Background aquifer pressure data collected during the CdV-16-4ip tests were plotted along with barometric pressure to determine the barometric effect on water levels.

Figure B-7.0-1 shows aquifer pressure data from CdV-16-4ip screen 1 during the test period along with barometric pressure data from TA-54 that have been corrected to equivalent barometric pressure in feet of water at the water table. The CdV-16-4ip data are referred to in the figure as the "apparent hydrograph"

because the measurements reflect the sum of water pressure and barometric pressure, having been recorded using a nonvented pressure transducer. The dates of the pumping periods for the CdV-16-4ip pumping tests are included in the figure for reference.

In Figure B-7.0-1, the hydrograph scale spans a much greater range than the barometric pressure scale, so that all of the hydrograph can be illustrated. To compare the hydrograph and barometric pressure directly, a portion of the hydrograph observed during recovery was replotted on Figure B-7.0-2 at the same scale as the barometric pressure curve. It is clear that barometric pressure fluctuations had little effect on the apparent hydrograph, implying a barometric efficiency near 100%.

Figure B-7.0-3 shows aquifer pressure data collected from CdV-16-4ip screen 2 during the screen 1 pumping test effort. The apparent hydrograph scale in Figure B-7.0-3 is much greater than the barometric pressure scale to illustrate the entire water-level data set. The hydrograph shows two episodes where the head over the transducer reached hundreds of feet. The first one corresponds to the pump installation just before the initial packer inflation. The subsequent rise in water level occurred when the nylon nitrogen line between the nitrogen tank and the downhole packer broke, allowing the packer to deflate briefly. The line was quickly repaired and the packer reinflated.

To compare the screen 2 hydrograph and barometric pressure directly, the hydrograph was replotted on Figure B-7.0-4 at the same scale as the barometric pressure curve. As observed in screen 1, it is clear that barometric pressure fluctuations had little effect on the apparent hydrograph from screen 2, implying a barometric efficiency near 100% for that zone as well.

Figure B-7.0-4 shows two anomalies. First, the head measured after the packer was reinflated following failure of the nylon packer line was about 1 ft greater than that observed when the pump was installed and the packer was initially inflated. There was no apparent explanation for this. It is possible that the sudden head increase that occurred when the packer deflated may have affected the transducer or the well construction materials (annular seal materials) and caused an apparent water-level change.

The second anomaly was the inexplicable rise in head of about 0.25 ft that occurred for several hours on March 4. Although there was no obvious explanation for the observed response, it may have been related to the apparent borehole instability induced by the water-hammer effect mentioned above.

Note that subsequent step-drawdown testing of the screen 2 interval suggested that this zone might be unstable. This was evidenced by a sudden deterioration in pumping performance during the step-drawdown test and production of solids with the pumped water, which are similar in appearance to bentonite annular seal material. The large head difference between screens 1 and 2 results in a severe water-hammer effect on the screen 2 zone when an inflatable packer separating the screens is deflated, allowing the zones to come in contact. This has occurred several times during well development, bridge plug installation and removal, and test pumping. These enormous hydraulic effects could have eroded the filter pack away from the screen, allowing overlying materials to collapse around the screen. A video log conducted following testing of screen 2 showed formation material in the screen slots and sediment-laden water in the screen. The anomalous water-level rise on March 4 may have been related to the instability of the annular fill materials in the screen 2 zone. When the screen 2 transducer was removed from the well after testing screen 1, bentonitic material was present on the transducer. It was analyzed and shown to be smectite clay, consistent with bentonite used for the annular seal in CdV-16-4ip.

Figure B-7.0-5 shows the apparent hydrograph recorded in screen 2 during the screen 2 pumping test effort. The data confirmed the near 100% barometric efficiency for the screen 2 zone.

Figure B-7.0-6 shows the apparent hydrograph recorded in screen 1 during the screen 2 pumping test. The apparent hydrograph data were plotted on a broad scale to accommodate showing all of the data. The water levels showed significant ongoing recovery in response to both the original screen 1 pumping test conducted a month earlier as well as a 12-h cross-flow period on March 20 when the pump was pulled from screen 1 and reset at screen 2.

Hydrograph data from nearby wells R-25 (screens 1, 2, 4, 5, 6, 7, and 8), R-25b, CdV-16-1(i), CdV-16-2(i)r, and R-63 were downloaded to check for a possible pumping response to the CdV-16-4ip tests. None of the monitored zones showed any response to pumping CdV-16-4ip screen 2. The only zone that showed a response to pumping CdV-16-4ip screen 1 was R-25 screen 2. The data corresponding to the pumping test period are shown in Figure B-7.0-7.

Because the Earth-tide fluctuations in the hydrograph were large, it was necessary to correct the water-level data by removing the Earth-tide effect. This was done using BETCO (barometric and Earth-tide correction) software—a mathematically complex correction algorithm that uses regression deconvolution (Toll and Rasmussen 2007, 104799) to modify the data. The BETCO correction not only removes barometric pressure effects, but can remove Earth-tide effects as well. The BETCO-corrected data for R-25 screen 2 are included in the data plot in Figure B-7.0-7. The drawdown observed in response to pumping CdV-16-4ip was approximately 0.4 ft.

B-8.0 WELL CDV-16-4IP SCREEN 1 DATA ANALYSIS

This section presents the data obtained from the CdV-16-4ip screen 1 pumping tests and the results of the analytical interpretations. Data are presented for the step-drawdown and 10-d tests.

B-8.1 Well CDV-16-4IP Screen 1 Test Description

Screen 1 was tested from February 24 to March 20, 2011. After setting the pump and filling the drop pipe on February 24, a step-drawdown test was conducted on February 25. Following recovery overnight, the 10-d test was begun on February 26 and followed by recovery data collection from March 8 to 20.

Figure B-8.1-1 shows the water-level data measured during the screen 1 pumping tests. Several important observations and conclusions can be made from the graph.

During the step-drawdown test, screen 1 was pumped for more than 7 h at rates of up to 20.7 gpm with a drawdown of around 10 ft. In contrast, the 10-d test, conducted at rates no greater than 11.8 gpm, produced drawdown in excess of 50 ft. The enormous increase in drawdown with extended pumping time implied severe boundary conditions for the screen 1 zone.

Consistent with this observation, following recovery overnight after the step-drawdown test, the water level remained 2.5 ft lower than the original static water level. Failure of recovery to near the starting level was another strong indication of a severely laterally limited permeable zone. Similarly, at the conclusion of the tests, the recovered water level remained 5 ft below the original static level after 12 d of recovery.

During pumping, at a drawdown of around 35 ft (head over the transducer of about 75 ft), there was a distinct reduction in the rate of drawdown. It is possible that the storage coefficient (specific yield) increased for the sediments below that depth. Although this sort of response could normally be ascribed to delayed-yield effects, the recovery data contradicted this idea, reinforcing the supposition of a change in storage coefficient with depth. Note that the same effect was repeated in the recovery data set. If the cause of the flattening of the curve during pumping had been related to delayed yield, the recovery response would have been reversed, i.e., a steep initial recovery response followed by a flat trend. The

actual recovery rate was slow initially and more rapid later on, consistent with the postulated change in specific yield. (Note that during recovery, the transition occurred at a slightly higher water level. This was because of the extra drawdown that existed in the well during the active pumping phase compared with the recovery phase when no pumping was occurring.)

Except for the early-time drawdown and late-time recovery, most of the data in Figure B-8.1-1 followed straight-line trends, an indication of limited aquifer extent. When pumping a laterally extensive aquifer, a linear plot of the drawdown or recovery data would show a steady flattening trend over time. Straight-line drawdown plots, on the other hand, result from pumping (draining) a zone of finite lateral size—analogueous to the water-level trend that would be observed when pumping water out of a bathtub or swimming pool.

The straight-line recovery plots are interesting. If the permeable zone were fully bounded, water levels would not recover. The actual ongoing recovery showed that the limited perched zone has indirect hydraulic connection to other recharge sources. The linear (straight-line) recovery trends during the first several days of recovery suggested a constant recharge input rate to the perched zone in which the upper CdV-16-4ip screen is placed, analogueous to the rate at which water flows over a weir. As the head over the transducer approached a height of about 100 ft (corresponding to about 10 ft of drawdown), the recovery curve began to flatten, suggesting that the water level had reached the elevation of the recharge source at an elevation of about 6645 ft amsl, which approximately corresponds to the contact between the Otowi Member of the Bandelier Tuff and the Puye Formation in the vicinity of CdV-16-4ip.

The conclusion from this cursory examination of the drawdown and recovery plots is that the pumped interval consists of highly permeable, severely laterally limited sediments that have an indirect hydraulic connection to a recharge source. This would be consistent with indirect hydraulic recharge to the perched intermediate zone from a nearby fault or fracture zone. It is also consistent with a laterally extensive perched zone connected to the pumped zone, but limited to a saturated thickness of about 10 ft.

Using the “bathtub” analogy, based on the linear changes in water level over time, it is possible to estimate the rate of the hypothesized recharge by comparing the drawdown slope during pumping with that during recovery. It can be shown that the recharge rate, R , can be computed as follows:

$$R = \frac{I_R Q}{I_R - I} \qquad \text{Equation B-17}$$

where R = recharge rate

I_R = drawdown slope during recovery

Q = discharge rate

I = drawdown slope during pumping

with all terms expressed in consistent units.

Figure B-8.1-2 shows the observed drawdown and recovery slopes along with the corresponding average pumping rates. Applying Equation B-17 to the 11.1-gpm interval yielded an estimated formation recharge rate of 4.40 gpm. Applying the equation to the 7.33-gpm rate yielded an estimated recharge rate of 5.26 gpm, in reasonable agreement with the first value. Averaging these values gives an estimated recharge rate of 4.83 gpm.

This calculation is based on the assumption that the storage coefficient (specific yield) has the same magnitude during recovery as during pumping. Often this is not the case because of hysteretic effects. In unconfined aquifers, the rate of recovery can be more rapid than that of drawdown because of a smaller effective storage coefficient during recovery. During pumping the capillary fringe above the water table increases in thickness, while during recovery it gets thinner (Bevan et al. 2005, 105186). If the rate of thinning during recovery exceeds the rate of growth during pumping, the effective storage coefficient during recovery will be less than that during pumping, resulting in a more rapid recovery rate than drawdown rate. Additionally, as the water table rebounds during recovery, it can trap air in the previously dewatered pore spaces, further decreasing the effective recovery storage coefficient. This means that the apparent recovery (recharge) rate could be exaggerated and overestimated. It follows that the computed estimated recharge rate of 4.83 gpm (930 ft³/d) is the maximum possible rate.

This recharge rate was used to estimate the areal extent of the contiguous dewatered perched zone. The area of the permeable perched zone can be computed as follows:

$$A = \frac{Q}{d_r S_y} \quad \text{Equation B-18}$$

where A = perched zone area, in square feet

Q = recharge rate, in cubic feet per day (930 ft³/d [4.83 gpm])

d_r = rate of change in the depth to water, in feet

S_y = specific yield (storage coefficient)

Figure B-8.1-3 shows estimated areal extent of the perched zone as a function of reasonable estimates of short-term specific yield for the water-level recovery response observed on March 8 and 9 when the rate of recovery, d_r, was 2.1 ft/d. The possible range of the perched zone area is large, because it is related to specific yield, which can only be estimated.

As an example, consider the case for a specific yield of 0.05. The corresponding perched zone area is 8857 ft². The data do not support a determination of the shape of the perched zone. Thus, this area could reflect (1) a circular zone having a radius of 53 ft (diameter of 106 ft); (2) a square area 94 ft on a side; (3) a linear strip 10 ft wide and 885.7 ft long; or (4) complex areas, such as dendritic zones with many interconnected branches. The pumping test data cannot provide any illumination regarding the nature of the shape of the connected permeable zone. The data confirm, however, that the perched zone is fairly small, regardless of the value of the specific yield.

During the pumping period, before cutting back the flow rate, at a drawdown of about 50 ft (head over the transducer of about 60 ft), the drawdown slope increased dramatically (Figure B-8.1-1). This increase was likely an indication that the permeable zone was being almost fully dewatered. This suggested that the most permeable sediments did not extend to the bottom of the well screen and that the effective thickness of permeable sediments was around 60 ft.

Note that on March 3 and 5, the water level was pulled below the bottom of the screen. This was attributable to intentional increases in pumping rate designed to temporarily dewater the well quickly to ascertain the amount of remaining available drawdown. These operations were performed as a precaution to avoid pulling the pumping level to the pump intake and causing cavitation of the pump over an extended period.

B-8.2 Well CdV-16-4ip Screen 1 Step-Drawdown Test

Step-drawdown testing of CdV-16-4ip began at 7:00 a.m. on February 25 at an initial discharge rate of 4.1 gpm. The rate was increased every 20 min at increments of around 1 gpm or less to a maximum rate of 20.7 gpm. During the final 20-min step, the rate was cut back to 10.6 gpm. The test was terminated at 2:20 p.m. after a total of 22 pumping steps had been conducted.

The many pumping steps, culminating in the high pumping rate of 20.7 gpm, were selected with the intention of gradually dewatering the entire formation thickness and thus indirectly providing a detailed picture of formation permeability as a function of depth. Unfortunately, the short-term yield of the zone was too great to allow dewatering of a significant portion of it quickly, thwarting this attempt.

Figure B-8.2-1 shows the discharge rates applied during the step-drawdown test, as a function of pumping time, along with the observed drawdown. As shown on the graph, when the pumping rate was reduced to 10.6 gpm during the final step, the drawdown leveled off at around 9 ft. Note that earlier (pumping time of 180 min), at a similar pumping rate, the drawdown was only about 3 ft. The subsequent tremendous increase in drawdown at a similar pumping rate was an indication of a severely laterally limited aquifer, as discussed previously.

To illustrate this further, drawdown responses for a hypothetical laterally extensive aquifer were computed and compared with the observed response. To support the calculations, a lower-bound transmissivity was estimated from the first step of the step-drawdown test for use in the well hydraulics equations.

At the end of the first 20 min of pumping, the discharge rate was 4.1 gpm with a resulting drawdown of 0.64 ft for a short-term specific capacity of 6.41 gpm/ft. In addition to specific capacity and pumping time, other input assumptions used in the calculations included a borehole radius of 0.60 ft (inferred from the volume of the filter pack required to backfill the screened zone), the pumping time of 20 min, and an assumption of fully penetrating conditions.

Applying the Brons and Marting method to these inputs yielded lower-bound transmissivity values for the upper perched zone shown in Figure B-8.2-2. As shown in the figure, the lower-bound transmissivity values ranged from about 4500 to 6500 gallons per day (gpd)/ft for typical, reasonable storage coefficient values.

The combinations of lower-bound transmissivity values and corresponding storage coefficients were used to simulate the 22-step pumping test by superimposing multiple calculations using the Cooper-Jacob equation. The calculations were performed to exactly match the observed drawdown during the first pumping step. The calculations corresponding to storage coefficient values of 0.01 and 0.1 are shown in Figure B-8.2-3.

As shown in the figure, the predicted drawdown after 440 min of pumping at the prescribed step rates was less than 3 ft, compared with the actual drawdown of nearly 9 ft. This was another strong indication that the actual drawdown was affected by severe aquifer boundaries. (Note that the use of lower-bound transmissivity values did not limit this conclusion. For higher transmissivity values, and corresponding reduced well inefficiency, the computed drawdown values would be even less than those shown.)

Thus, the step-drawdown test provided ample evidence of a severely laterally limited saturated zone, consistent with conclusions drawn from examination of the pumping and recovery hydrograph discussed previously.

B-8.3 Well CdV-16-4ip Screen 1 10-d Test

At 8:00 a.m. on February 26, the 10-d pumping test was initiated at a discharge rate of 11.8 gpm. Over time, as the drawdown in the well increased substantially, the discharge rate declined gradually because of the increased pumping lift. By March 5 (the eighth day of pumping), the rate had declined to 10.7 gpm. Because of concerns of drawing the pumping water level to the pump intake (causing cavitation), on March 5 the discharge rate was cut back to 7.9 gpm at 3:40 p.m. and then to 7.33 gpm at 3:50 p.m., where it remained for the balance of the pumping test. Figure B-8.3-1 shows a summary of the pumping rates measured during the test.

The pump was shut off at 6:00 a.m. on March 8, and recovery data were collected until 7:08 a.m. Mountain Daylight Time (6:08 a.m. Mountain Standard Time) on March 20 when the pump was pulled from the well.

Figure B-8.3-2 shows a semilog plot of the drawdown data recorded during the screen 1 10-d test. The earliest data likely best represent formation properties while the subsequent data show continuous slope increase, consistent with dewatering a limited saturated zone. The lone exception to this was the inflection point corresponding to a probable increase in specific yield (storage coefficient) at depth.

Figure B-8.3-3 shows late data from the screen 1 test. It is evident that the rate of water-level descent increased dramatically before the discharge rate was cut back, signaling that most of the saturated thickness of permeable sediments had been dewatered, and the lower 15 ft of screen was installed in a relatively nonproductive zone.

Figure B-8.3-4 shows an analysis of the earliest data from the test. The casing and filter pack storage times are shown on the graph for reference. Calculations made from the line of fit shown on the graph included a transmissivity of 4060 gpd/ft and a storage coefficient of 0.35 for the sediments penetrated by the cone of depression up to that point. The anomalously large storage coefficient implied that even the earliest data were affected by the formation boundary. This is because an artificially steep slope (caused by the negative boundary) leads to an overestimate of storage coefficient when standard equations are applied to the data. Boundary effects also cause the transmissivity value to be underestimated because the transmissivity value is computed inversely as a function of the slope of the line of fit. These conditions indicate the actual transmissivity was greater than 4060 gpd/ft.

Figure B-8.3-5 shows an analysis of the earliest data from the first step of the step-drawdown test that was conducted before the 10-d test. As shown on the graph, the analysis yielded apparent values of 3480 gpd/ft for the transmissivity and 0.66 for the storage coefficient of the sediments penetrated by the cone of depression up to that point. Again, the anomalously large storage coefficient confirmed that boundary effects were present almost immediately in the pumping data sets from screen 1. As before, this indicated that the apparent transmissivity value was an underestimate and that the true value was in excess of 3480 gpd/ft.

Figure B-8.3-6 shows an analysis of the drawdown data observed in R-25 screen 2 during the step-drawdown and 10-d tests. The R-25 screen 2 water-level data have been corrected for Earth tides and partially corrected for barometric pressure effects (Figure B-7.0-7). A modification was made to the pumping rates in the analysis shown. The R-25 screen 2 plot showed a flattening response at around 3000 min, corresponding to the inflection point observed in the screen 1 hydrograph that may have resulted from a change in storage coefficient. Furthermore, after 10,000 min, when the discharge rate was cut back to 7.33 gpm, the data appeared to show a response. This led to the conclusion that the response at R-25 screen 2 was tied to pumping changes in the perched zone and was independent of the possible recharge source providing the steady rate of 4.83 gpm. Because of this, it was conjectured that the R-25 screen 2 response was a function of the net withdrawal from the perched zone, i.e., the

difference between the pumping rates and the independent recharge rate of 4.83 gpm. This conjecture is uncertain because of the small water-level changes involved and the uncertain barometric pressure corrections.

The step-drawdown test averaged a discharge rate of 12.2 gpm, which is a net withdrawal rate about 7.4 gpm greater than the hypothesized recharge rate. The first 7-plus days of the 10-d test averaged around 11.2 gpm, about 6.4 gpm greater than the hypothesized recharge rate. Finally, after the pumping rate was cut back during the 10-d test, the pumping still averaged 2.5 gpm more than the hypothesized recharge rate. Thus, the R-25 screen 2 data were analyzed as though the respective pumping rates were 7.4, 6.4, and 2.5 gpm.

The analysis shown in Figure B-8.3-6 compares the data to a theoretical type curve based on these discharge rates. The computed hydraulic parameter values appear reasonable although their reliability may be questionable because the applied theory did not account for boundary conditions known to exist.

The comparison was revealing, however, in that the actual data showed a muted response compared with the type curve. For example, during the shutdown period between the step-drawdown test and the 10-d test, the type curve suggested that the water levels in R-25 screen 2 should reverse, showing recovery before trending downward again. Instead, the actual response was muted, showing a slight water-level flattening but no reversal. Likewise, when the discharge rate was cut back to 7.33 gpm, the data showed a small effect, whereas the type curve predicted a more significant reduction in drawdown. This suggested a diffuse, indirect connection between the pumped zone and R-25 screen 2.

Figure B-8.3-7 shows the recovery data recorded following shutdown of the screen 1 pumping test. The bulk of the recovery response simply reflected the resaturation of dewatered sediments at a nearly constant recharge rate (roughly 4.83 gpm), initially through a depth interval having a large specific yield (storage coefficient) and later through shallower depths where the specific yield was smaller.

Once the residual drawdown was less than 10 ft, the recovery rate was lower, yielding a calculated transmissivity of 140 gpd/ft. The transmissivity value determined from the late-time recovery analysis can be thought of as an "effective" value for the area-wide sediments. The sediments that compose the perched aquifer likely have variable permeability and zones of saturation, with good permeability and saturation in some directions and poor flow characteristics in other directions.

Several analyses (time-drawdown analyses from the step-drawdown and 10-d tests and specific capacity analysis) implied a minimum transmissivity for the screen 1 zone ranging from about 4000 to 7000 gpd/ft. Given the estimated transmissivity of the pumped perched zone compared with that of surrounding sediments from Figure B-8.3-7, the flow regime appears to consist of a thick, highly permeable saturated zone of severely limited areal extent with indirect/muted hydraulic connection to surrounding saturated materials.

As a final illustration, Figure B-8.3-8 compares the drawdown change and recovery magnitude as a function of pumping/recovery time. Theoretically, these curves should coincide at early and middle times, diverging slightly at late times. It is apparent that the curves are very different. This further reinforces the idea that the bulk of the data do not necessarily reflect aquifer permeability or support aquifer property calculation, but rather are an artifact of simply draining and refilling the perched zone.

B-9.0 WELL CDV-16-4IP SCREEN 2 DATA ANALYSIS

This section presents the data obtained from the CdV-16-4ip screen 2 pumping tests and the results of the analytical interpretations. Data are presented for the step-drawdown and 10-d tests.

B-9.1 Well CdV-16-4ip Screen 2 Test Description

Screen 2 was tested from March 20 to April 20, 2011. After setting the pump and filling the drop pipe on March 20, a step-drawdown test was conducted on March 21. Following recovery overnight, the 10-d test was begun on March 22 and followed by recovery data collection from April 1 to 20.

Step-drawdown testing began at 7:30 a.m. on March 21 at an initial discharge rate of 2.2 gpm. The rate was increased every 60 min at increments of around 2 to 3 gpm. When the rate reached 13.7 gpm, the pumping water level reached the pump intake, causing cavitation, so the test was terminated at that time. About that same time, the water produced from the well became turbid with a colloidal-appearing content, having the color of bentonite grout material. It appeared as though the borehole was unstable and that subsurface material sediments or seals may have moved suddenly.

At 12:00 p.m. on March 22, the 10-d pumping test was initiated at a discharge rate of 5 gpm. Over time, the rate remained fairly steady, ranging from about 4.9 gpm to a little more than 5.1 gpm.

The pump was shut off at 12:00 p.m. on April 1, and recovery data were collected until 7:40 a.m. on April 20 when brief pumping was performed in an attempt to collect water samples for radon analysis.

B-9.2 Well CdV-16-4ip Screen 2 Step-Drawdown Test

Figure B-9.2-1 shows a plot of the discharge rates applied during the step-drawdown test along with the resulting drawdown observed in screen 2. The locations of the top and bottom of the well screen as well as the pump intake are shown in the figure for reference.

Remarkably, the specific capacity remained essentially constant through all pumping steps but the last one, even though the well screen was progressively dewatered by a greater amount with each increase in pumping rate. This was because the screen was sealed well enough to remain saturated even under vacuum conditions. The presence of a vacuum was confirmed by observing the lowest measured head, which was 17 ft below the pump intake.

During the last step, when the discharge rate was increased from 11.56 gpm to 13.26 gpm, it appeared that the vacuum seal was “broken” because the drawdown increased disproportionately compared with the increase in pumping rate. Soon thereafter, the specific capacity continued to decline as evidenced by the discharge rate declining more rapidly than the drawdown. For example, during the final minutes of the test, the discharge rate declined 22.3% from its peak value while the drawdown declined only 7.6%.

The step-drawdown test showed that the flow remained laminar at nearly all pumping rates. Further, it showed that the perched aquifer screened zone remained sealed from atmospheric pressure for most pumping rates, although the seal eventually broke, allowing entry of air into the pumped zone. This reaction was accompanied by release of fines into the well as evidenced by the sudden clay content of the water, which was noted in the discharge at the end of the step-drawdown test.

B-9.3 Well CdV-16-4ip Screen 2 10-d Test

Figure B-9.3-1 shows a plot of the discharge rates applicable to the screen 2 10-d pumping test. The discharge rate remained near 5.0 gpm for the duration of the pumping test.

Figure B-9.3-2 shows a semilog plot of the corrected drawdown data collected from the 10-d constant-rate pumping test. The estimated casing-storage times are shown on the graph for reference. (The calculation of casing-storage time was based on the assumption of complete drainage of the casing, screen, and filter pack. If a partial vacuum persisted in the well, these calculations would be

overestimates [conservative].) A minor amount of dewatering of the well screen occurred late in the test, so that a small component of the drawdown was corrected for the effects of dewatering using Equation B-13.

At first glance, the data trace appeared to reflect classical unconfined aquifer response showing delayed yield. The early and late slopes produced about the same transmissivity (400 gpd/ft), while the intermediate data showed a flatter slope. However, as described below, the recovery data contradicted this interpretation. Clearly, the intermediate data and the initial portion of the late data segment showed erratic drawdown response. It is possible that the instability of the annular fill materials in the pumped zone contributed to the variation in observed water levels, affecting much of the data set.

Figure B-9.3-3 shows the recovery data collected following shutdown of the 10-d pumping test. The transmissivity estimated from the early data was 660 gpd/ft, making the computed hydraulic conductivity 15.2 gpd/ft², or 2.0 ft/d. The subsequent data showed a slope increase and a calculated transmissivity of 300 gpd/ft, similar to that obtained from the late drawdown data, and about half the early-time value.

The steepening of the recovery curve after a little more than an hour of recovery could have a couple of causes. It might show a reduction in the transmissivity of the sediments at a distance from the pumped well. Alternatively, it might signal the presence of a hydraulic boundary. The nearly 2:1 ratio of computed transmissivity values can be an indication of an approximately linear boundary near the pumped well, with the aquifer extent limited in that direction, but far reaching in the opposite direction. Either interpretation suggests an areally extensive saturated perched zone at screen 2. However, nearby observation wells were monitored during the 10-d test, including R-25 screen 4, which is at a similar elevation to the lower screen at CdV-16-4ip and 430 ft away. No apparent response to pumping the lower screen at CdV-16-4ip was observed in any of the surrounding wells or screens.

The late data on Figure B-9.3-3 suggested the possibility of additional formation inhomogeneities, including an area of increased transmissivity at a great distance from the pumped well. Alternatively, this type of response could be because of hysteretic effects associated with temporal storage coefficient changes during refilling of the formation pore spaces and movement of the capillary zone. Finally, it is possible that it is a delayed response to large barometric pressure fluctuations that occurred from April 9 to 11.

Figure B-9.3-4 shows a comparison of drawdown and recovery versus elapsed time for the screen 2 pumping test. Ideally, these curves should coincide at early and middle times, diverging only at late times. However, the two curves do not match very well. The drawdown curve showed the steep, flat, and steep sequence of slopes discussed earlier, whereas the recovery curve showed an essentially opposite trend, with an early flat slope, a steeper intermediate slope, and a flat final slope. As discussed previously, possible reasons for this included instability in the sediments and backfill materials at screen 2 contributing to erratic response during the pumping portion of the test and hysteretic effects influencing the late recovery data.

B-9.4 Well CdV-16-4ip Screen 2 Specific Capacity Data

Specific capacity data were used along with well geometry to estimate a lower-bound hydraulic conductivity value for the permeable zone penetrated by CdV-16-4ip screen 2. This was done to provide a frame of reference for evaluating the foregoing analyses. Two sets of computations were made—one set for the drawdown observed at the end of the pumping test and another for the early recovery response before the boundary/inhomogeneity effect. The former calculations identified an overall lower-bound transmissivity, while the latter ones determined a lower-bound transmissivity for the zone near the well.

At the end of 14,400 min of pumping, the discharge rate was 5.0 gpm with a resulting drawdown of 19.8 ft and a dewatering-corrected drawdown of 18.8 ft. This resulted in an actual specific capacity of 0.253 gpm/ft and a corrected specific capacity of 0.266 gpm/ft. In addition to corrected specific capacity and pumping time, other input values used in the calculations included a borehole radius of 0.51 ft (inferred from the volume of the filter pack required to backfill the screened zone), a screen length of 31.1 ft, and a saturated thickness of 43.3 ft.

Applying the Brons and Marting method to these inputs for a range of storage coefficient values yielded the lower-bound transmissivity estimates shown by the lower curve in Figure B-9.4-1—averaging a little more than 400 gpd/ft. This was consistent with the combination of the near-well transmissivity of 660 gpd/ft and distant transmissivity values of 300 to 400 ft determined from the test data.

During recovery, the corrected residual drawdown declined from 18.8 ft to about 10.0 ft (a recovery distance of 8.8 ft) after 80 min ($t/t' = 180$). Applying the Brons and Marting method to these inputs for a range of storage coefficient values yielded the lower-bound transmissivity estimates shown by the upper curve in Figure B-9.4-1—averaging around 600 gpd/ft. This was reasonably consistent with the pumping test value of 660 gpd/ft.

The close correspondence between the lower-bound transmissivity values and those determined from the pumping test data suggested a fairly high well efficiency for screen 2.

B-10.0 SUMMARY

Constant-rate pumping tests were conducted on CdV-16-4ip screens 1 and 2. The tests were performed to gain an understanding of the hydraulic characteristics of the screened zones and the degree of interconnection between them. Numerous observations and conclusions were drawn from the tests as summarized below.

The static water level observed in screen 1 was substantially higher (281 ft) than that in screen 2, showing a strong downward hydraulic gradient, highly resistive sediments separating the screened zones, and little hydraulic connection between the screens. Testing confirmed this, showing no drawdown in either zone because of pumping the other.

A comparison of barometric pressure and CdV-16-4ip water-level data showed a high barometric efficiency for both zones.

Screen 1

The 69-ft-thick saturated perched zone at screen 1 is highly permeable, with lower-bound transmissivity values ranging from about 4000 to 7000 gpd/ft. With extended pumping, however, drawdown increased dramatically. This corresponded to a lower-bound hydraulic conductivity on the order of 100 gpd/ft², or 13 ft/d.

The nearly immediate onset of boundary effects before the cessation of casing storage precluded determining the true formation transmissivity.

CdV-16-4ip screen 1 was pumped at 4.1 gpm for 20 min, resulting in a drawdown of 0.64 ft for a short-term specific capacity of 6.41 gpm/ft.

The perched zone is severely limited in lateral extent. The brief (440-min) step-drawdown test showed pronounced boundary effects. The 10-d test, at discharge rates ranging from 11.8 to 7.33 gpm, effectively dewatered the bulk of the perched interval in the immediate vicinity of the pumped well.

The perched zone appeared to be recharged at a rate of about 4.8 gpm from laterally adjacent sediments during the 10-d pumping period and much of the recovery period. This probably represents the maximum sustainable yield that could realistically be obtained from screen 1 over time. The actual long-term yield might be less, as a function of overall recharge rates to the perched zone and adjacent hydraulically connected sediments.

The pumping test showed that screen 1 is installed in a moderate-transmissivity, but laterally limited, pocket of material within lower-transmissivity surrounding material. Late-time recovery data suggested an area-wide transmissivity of about 130 gpd/ft using the standard infinite-aquifer model. The actual makeup of contributing water bearing sediment might be very different, possibly consisting of a complex matrix of indirectly hydraulically connected zones, possibly associated with local faults or fractures.

Water levels were monitored in several wells during the screen 1 pumping test. Only R-25 screen 2 (430.4 ft away) showed a response to pumping. The hydraulic response at R-25 screen 2 was muted or "sluggish" compared with what would be expected theoretically, suggesting a somewhat indirect hydraulic connection between CdV-16-4ip screen 1 and R-25 screen 2. The total drawdown observed in R-25 screen 2 was 0.4 ft.

Screen 2

The 43.3-ft-thick perched zone at screen 2 showed good permeability. The transmissivity in the vicinity was calculated at 660 gpd/ft, with an average hydraulic conductivity of 15.2 gpd/ft², or 2.0 ft/d.

At the end of 14,400 min of pumping, the discharge rate was 5.0 gpm with a resulting drawdown of 19.8 ft and a corrected drawdown of 18.8 ft. This resulted in an actual specific capacity of 0.253 gpd/ft and a corrected specific capacity of 0.266 gpm/ft.

Later data suggested either a reduction (approximately half) in transmissivity at distance from the pumped well or perhaps a formation boundary having the same effect on the data.

Late-time data suggested an areally extensive perched zone, very different from that observed at screen 1.

Lower-bound transmissivity values estimated from both late pumping data and early recovery data were consistent with values determined from the pumping test and suggested a fairly high well efficiency.

Water levels were monitored in several wells during the screen 2 pumping test. None of the monitored zones showed any response to pumping.

Bentonite was recovered on the screen 2 transducer during the screen 1 pumping test. Also, water pumped from screen 2 during the step-drawdown test appeared to contain bentonite near the end of the pumping period, coinciding with a distinct reduction in screen 2 yield. It is possible that the water-hammer effect associated with packer deflation that exposed the screen 2 zone to screen 1 water levels (about 290 ft higher) may have compromised the annular seal above screen 2.

The hydraulic stress caused by deflating the packer following the screen 2 pumping test dislodged the pressure transducer from the transducer cage in which it was housed.

B-11.0 REFERENCES

The following list includes all documents cited in this appendix. Parenthetical information following each reference provides the author(s), publication date, and ER ID. This information is also included in text citations. ER IDs are assigned by the Environmental Programs Directorate's Records Processing Facility (RPF) and are used to locate the document at the RPF and, where applicable, in the master reference set.

Copies of the master reference set are maintained at the NMED Hazardous Waste Bureau and the Directorate. The set was developed to ensure that the administrative authority has all material needed to review this document, and it is updated with every document submitted to the administrative authority. Documents previously submitted to the administrative authority are not included.

- Bevan, M.J., A.L. Endres, D.L. Rudolph, and G. Parkin, December 2005. "A Field Scale Study of Pumping-Induced Drainage and Recovery in an Unconfined Aquifer," *Journal of Hydrology*, Vol. 315, No. 1–4, pp. 52–70. (Bevan et al. 2005, 105186)
- Bradbury, K.R., and E.R. Rothschild, March-April 1985. "A Computerized Technique for Estimating the Hydraulic Conductivity of Aquifers from Specific Capacity Data," *Ground Water*, Vol. 23, No. 2, pp. 240-246. (Bradbury and Rothschild 1985, 098234)
- Brons, F., and V.E. Marting, 1961. "The Effect of Restricted Fluid Entry on Well Productivity," *Journal of Petroleum Technology*, Vol. 13, No. 2, pp. 172-174. (Brons and Marting 1961, 098235)
- Cooper, H.H., Jr., and C.E. Jacob, August 1946. "A Generalized Graphical Method for Evaluating Formation Constants and Summarizing Well-Field History," *American Geophysical Union Transactions*, Vol. 27, No. 4, pp. 526-534. (Cooper and Jacob 1946, 098236)
- Driscoll, F.G., 1986. Excerpted pages from *Groundwater and Wells*, 2nd Ed., Johnson Filtration Systems Inc., St. Paul, Minnesota. (Driscoll 1986, 104226)
- Hantush, M.S., July 1961. "Drawdown around a Partially Penetrating Well," *Journal of the Hydraulics Division, Proceedings of the American Society of Civil Engineers*, Vol. 87, No. HY 4, pp. 83-98. (Hantush 1961, 098237)
- Hantush, M.S., September 1961. "Aquifer Tests on Partially Penetrating Wells," *Journal of the Hydraulics Division, Proceedings of the American Society of Civil Engineers*, pp. 171–195. (Hantush 1961, 106003)
- Kruseman, G.P., N.A. de Ridder, and J.M. Verweij, 1991. Excerpted page from *Analysis and Evaluation of Pumping Test Data*, International Institute for Land Reclamation and Improvement, Netherlands. (Kruseman et al. 1991, 106681)
- Schafer, D.C., January-February 1978. "Casing Storage Can Affect Pumping Test Data," *The Johnson Drillers Journal*, pp. 1-6, Johnson Division, UOP, Inc., St. Paul, Minnesota. (Schafer 1978, 098240)
- Theis, C.V., 1934-1935. "The Relation Between the Lowering of the Piezometric Surface and the Rate and Duration of Discharge of a Well Using Ground-Water Storage," *American Geophysical Union Transactions*, Vol. 15-16, pp. 519-524. (Theis 1934-1935, 098241)
- Toll, N.J., and T.C. Rasmussen, January–February 2007. "Removal of Barometric Pressure Effects and Earth Tides from Observed Water Levels," *Ground Water*, Vol. 45, No. 1, pp. 101–105. (Toll and Rasmussen 2007, 104799)

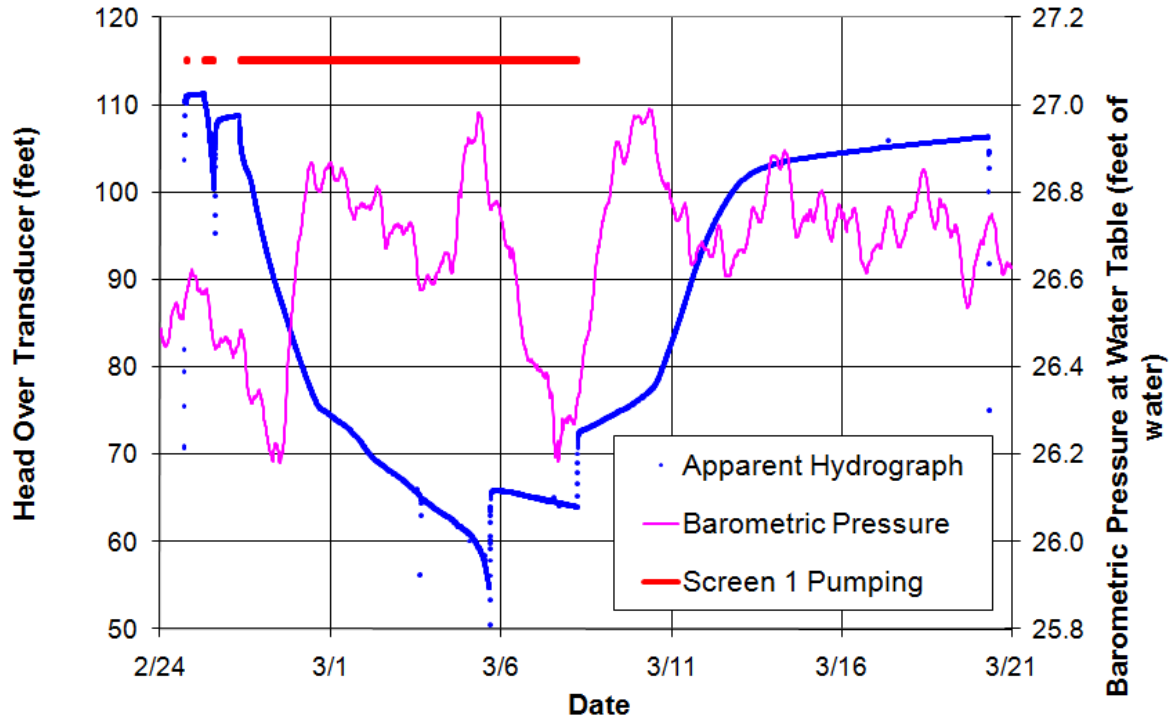


Figure B-7.0-1 Well CdV-16-4ip screen 1 apparent hydrograph

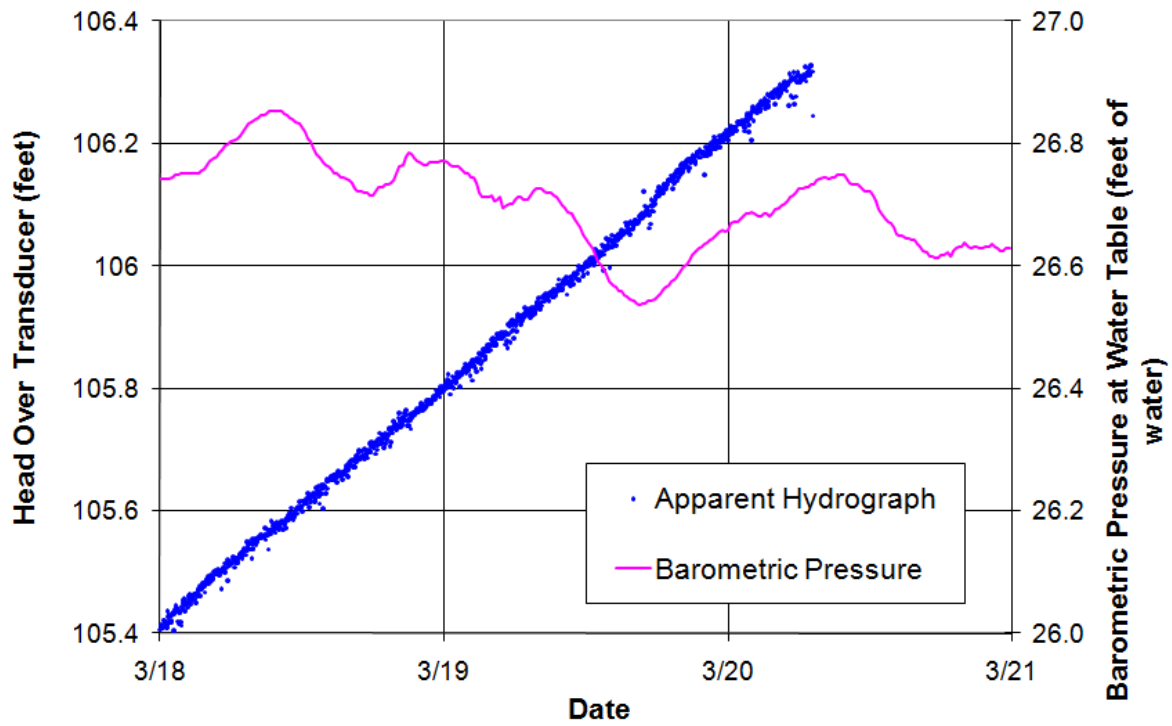


Figure B-7.0-2 Well CdV-16-4ip screen 1 apparent hydrograph—expanded scale

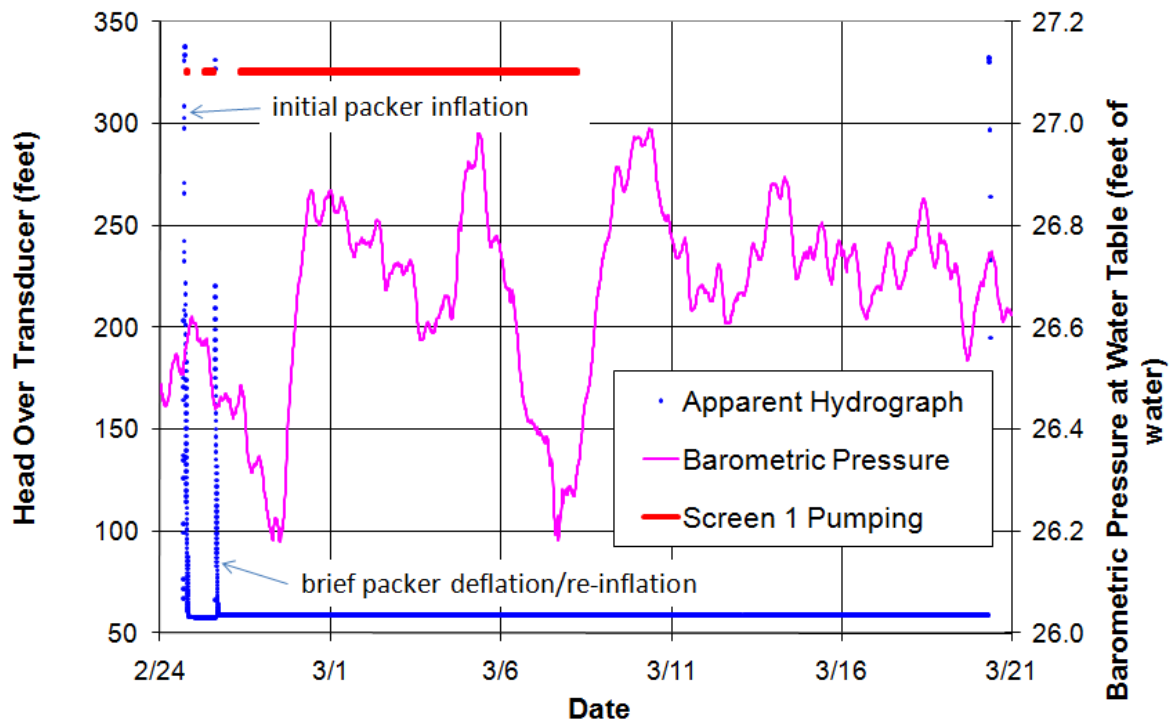


Figure B-7.0-3 Well CdV-16-4ip screen 2 apparent hydrograph during screen 1 pumping test

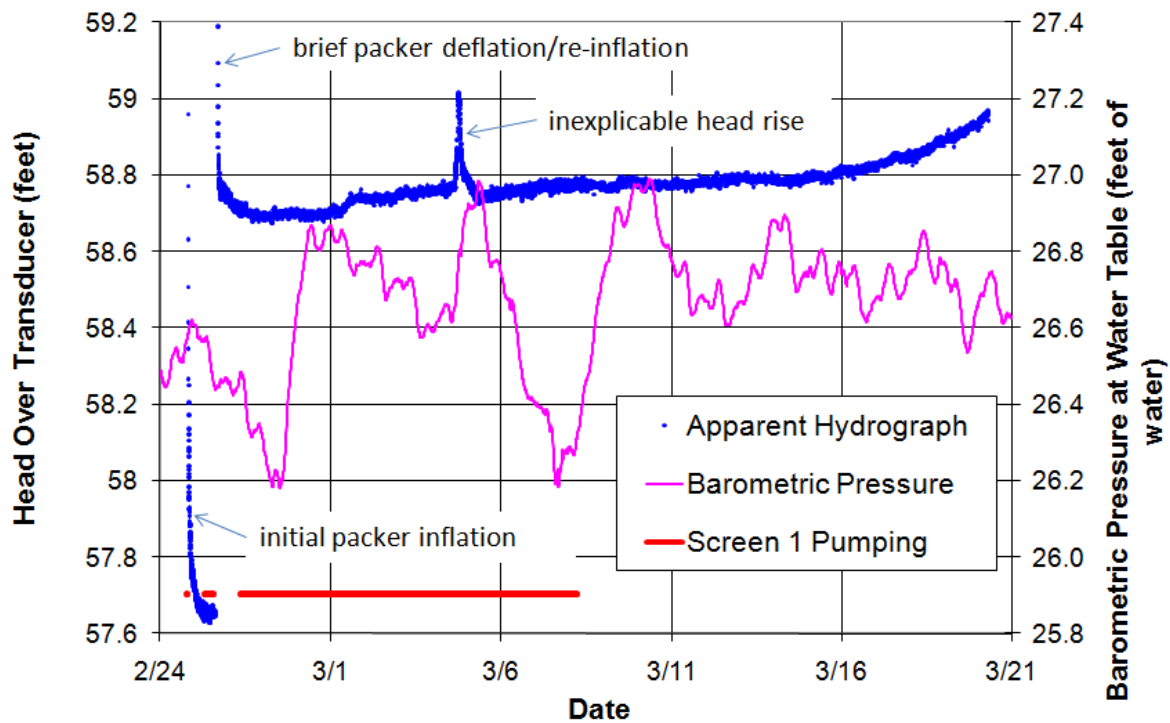


Figure B-7.0-4 Well CdV-16-4ip screen 2 apparent hydrograph during screen 1 pumping test—expanded scale

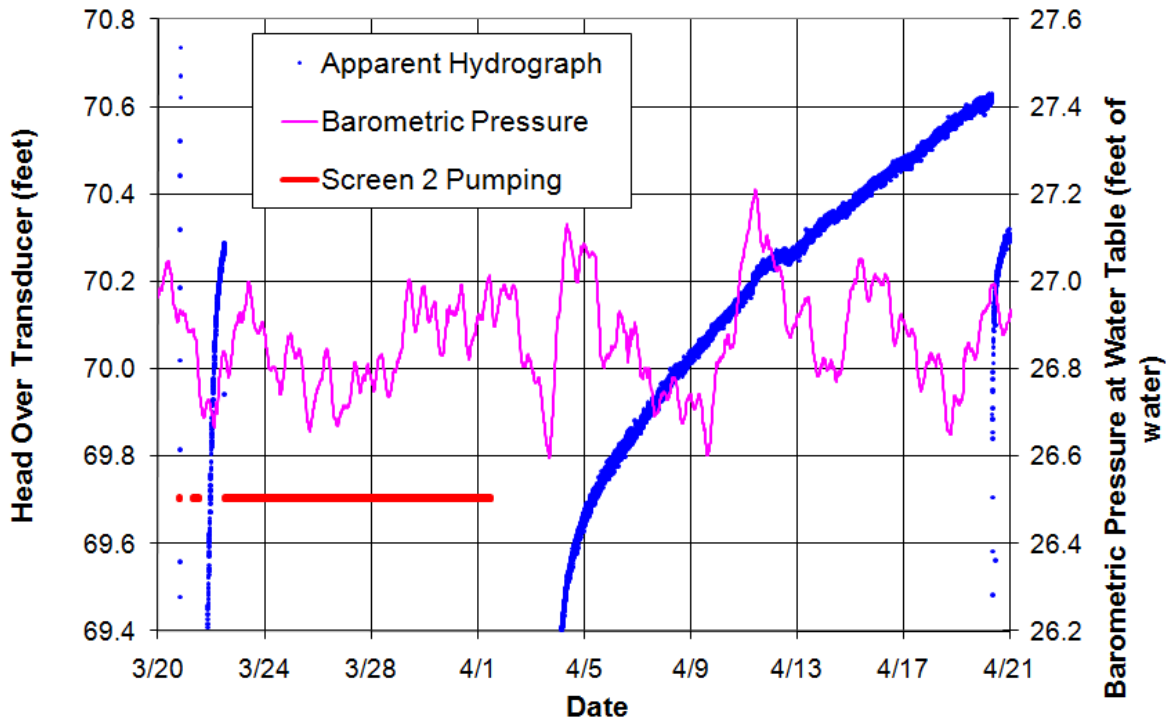


Figure B-7.0-5 Well CdV-16-4ip screen 2 apparent hydrograph

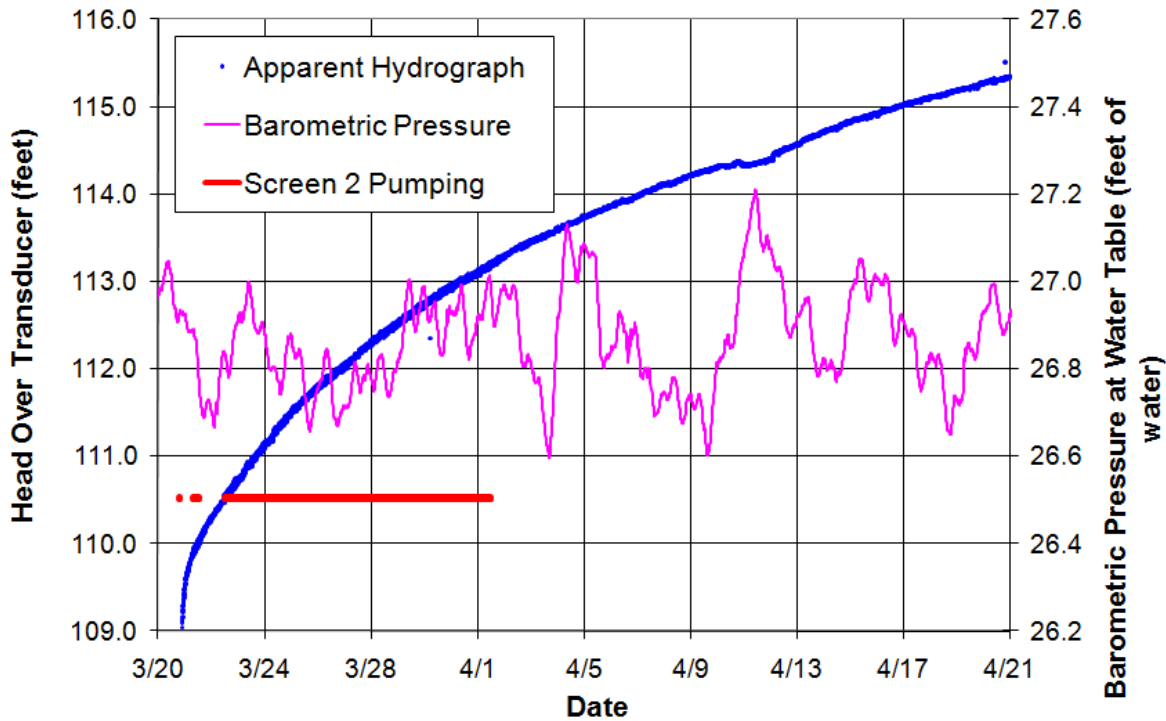


Figure B-7.0-6 Well CdV-16-4ip screen 1 apparent hydrograph during screen 2 pumping test

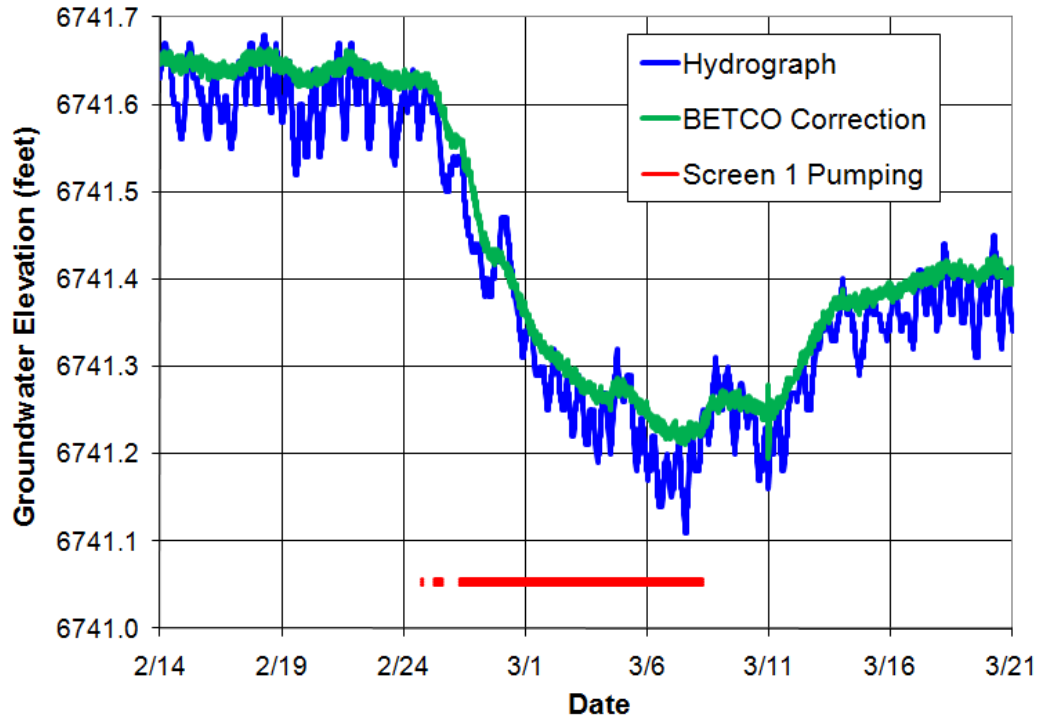


Figure B-7.0-7 Well R-25 screen 2 hydrograph during CdV-16-4ip screen 1 pumping test

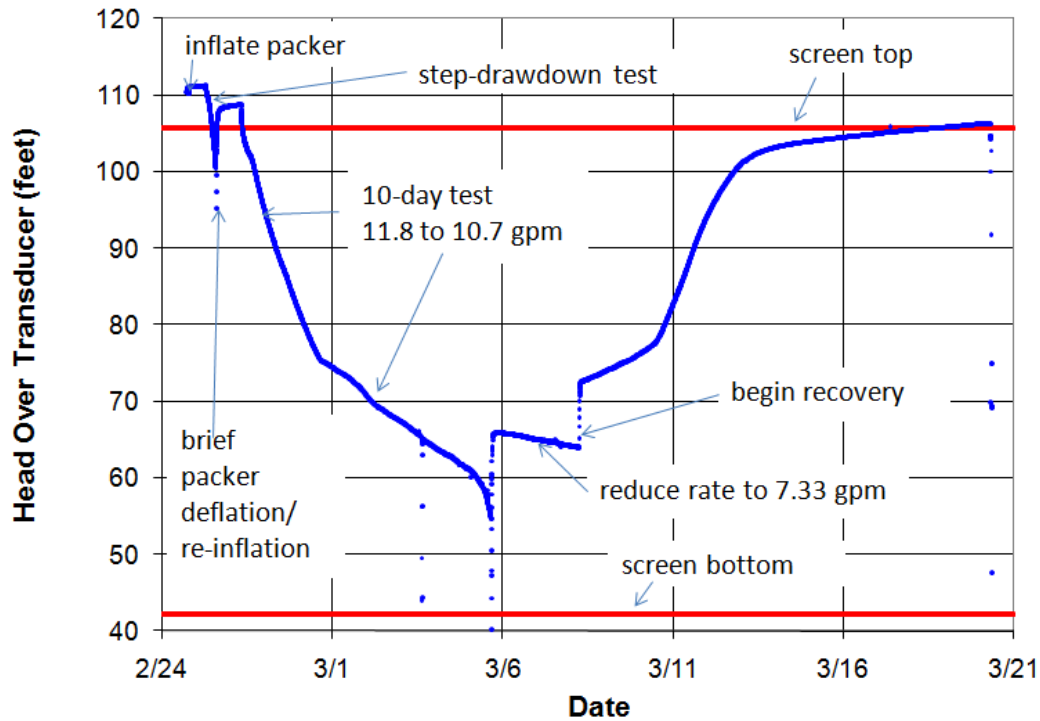


Figure B-8.1-1 Well CdV-16-4ip screen 1 summary of activities

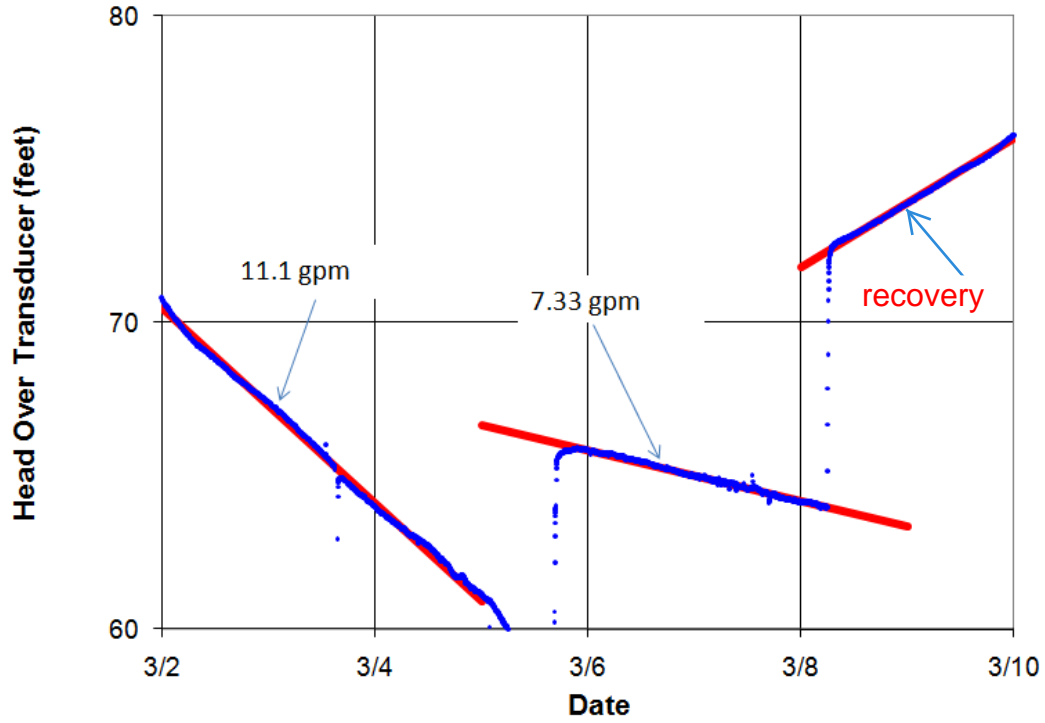


Figure B-8.1-2 Well CdV-16-4ip screen 1 drawdown and recovery linear trends

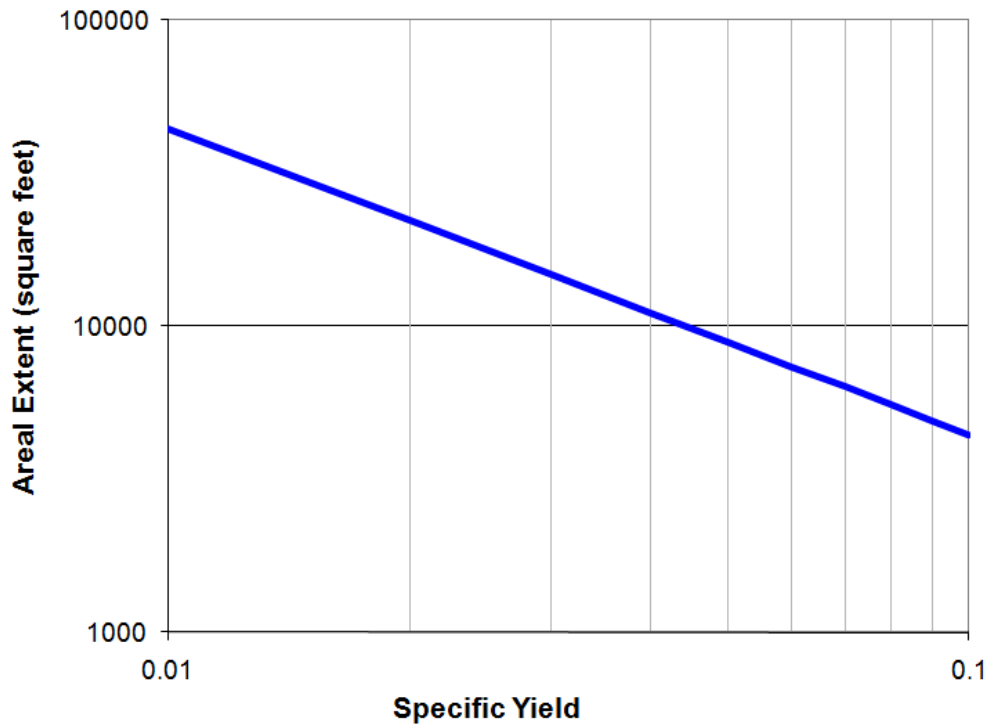


Figure B-8.1-3 Estimated areal extent of screen 1 perched zone

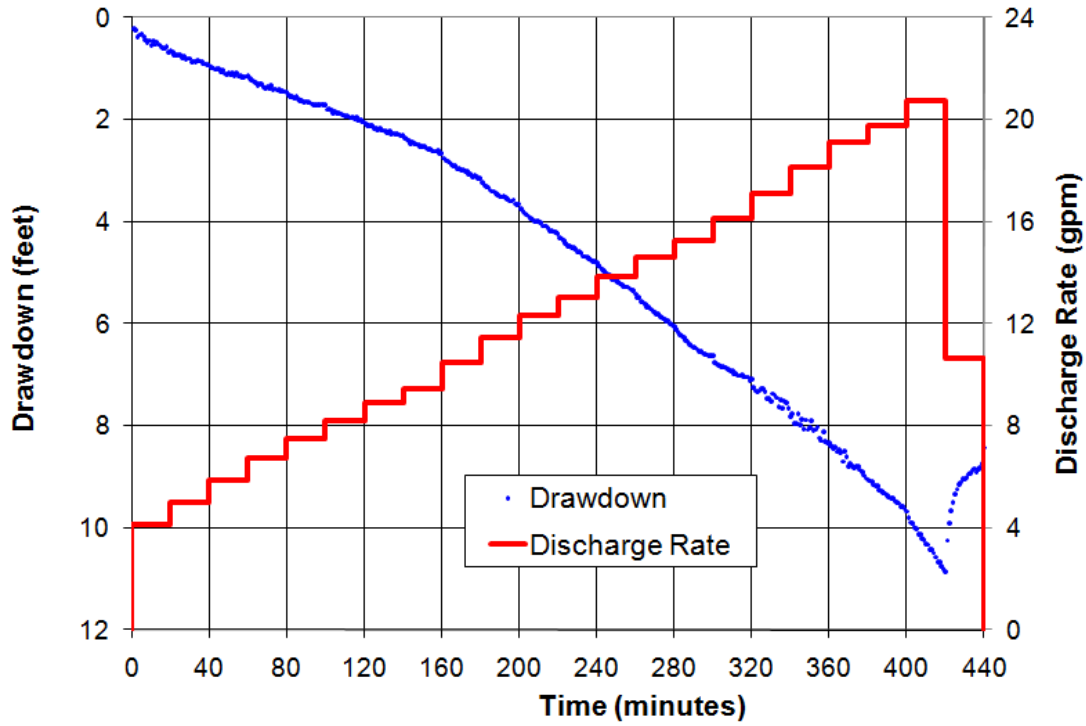


Figure B-8.2-1 Well CdV-16-4ip screen 1 step-drawdown test

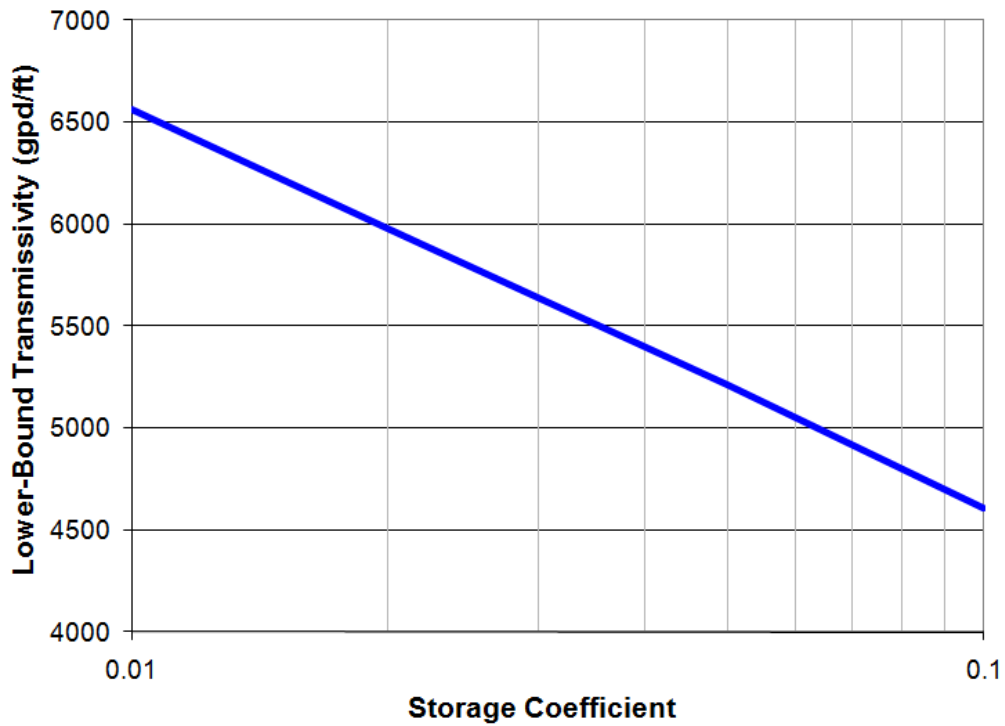


Figure B-8.2-2 Well CdV-16-4ip screen 1 lower-bound transmissivity

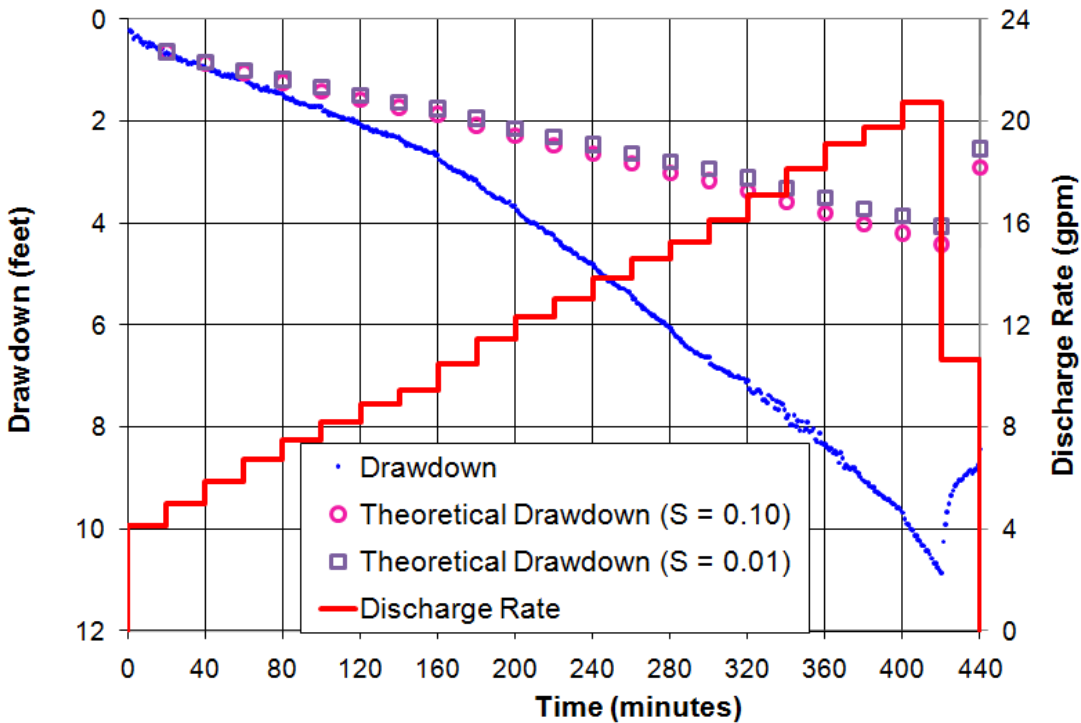


Figure B-8.2-3 Well CdV-16-4ip screen 1 theoretical drawdown

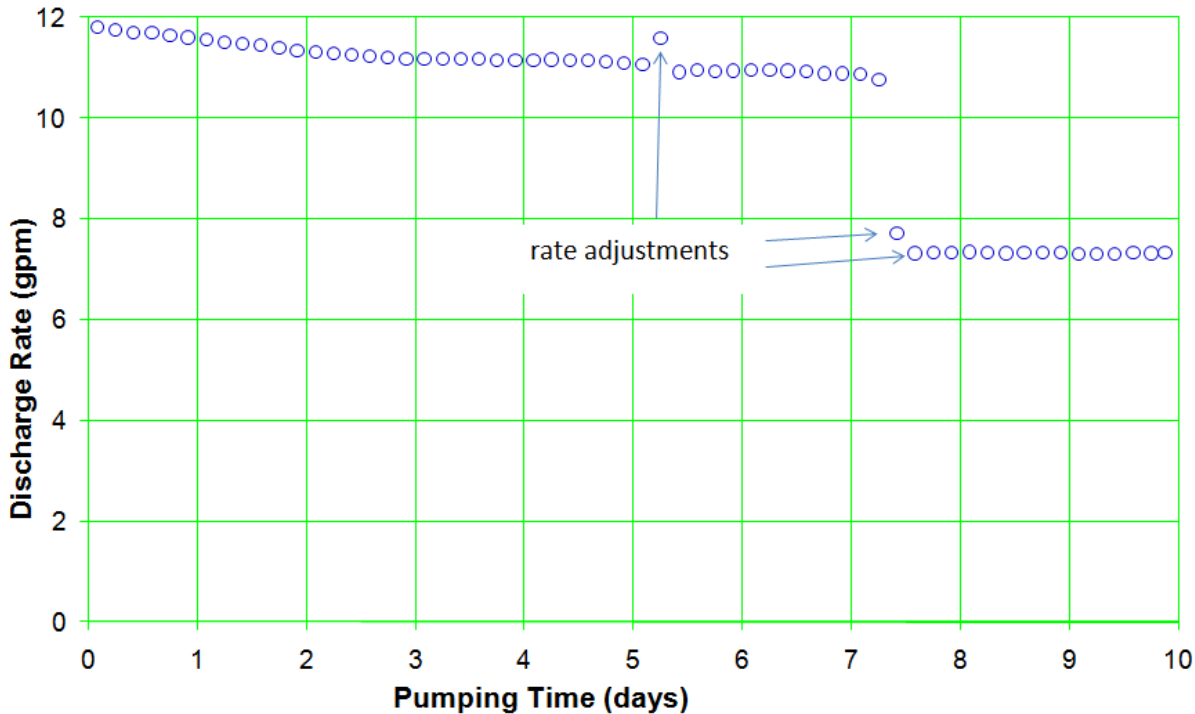


Figure B-8.3-1 Well CdV-16-4ip screen 1 pumping rates

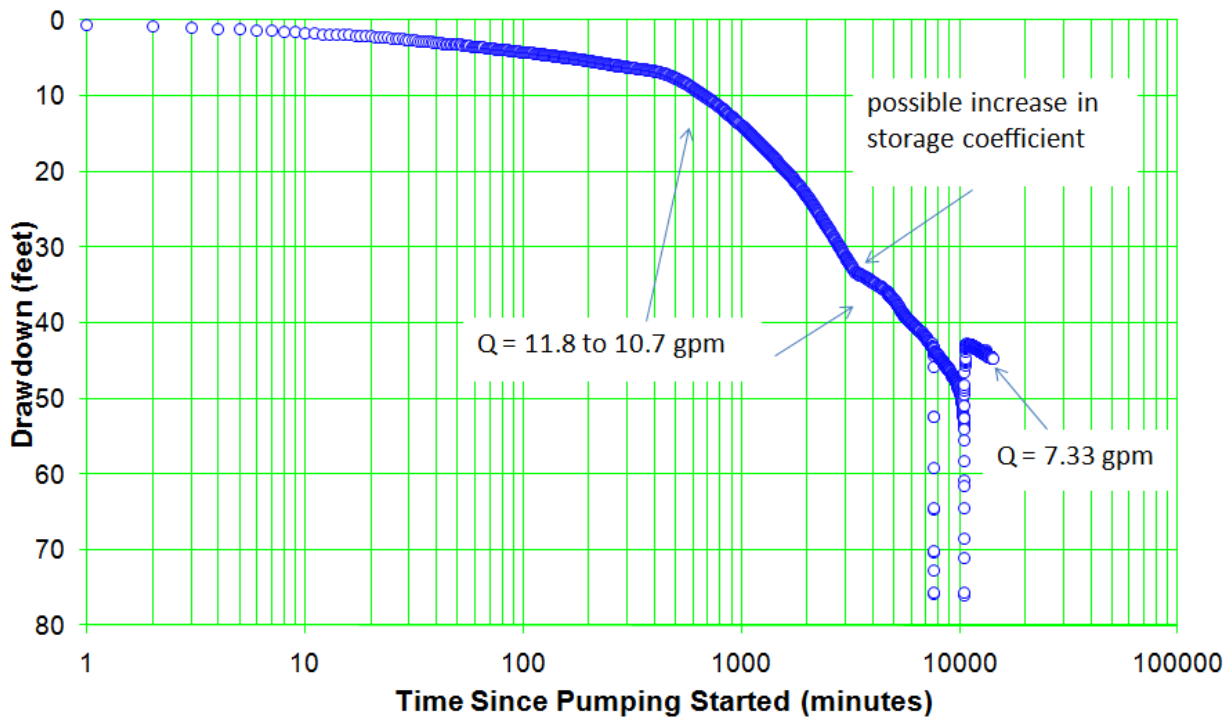


Figure B-8.3-2 Well CdV-16-4ip screen 1 drawdown

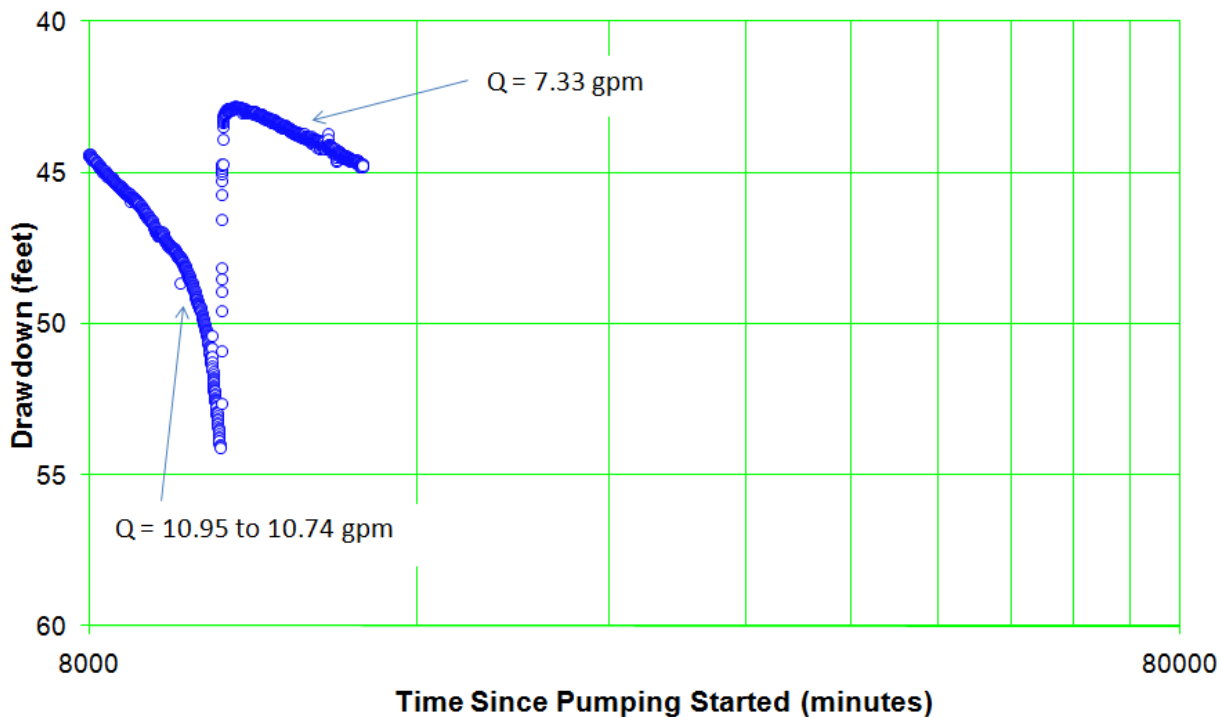


Figure B-8.3-3 Well CdV-16-4ip screen 1 late-time drawdown

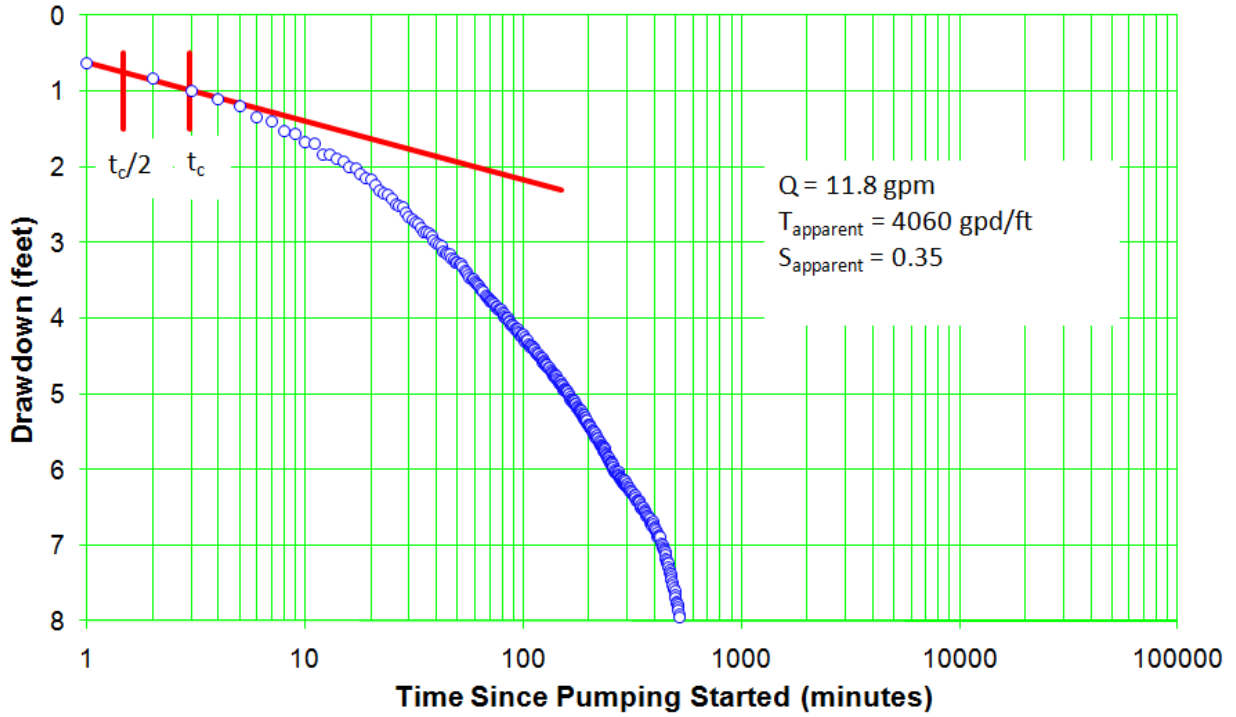


Figure B-8.3-4 Well CdV-16-4ip screen 1 early-time drawdown

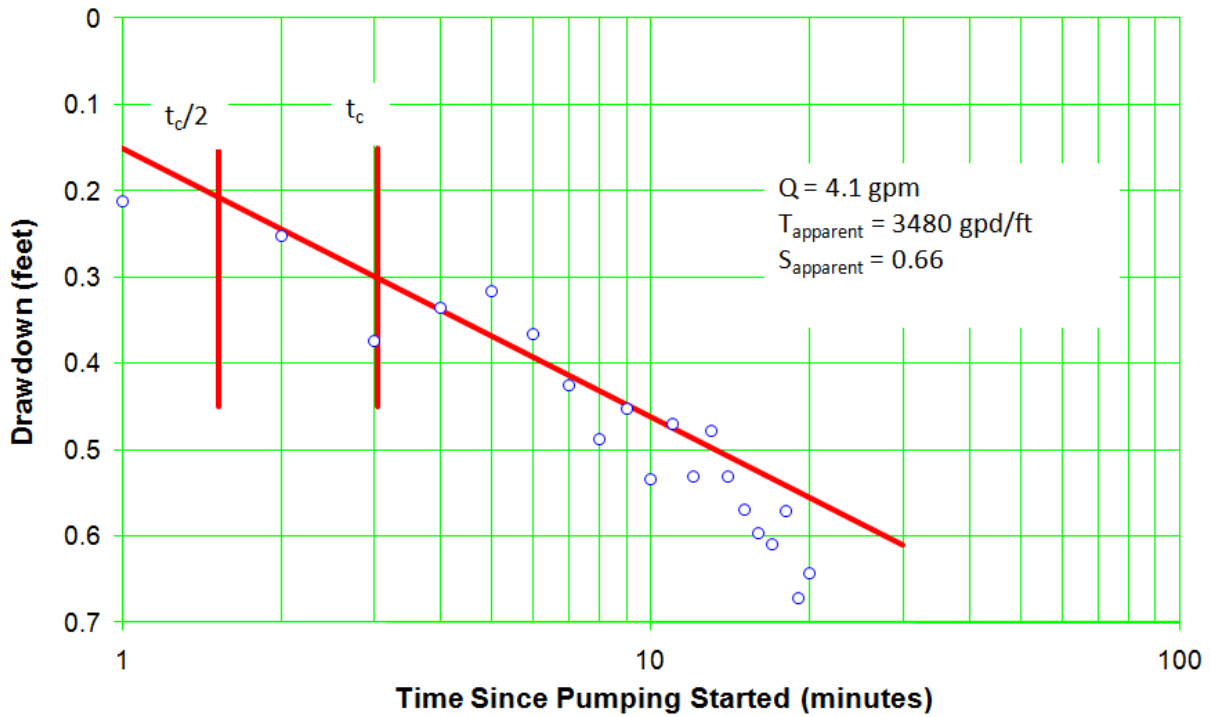


Figure B-8.3-5 Well CdV-16-4ip screen 1 step 1 drawdown

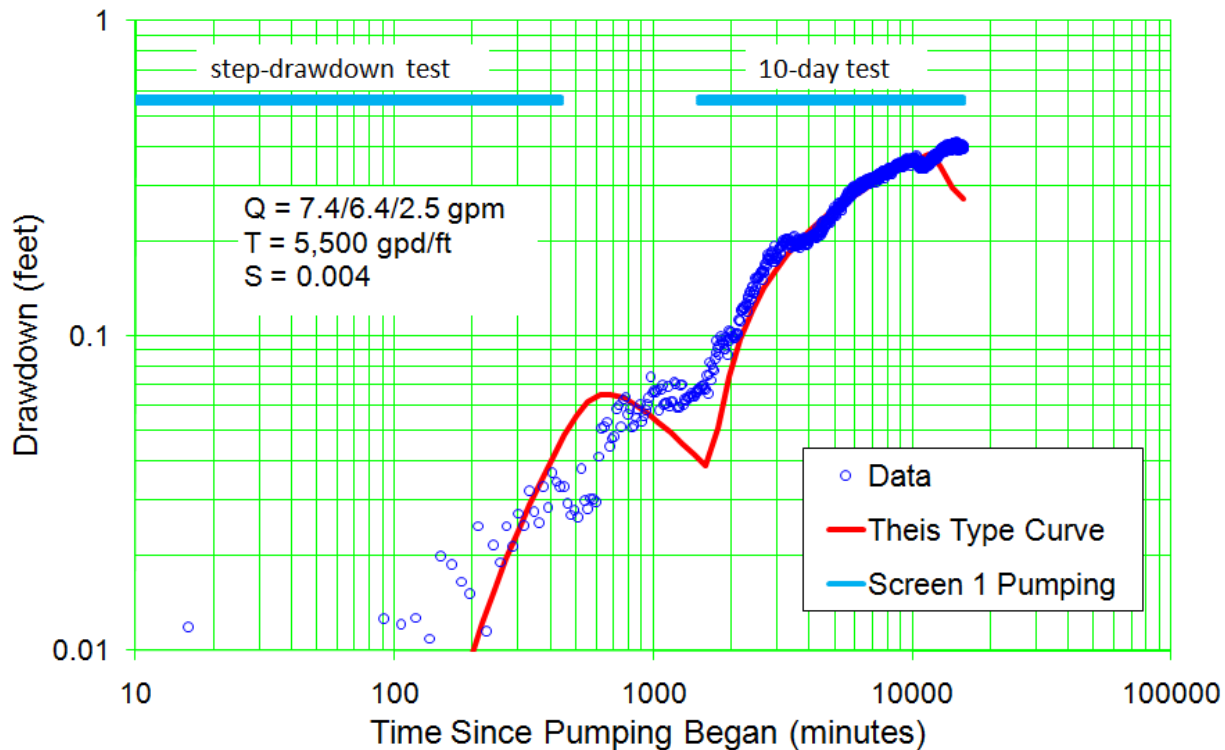


Figure B-8.3-6 Well R-25 screen 2 drawdown

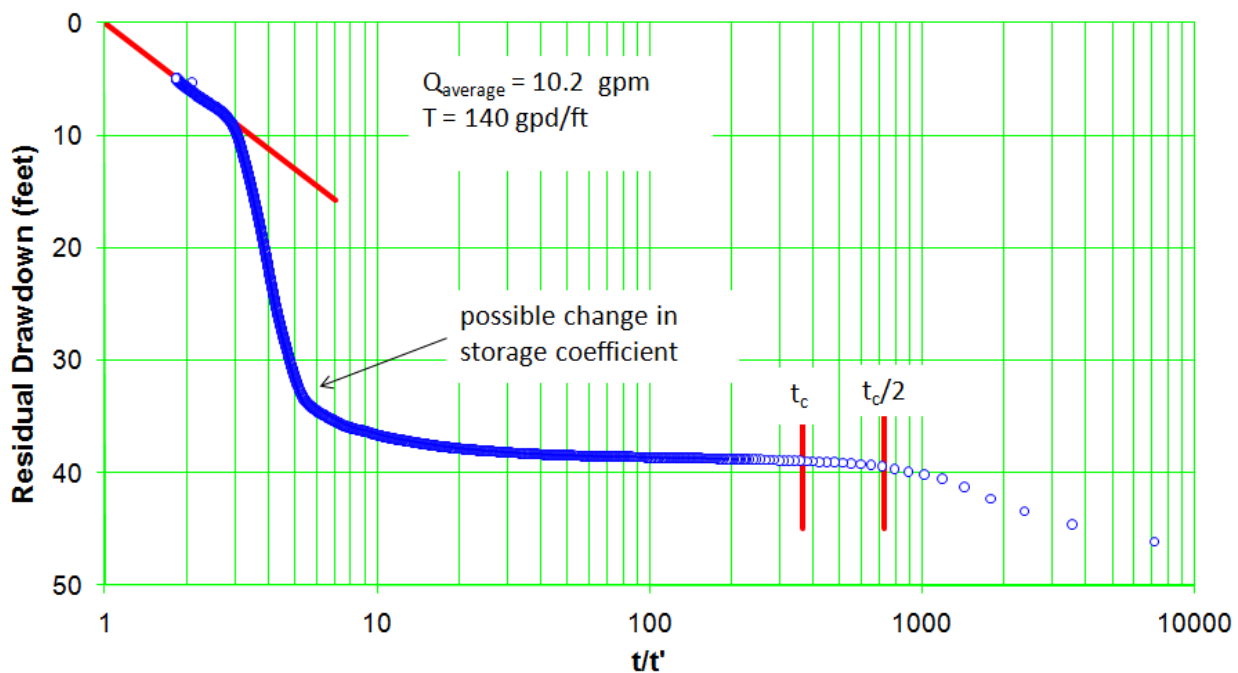


Figure B-8.3-7 Well CdV-16-4ip screen 1 recovery

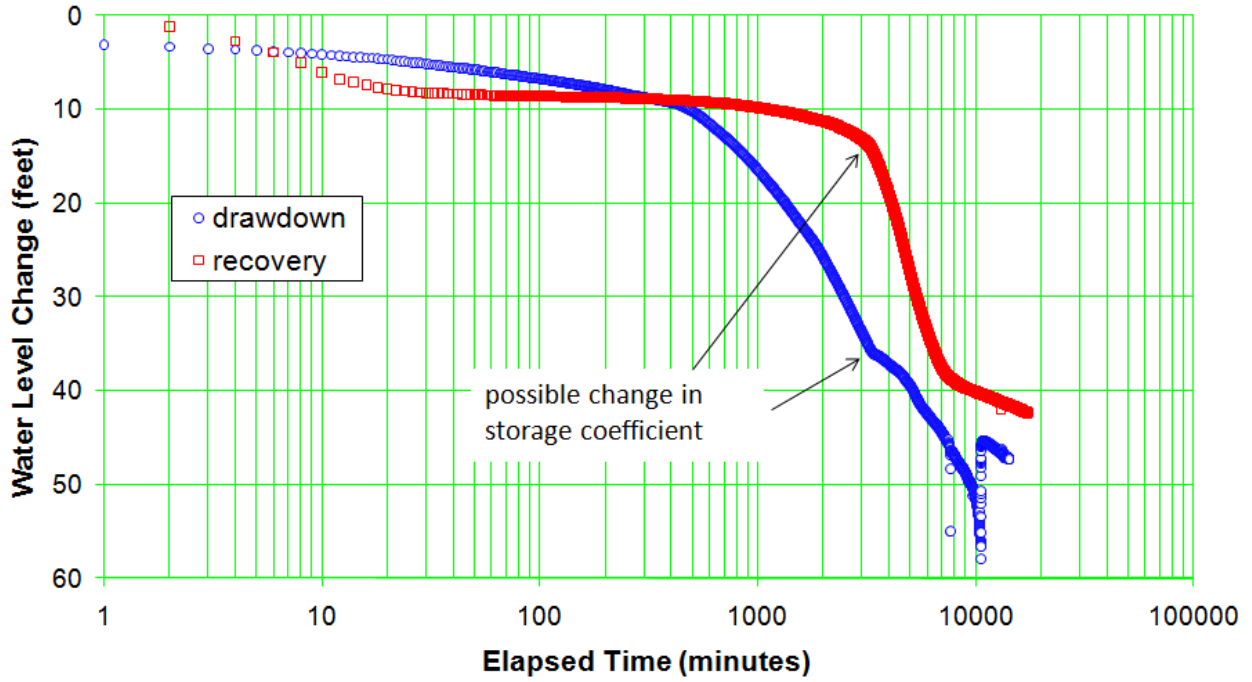


Figure B-8.3-8 Well CdV-16-4ip screen 1 drawdown and recovery comparison

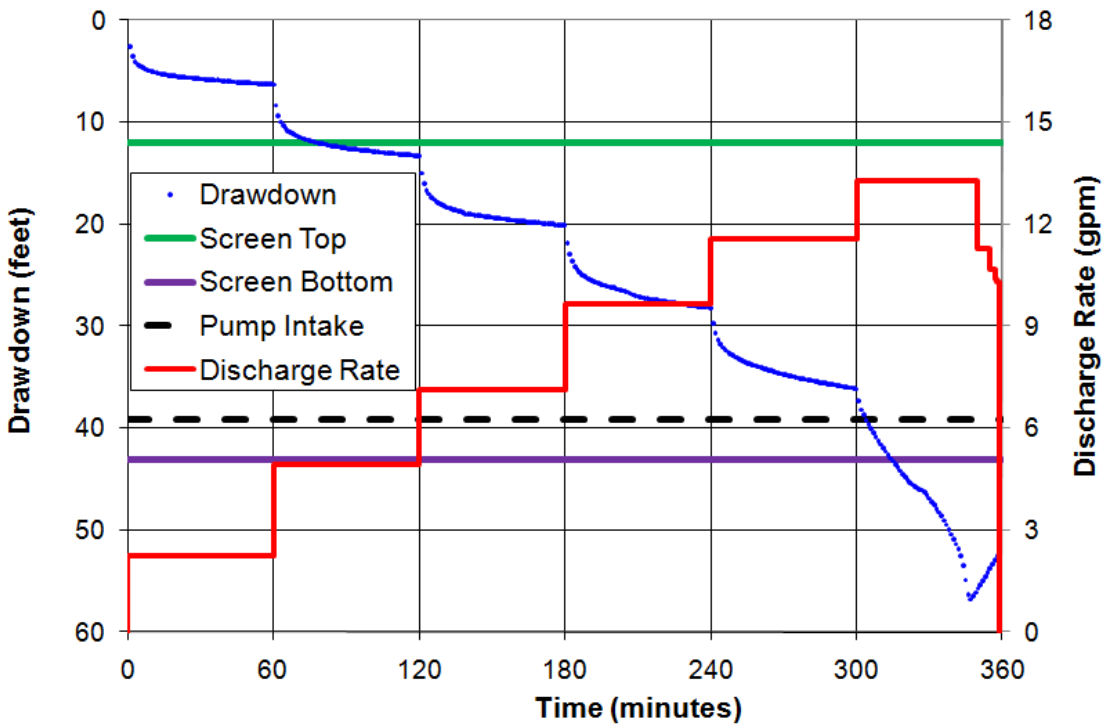


Figure B-9.2-1 Well CdV-16-4ip screen 2 step-drawdown test

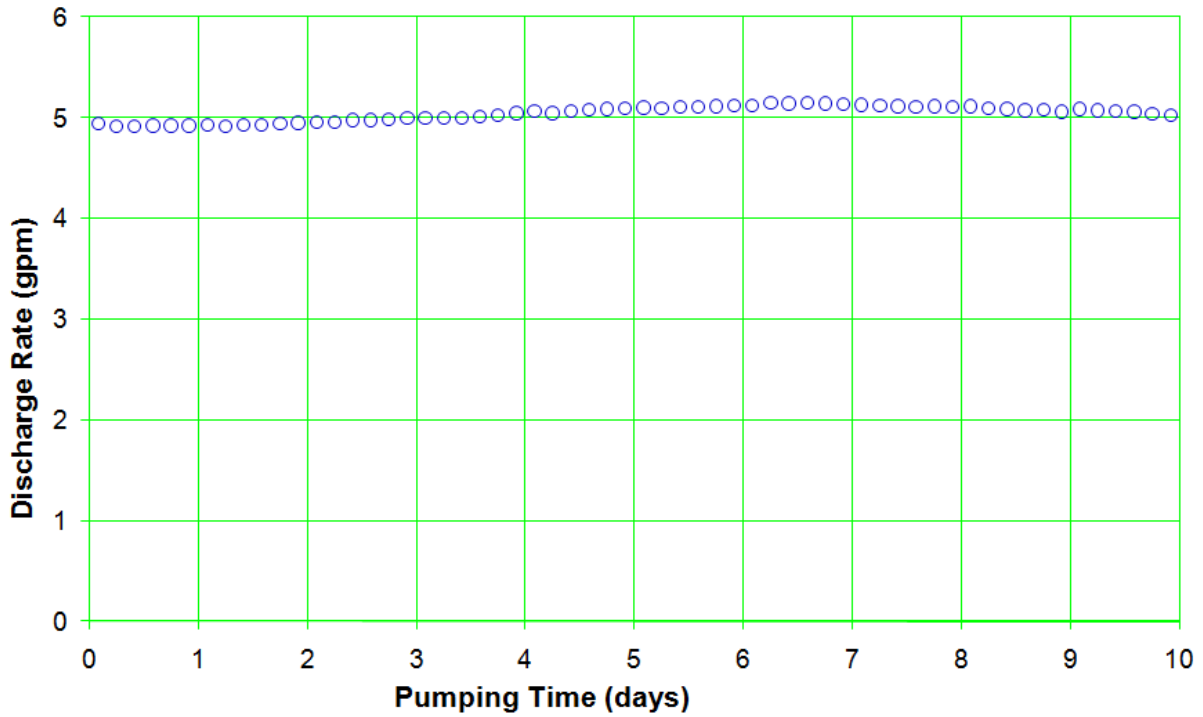


Figure B-9.3-1 Well CdV-16-4ip screen 2 pumping rates

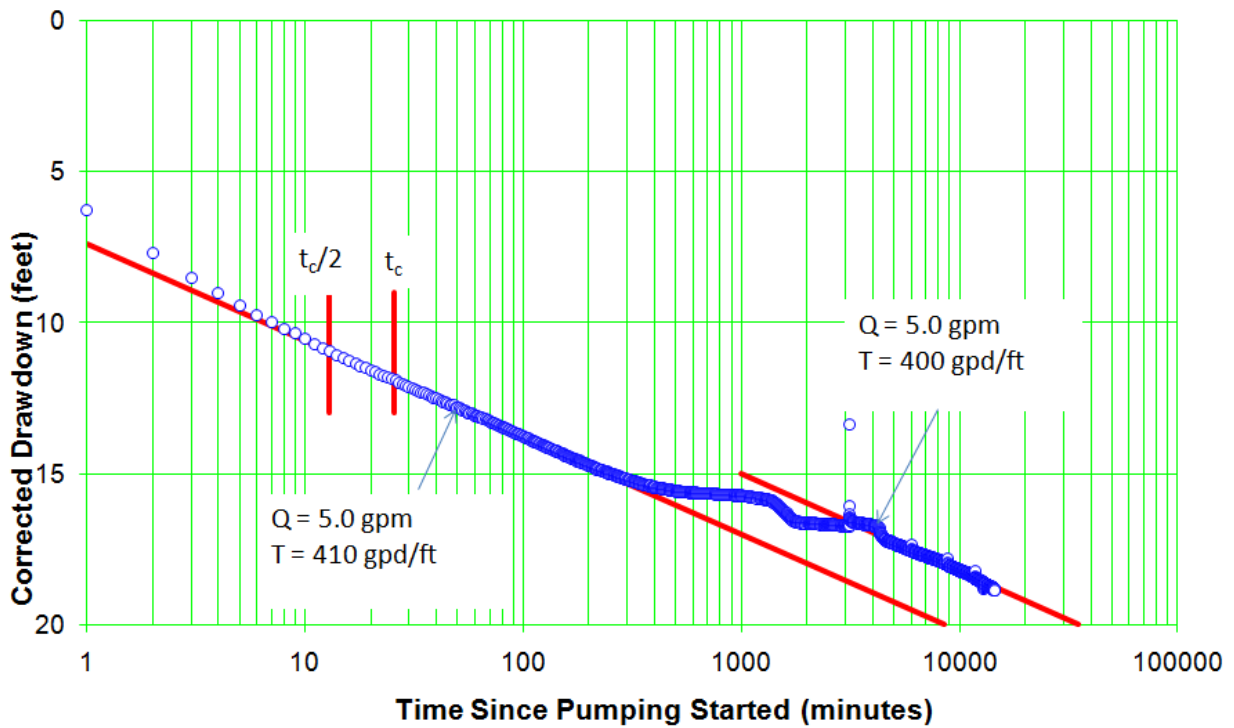


Figure B-9.3-2 Well CdV-16-4ip screen 2 corrected drawdown

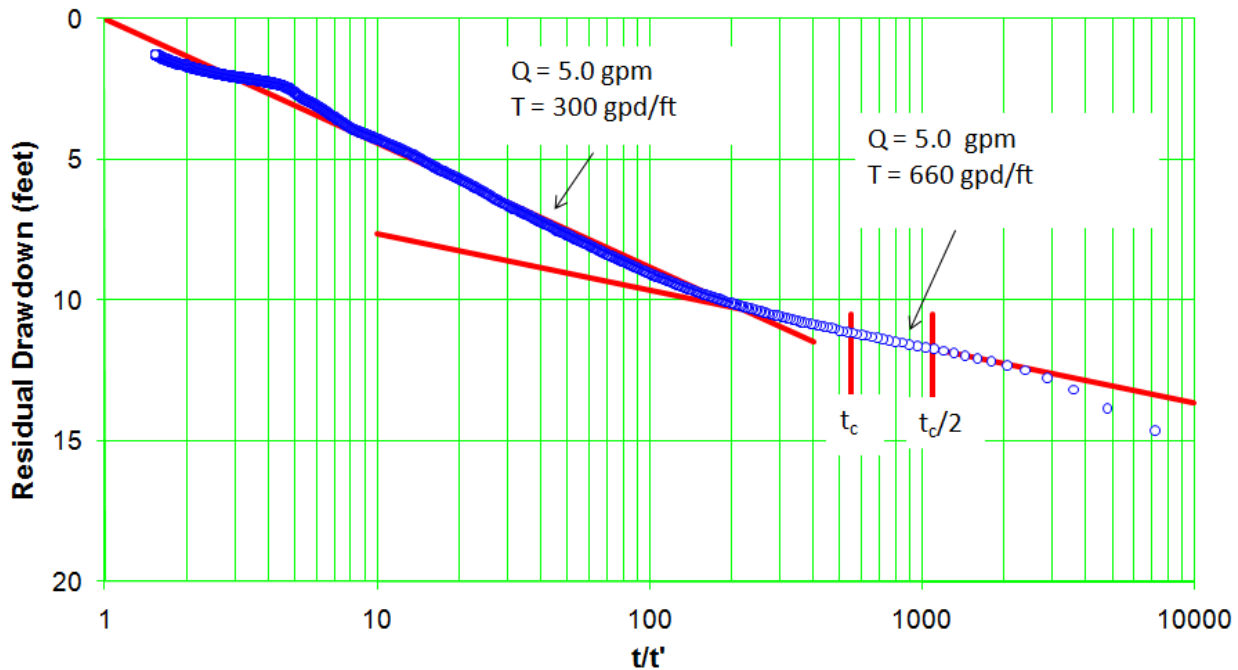


Figure B-9.3-3 Well CdV-16-4ip screen 2 recovery

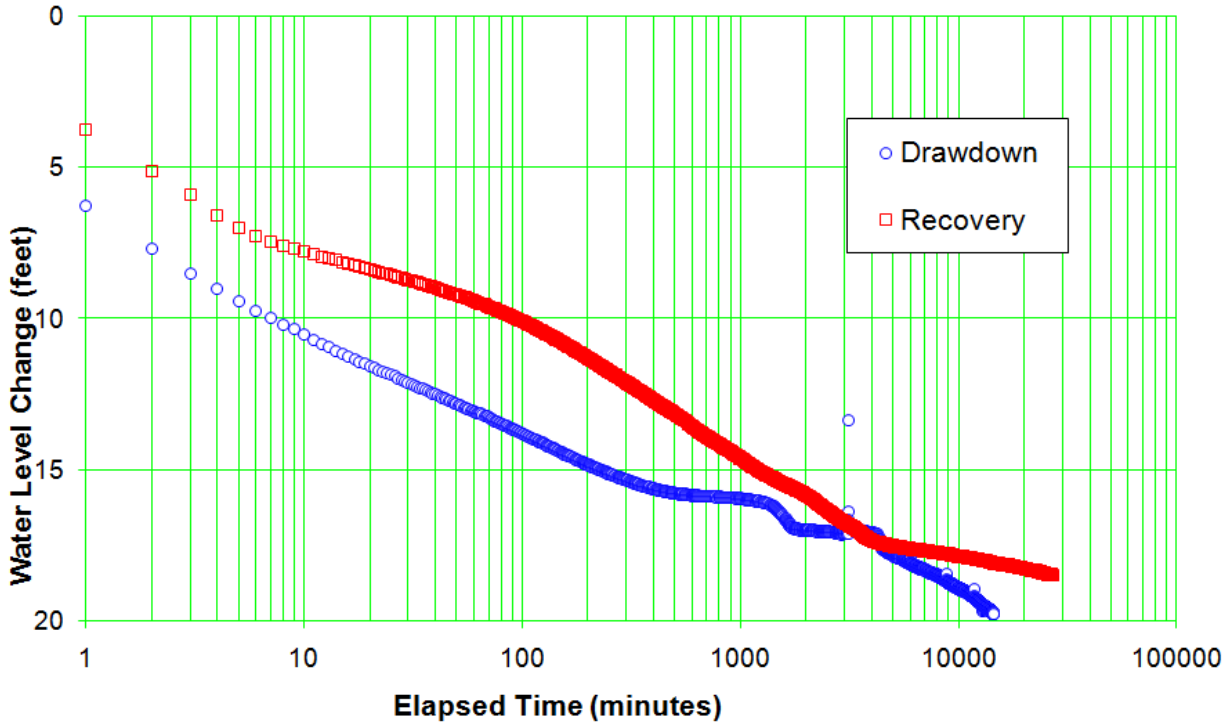


Figure B-9.3-4 Well CdV-16-4ip screen 2 drawdown and recovery comparison

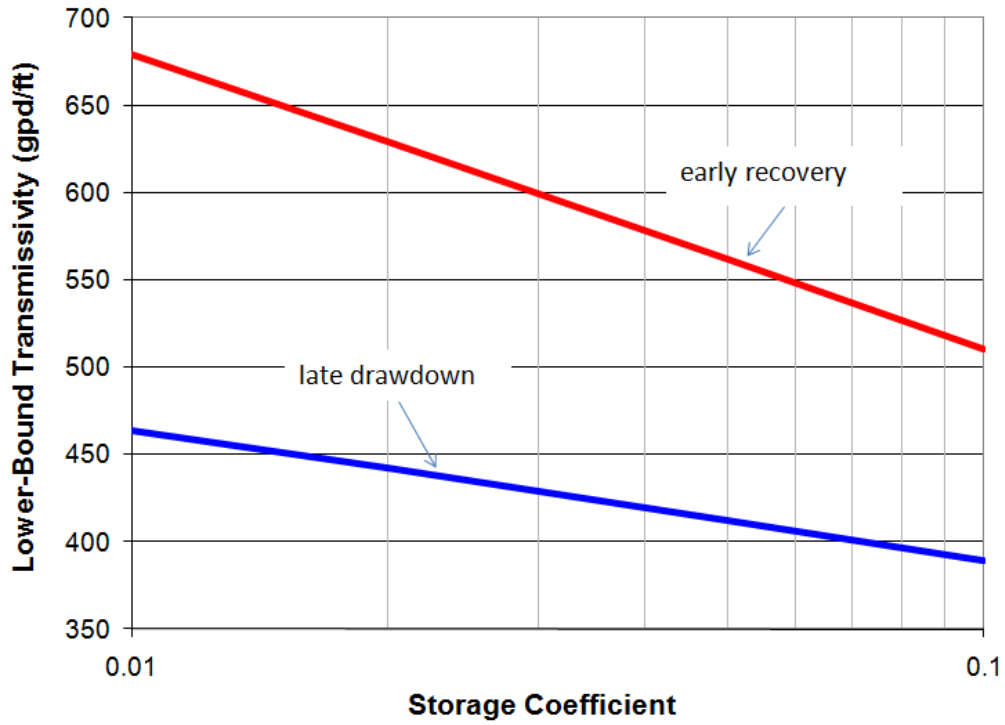


Figure B-9.4-1 Well CdV-16-4ip screen 2 lower-bound transmissivity

Appendix C

Well R-25b Pump Test Analysis

C-1.0 INTRODUCTION

This appendix describes the hydraulic analysis of a pumping test conducted in April 2011 at well R-25b, a perched zone well located at Technical Area 16 (TA-16) next to R-25. The test on R-25b was conducted to characterize the saturated materials, quantify the magnitude of the hydraulic properties of the screened interval, and check for pumping effects in nearby screened intervals. Testing consisted of pumping the well for 24 h using the dedicated Bennett pump already installed in the well.

Unlike most of the R-well pumping tests conducted on the Pajarito Plateau, an inflatable packer system was not used in R-25b to try to eliminate casing storage effects on the test data. The dedicated pumping system did not include an inflatable packer. Further, the static water level fell within the well screen, thus ensuring that dewatering of the screen and filter pack would occur, causing-storage effects regardless of the testing approach applied to the well.

Conceptual Hydrogeology

R-25b lies within the Otowi Member of the Bandelier Tuff, above the Puye Formation. The well screen is 20.8 ft long, extending from 750.0 to 770.8 ft below ground surface (bgs), from elevation 6767.0 to 6746.2 ft above mean sea level (amsl). The static water level measured on April 22, 2011, at the start of the pumping test, was 751.9 ft bgs (elevation 6765.1 ft amsl). The brass cap elevation at the well is at 7517.0 ft amsl. Because of the location of the water table 1.9 ft below the top of the well screen, unconfined conditions were assumed for R-25b.

Several wells and screen intervals were monitored during the R-25b pumping test. Only R-25 screens 1 and 2 showed response to pumping R-25b. R-25 screen 1 is 20.8 ft long, located within the Otowi Member of the Bandelier Tuff and screened between elevations 6778.5 and 6757.7 ft amsl, with a static water level slightly above the screen at 6779.3 ft amsl. R-25 screen 2 is 10.8 ft long, lying within the Puye Formation between elevations 6633.5 and 6622.7 ft amsl, with a static water level well above the screen at 6741.4 ft amsl.

Because of the drawdown response observed in R-25 screens 1 and 2 during the R-25b pumping test, in the hydraulic analysis described below it was assumed that the three screened intervals were within the same hydrologic unit. The zone of saturation was considered to extend from the R-25 screen 1 static water level (6779.3 ft amsl) to the base of R-25 screen 2 (6622.7 ft amsl), a span of 156.6 ft. Thus, the analysis considered the partial penetration of the well in the perched-intermediate zone.

R-25b Testing

R-25b was tested by operating the dedicated Bennett pump for 24 h from 7:16 a.m. on April 22 to 7:16 a.m. on April 23. The discharge rate began at 0.65 gallons per minute (gpm) but declined to 0.58 gpm by the end of the test, averaging 0.60 gpm for the 24-h pumping period. Following shutdown of the pumping test, recovery data were recorded for a little more than 2 d until 9:34 a.m. on April 25.

C-2.0 BACKGROUND DATA

The background water-level data collected in conjunction with running the pumping tests allow the analyst to see what water-level fluctuations occur naturally in the aquifer and help distinguish between water-level changes caused by conducting the pumping test and changes associated with other causes.

Background water-level fluctuations have several causes, among them barometric pressure changes, operation of other wells in the aquifer, Earth tides, and long-term trends related to weather patterns. The background data hydrographs from the monitored wells were compared with barometric pressure data from the area to determine if a correlation existed.

Previous pumping tests on the plateau have demonstrated a barometric efficiency for most wells of between 90% and 100%. Barometric efficiency is defined as the ratio of water-level change divided by barometric pressure change, expressed as a percentage. In the initial pumping tests conducted on the early R-wells, downhole pressure was monitored using a vented pressure transducer. This equipment measures the difference between the total pressure applied to the transducer and the barometric pressure, this difference being the true height of water above the transducer.

Subsequent pumping tests have utilized nonvented transducers. These devices simply record the total pressure on the transducer, that is, the sum of the water height plus the barometric pressure. This results in an attenuated “apparent” hydrograph in a barometrically efficient well. Take as an example a 90% barometrically efficient well. When a vented transducer is used for monitoring, an increase in barometric pressure of 1 unit causes a decrease in recorded downhole pressure of 0.9 unit because the water level is forced downward 0.9 unit by the barometric pressure change. However, using a nonvented transducer, the total measured pressure increases by 0.1 unit (the combination of the barometric pressure increase and the water-level decrease). Thus, the resulting apparent hydrograph changes by a factor of 100 minus the barometric efficiency, and in the same direction as the barometric pressure change rather than in the opposite direction.

The R-25b pumping test was conducted using the dedicated transducer that is vented. Therefore, changes in barometric pressure directly raised and lowered water levels in the well, affecting the measured head values. This, coupled with a high-barometric efficiency (described below), required data to be corrected for barometric pressure effects before analysis.

Barometric pressure data were obtained from TA-54 tower site from the Waste and Environmental Services Division-Environmental Data and Analysis (WES-EDA). The TA-54 measurement location is at an elevation of 6548 ft amsl, whereas the wellhead elevation is at 7517 ft amsl. The static water level in R-25b was 751.9 ft below land surface, making the water-table elevation 6765.1 ft amsl. Therefore, the measured barometric pressure data from TA-54 had to be adjusted to reflect the pressure at the elevation of the water table within R-25b.

The following formula was used to adjust the measured barometric pressure data:

$$P_{WT} = P_{TA54} \exp \left[- \frac{g}{3.281R} \left(\frac{E_{R-25b} - E_{TA54}}{T_{TA54}} + \frac{E_{WT} - E_{R-25b}}{T_{WELL}} \right) \right] \quad \text{Equation C-1}$$

where P_{WT} = barometric pressure at the water table inside R-25b

P_{TA54} = barometric pressure measured at TA-54

g = acceleration of gravity, in m/s² (9.80665 m/s²)

R = gas constant, in J/kg/degrees kelvin (287.04 J/kg/K)

E_{R-25b} = land surface elevation at R-25b site, in feet (7517 ft)

E_{TA54} = elevation of barometric pressure measuring point at TA-54, in feet (6548 ft)

E_{WT} = elevation of the water level in R-25b, in feet (6765.1 ft)

T_{TA54} = air temperature near TA-54, in degrees kelvin (assigned a value of 56.8°F, or 286.9 K)

T_{WELL} = air temperature inside R-25b, in degrees kelvin (assigned a value of 50.6°F, or 2283.5 K)

This formula is an adaptation of an equation WES-EDA provided. It can be derived from the ideal gas law and standard physics principles. An inherent assumption in the derivation of the equation is that the air temperature between TA-54 and the well is temporally and spatially constant and that the temperature of the air column in the well is similarly constant.

The corrected barometric pressure data reflecting pressure conditions at the water table were compared with the water-level hydrograph to discern the correlation between the two and determine whether water-level corrections would be needed before data analysis.

C-3.0 IMPORTANCE OF EARLY DATA

When pumping or recovery first begins, the vertical extent of the cone of depression is limited to approximately the well screen length, the filter pack length, or the aquifer thickness in relatively thin permeable strata. For many pumping tests on the plateau, the early pumping period is the only time the effective height of the cone of depression is known with certainty because, soon after startup, the cone of depression expands vertically through permeable materials above and/or below the screened interval. Thus, the early data often offer the best opportunity to obtain hydraulic conductivity information because conductivity would equal the earliest-time transmissivity divided by the well screen length.

Unfortunately, in many pumping tests (including the R-25b test), casing-storage effects dominate the early-time data, potentially hindering the effort to determine the transmissivity of the screened interval. The duration of casing-storage effects can be estimated using the following equation (Schafer 1978, 098240):

$$t_c = \frac{0.6(D^2 - d^2)}{\frac{Q}{s}}$$

Equation C-2

where t_c = duration of casing storage effect, in minutes

D = inside diameter of well casing, in inches (approximately 5.1 in.)

d = outside diameter of drop pipe or tubing bundle, in inches

Q = discharge rate, in gallons per minute

s = drawdown observed in pumped well at time t_c , in feet

The calculated casing storage time is quite conservative. Often, the data show that significant effects of casing storage have dissipated after about half the computed time.

For wells screened across the water table or wells in which the filter pack can drain during pumping, there can be an additional storage contribution from the filter pack. The following equation provides an estimate of the storage duration accounting for both casing and filter-pack storage:

$$t_c = \frac{0.6[(D^2 - d^2) + S_y(D_B^2 - D_C^2)]}{\frac{Q}{s}} \quad \text{Equation C-3}$$

where S_y = short term specific yield of filter media (typically 0.2)

D_B = diameter of borehole, in inches (13 in., based on backfill volume)

D_C = outside diameter of well casing, in inches (5.563 in.)

This equation was derived from Equation C-2 on a proportional basis by increasing the computed time in direct proportion to the additional volume of water expected to drain from the filter pack. (To prove this, note that the left hand term within the brackets is directly proportional to the annular area [and volume] between the casing and drop pipe while the right hand term is proportional to the area [and volume] between the borehole and the casing, corrected for the drainable porosity of the filter pack. Thus, the summed term within the brackets accounts for all of the volume [casing water and drained filter pack water] appropriately.)

In some instances, it is possible to eliminate casing storage effects by setting an inflatable packer above the tested screen interval before conducting the test. This approach was not applicable to the R-25b test, because the pumping test was conducted using the dedicated Bennett pump and no packer. In addition, the static water level fell with the well screen, thus ensuring that dewatering of the screen and filter pack would occur regardless of the pumping approach selected for testing.

C-4.0 TIME-DRAWDOWN METHODS

Time-drawdown data can be analyzed using a variety of methods. Among them is the Theis method (1934-1935, 098241). The Theis equation describes drawdown around a well as follows:

$$s = \frac{114.6Q}{T} W(u) \quad \text{Equation C-4}$$

where

$$W(u) = \int_u^{\infty} \frac{e^{-x}}{x} dx \quad \text{Equation C-5}$$

and

$$u = \frac{1.87r^2S}{Tt} \quad \text{Equation C-6}$$

and where s = drawdown, in feet

Q = discharge rate, in gallons per minute

T = transmissivity, in gallons per day per foot

S = storage coefficient (dimensionless)

t = pumping time, in days

r = distance from center of pumpage, in feet

To use the Theis method of analysis, the time-drawdown data are plotted on a log-log scale. Then, Theis curve matching is performed using the Theis type curve—a plot of the Theis well function $W(u)$ versus $1/u$. Curve matching is accomplished by overlaying the type curve on the data plot and, while keeping the coordinate axes of the two plots parallel, shifting the data plot to align with the type curve, effecting a match position. An arbitrary point, referred to as the match point, is selected from the overlapping parts of the plots. Match-point coordinates are recorded from the two graphs, yielding four values: $W(u)$, $1/u$, s , and t . Using these match-point values, transmissivity and storage coefficient are computed as follows:

$$T = \frac{114.6Q}{s} W(u) \quad \text{Equation C-7}$$

$$S = \frac{Tut}{2693r^2} \quad \text{Equation C-8}$$

where T = transmissivity, in gallons per day per foot

S = storage coefficient

Q = discharge rate, in gallons per minute

$W(u)$ = match-point value

s = match-point value, in feet

u = match-point value

t = match-point value, in minutes

An alternative solution method applicable to time-drawdown data is the Cooper-Jacob method (1946, 098236), a simplification of the Theis equation that is mathematically equivalent to the Theis equation for most pumped well data. The Cooper-Jacob equation describes drawdown around a pumping well as follows:

$$s = \frac{264Q}{T} \log \frac{0.3Tt}{r^2 S} \quad \text{Equation C-9}$$

The Cooper-Jacob equation is a simplified approximation of the Theis equation and is valid whenever the u value is less than about 0.05. For small radius values (e.g., corresponding to borehole radii), u is less than 0.05 at very early pumping times and therefore is less than 0.05 for most or all measured drawdown

values. Thus, for the pumped well, the Cooper-Jacob equation usually can be considered a valid approximation of the Theis equation. An exception occurs when the transmissivity of the aquifer is very low. In that case, some of the early pumped well drawdown data may not be well approximated by the Cooper-Jacob equation.

According to the Cooper-Jacob method, the time-drawdown data are plotted on a semilog graph, with time plotted on the logarithmic scale. Then a straight line of best fit is constructed through the data points and transmissivity is calculated using:

$$T = \frac{264Q}{\Delta s} \quad \text{Equation C-10}$$

where T = transmissivity, in gallons per day per foot

Q = discharge rate, in gallons per minute

Δs = change in head over one log cycle of the graph, in feet

Because many of the test wells completed on the plateau are severely partially penetrating, an alternate solution considered for assessing aquifer conditions is the Hantush equation for partially penetrating wells (Hantush 1961, 098237; Hantush 1961, 106003). The Hantush equation is as follows:

$$\text{Equation C-11}$$

$$s = \frac{Q}{4\pi T} \left[W(u) + \frac{2b^2}{\pi^2(l-d)(l'-d')} \sum_{n=1}^{\infty} \frac{1}{n^2} \left(\sin \frac{n\pi l}{b} - \sin \frac{n\pi d}{b} \right) \left(\sin \frac{n\pi l'}{b} - \sin \frac{n\pi d'}{b} \right) W \left(u, \sqrt{\frac{K_z}{K_r}} \frac{n\pi r}{b} \right) \right]$$

where, in consistent units, s , Q , T , t , r , S , and u are as previously defined and

b = aquifer thickness

d = distance from top of aquifer to top of well screen in pumped well

l = distance from top of aquifer to bottom of well screen in pumped well

d' = distance from top of aquifer to top of well screen in observation well

l' = distance from top of aquifer to bottom of well screen in observation well

K_z = vertical hydraulic conductivity

K_r = horizontal hydraulic conductivity

In this equation, $W(u)$ is the Theis well function and $W(u,\beta)$ is the Hantush well function for leaky aquifers where

$$\beta = \sqrt{\frac{K_z}{K_r}} \frac{n\pi r}{b} \quad \text{Equation C-12}$$

Note that for single-well tests, $d = d'$ and $l = l'$.

Unconfined Aquifer Drawdown Correction

For unconfined aquifers, the saturated aquifer thickness is reduced below the original thickness during testing. This results in drawdown values that deviate from theoretical predictions, because well hydraulics formulas are based on 100% aquifer saturation. Before analysis, the actual drawdown values must be corrected for dewatering effects using the following formula (Kruseman et al. 1991, 106681):

$$s_c = s_a - \frac{s_a^2}{2b} \quad \text{Equation C-13}$$

where s_c = corrected drawdown, in feet

S_a = observed drawdown, in feet

b = saturated aquifer thickness, in feet

Assumptions required for validity of Equation C-13 are (1) homogeneous hydraulic conductivity, (2) full penetration of the producing zone by the well screen, and (3) no head loss associated with vertical flow. This last assumption is satisfied by one of two extremes—either zero permeability in the vertical direction so no flow (and therefore no head loss) occurs vertically, or infinite vertical permeability. Failure to meet any of these three assumptions leads to modest errors in application of the drawdown correction equation.

R-25b data were affected by both dewatering and partial penetration. When the screen is partially penetrating, Equation 13 tends to overestimate the degree of correction required, putting the effective drawdown between the measured and corrected values.

C-5.0 RECOVERY METHODS

Recovery data were analyzed using the Theis recovery method. This is a semilog analysis method similar to the Cooper-Jacob procedure.

In this method, residual drawdown is plotted on a semilog graph versus the ratio t/t' , where t is the time since pumping began and t' is the time since pumping stopped. A straight line of best fit is constructed through the data points and T is calculated from the slope of the line as follows:

$$T = \frac{264Q}{\Delta s} \quad \text{Equation C-14}$$

The recovery data are particularly useful compared with time-drawdown data. Because the pump is not running, spurious data responses associated with dynamic discharge rate fluctuations are eliminated. The result is the data set is generally “smoother” and easier to analyze.

Recovery data also can be analyzed using the Hantush equation for partial penetration. This approach is generally applied to the early data in a plot of recovery versus recovery time.

C-6.0 SPECIFIC CAPACITY METHOD

The specific capacity of the pumped well can be used to obtain a lower-bound value of hydraulic conductivity. The hydraulic conductivity is computed using formulae that are based on the assumption that the pumped well is 100% efficient. The resulting hydraulic conductivity is the value required to sustain

the observed specific capacity. If the actual well is less than 100% efficient, it follows that the actual hydraulic conductivity would have to be greater than calculated to compensate for well inefficiency. Thus, because the efficiency is unknown, the computed hydraulic conductivity value represents a lower bound. The actual conductivity is known to be greater than or equal to the computed value.

For fully penetrating wells, the Cooper-Jacob equation can be iterated to solve for the lower-bound hydraulic conductivity. However, the Cooper-Jacob equation (assuming full penetration) ignores the contribution to well yield from permeable sediments above and below the screened interval. To account for this contribution, it is necessary to use a computation algorithm that includes the effects of partial penetration. One such approach was introduced by Brons and Marting (1961, 098235) and augmented by Bradbury and Rothschild (1985, 098234).

Brons and Marting introduced a dimensionless drawdown correction factor, s_p , approximated by Bradbury and Rothschild as follows:

$$s_p = \frac{1 - \frac{L}{b}}{\frac{L}{b}} \left[\ln \frac{b}{r_w} - 2.948 + 7.363 \frac{L}{b} - 11.447 \left(\frac{L}{b} \right)^2 + 4.675 \left(\frac{L}{b} \right)^3 \right] \quad \text{Equation C-15}$$

In this equation, L is the well screen length, in feet. Incorporating the dimensionless drawdown parameter, the conductivity is obtained by iterating the following formula:

$$K = \frac{264Q}{sb} \left(\log \frac{0.3Tt}{r_w^2 S} + \frac{2s_p}{\ln 10} \right) \quad \text{Equation C-16}$$

The Brons and Marting procedure can be applied to both partially penetrating and fully penetrating wells.

To apply this procedure, a storage coefficient value must be assigned. Storage coefficient values generally range from 10^{-5} to 10^{-3} for confined aquifers and 0.01 to 0.25 for unconfined aquifers (Driscoll 1986, 104226). Unconfined conditions were assumed for R-25b and a storage coefficient range of 0.01 to 0.10 was arbitrarily assigned. The calculation result is not particularly sensitive to the choice of storage coefficient value, so a rough estimate is generally adequate to support the calculations.

The analysis also requires assigning a value for the saturated aquifer thickness, b . For R-25b, an estimated thickness of 156.6 ft was used in the calculations—the distance between the static water level in R-25 screen 1 (6779.3 ft amsl) and the base of R-25 screen 2 (6622.7 ft amsl). For partially penetrating conditions, the calculations are not particularly sensitive to the choice of aquifer thickness because sediments far above or below the screen typically contribute little flow.

C-7.0 BACKGROUND DATA ANALYSIS

Background aquifer pressure data collected during the R-25b tests were plotted along with barometric pressure to determine the barometric effect on water levels.

Figure C-7.0-1 shows groundwater elevation data from R-25b during the test period along with barometric pressure data from TA-54 that have been corrected to equivalent barometric pressure in feet of water at the water table. The time of the pumping period for the R-25b pumping test is included on the figure for reference.

The barometric pressure data were plotted in Figure C-7.0-1 on a reverse scale to emphasize the correlation between barometric pressure and water levels. R-25b showed significant pressure change in response to barometric pressure fluctuations, with the data on April 24 and 25 showing water-level changes having the same magnitude as the barometric pressure fluctuations. This value implied a barometric efficiency near 100% for R-25b and indicated that water-level data would require correction for atmospheric effects.

Hydrograph data from nearby wells R-25 screens 1 and 2 (about 55 ft away) were obtained to check for a possible pumping response to the R-25b test. Of note is that the R-25 data were recorded using nonvented dedicated transducers in contrast to the vented type installed in R-25b. The screen-2 data required correction for barometric-pressure and Earth-tide effects. This correction was done using BETCO (barometric and earth tide correction) software—a mathematically complex correction algorithm that uses regression deconvolution (Toll and Rasmussen 2007, 104799) to modify the data. The BETCO correction removes the effects of barometric pressure as well as Earth tide effects.

Figure C-7.0-2 shows the data collected from R-25 screen 1. Note that the water-level scale has been expanded by a factor of 5 compared with the barometric pressure scale to illustrate the water-level changes more clearly. There was a clear response to pumping R-25b of a few hundredths of a foot of drawdown. Including data both before and after the pumping test, the overall water levels appeared to show a declining trend of about 0.005 ft/d. This trend was mathematically removed from the computed drawdown for R-25 screen 1 before analysis.

Figure C-7.0-3 shows the data collected from R-25 screen 2 along with the BETCO correction. Note that the water-level scale has been expanded by a factor of 5 compared with the barometric pressure scale to illustrate the water-level changes more clearly. The corrected data show a likely response to pumping R-25b. The data shortly before and after the test also show a background trend—this one about 0.006 ft/d. This trend was mathematically removed from the computed drawdown for R-25 screen 2 before analysis.

C-8.0 WELL R-25b DATA ANALYSIS

This section presents the data obtained from the R-25b pumping test and the results of the analytical interpretations. Data are presented for drawdown and recovery from the 24-h constant-rate test.

C-8.1 Well R-25b 24-Hour Constant-Rate Test

Figure C-8.1-1 shows the discharge rates measured during the R-25b pumping test. The rate started out at 0.65 gpm, declining to 0.60 gpm halfway through the test, and about 0.58 gpm during the latter stages of pumping.

Figure C-8.1-2 shows a semilog plot of the drawdown data collected from the 24-h constant-rate pumping test. The casing and filter pack storage times are shown in the figure for reference. Clearly, the bulk of the data were storage affected and thus did not support a rigorous analysis. By the time storage effects had subsided, discharge-rate fluctuations affected the data. The data were not considered analyzable because of the lack of sufficient discharge rate detail, the likelihood that the magnitude of the corrections would be larger than temporal changes in the corrected drawdown values, and the fact that discharge rate changes themselves induced additional incremental storage effects of large duration.

The data from R-25 screen 1 were analyzed by applying the Hantush equation to correct for partial penetration effects. Analysis was conducted by varying the vertical anisotropy ratio from 10^{-2} to 10^{-5} and observing the computed results. In general, the results of the analysis were not considered satisfactory.

Figure C-8.1-3 shows a typical plot of Hantush-corrected data for an assigned vertical anisotropy ratio of 10^{-5} . Figures C-8.1-4 and C-8.1-5 show hydraulic conductivity and storage coefficient values determined from the analysis as a function of anisotropy. As shown by subsequent analyses (described below), the computed hydraulic conductivity values appeared unrealistically large, suggesting an invalid analysis. It was possible that delayed yield had the effect of flattening the drawdown curve (Figure C-8.1-3) leading to an overestimate of hydraulic conductivity.

Figures C-8.1-6 through C-8.1-10 show Hantush curve matching solutions for R-25 screen 2 for anisotropy ratios of 10^{-1} through 10^{-5} , respectively. The type curves were limited to the early data, before apparent stabilization, because the late data may have reflected the effects of delayed yield. Figures C-8.1-11 and C-8.1-12 provide summaries of the computed hydraulic conductivity and storage coefficient values as a function of anisotropy. The most severe anisotropy values led to unrealistically low storage coefficient values. This effect suggested the vertical anisotropy values in the range of 10^{-3} through 10^{-1} were the most realistic for the lower portion of the saturated perched zone. On the other hand, it is possible that the vertical anisotropy of the uppermost strata (closer to R-25 screen 1) could be more severe, based on the large head difference between R-25 screen 1 and R-25b even though the screens in the two wells actually overlap slightly in elevation. (The large head difference between these two screens also could be a function of heterogeneity or preferential focused infiltration recharge of the perched zone in the vicinity of R-25b.)

The Hantush analyses of the R-25 screen 2 test data suggested a hydraulic conductivity on the order of about 0.3 ft/d. To put this result in perspective, however, it is important to point out that the computations were based on corrected water-level changes of about only 0.01 ft from a data set (R-25 screen 2 apparent hydrograph) in which the magnitude of the background “noise” was 10 times greater at nearly 0.10 ft. This limited the confidence that could be placed in the results of this particular analysis.

Figure C-8.1-13 shows a plot of the R-25b recovery data following the 24-h pumping test. The casing and filter-pack storage times are shown on the figure for reference. Clearly, most of the data were storage affected and were not analyzable.

Figure C-8.1-14 shows an expanded-scale plot of the late recovery data from R-25b. The transmissivity value obtained from the analysis was 240 gallons per day (gpd)/ft. However, the data shown on the graph were not corrected for barometric pressure changes. Therefore, a subset of the data points were corrected manually for barometric effects and plotted on the graph shown in Figure C-8.1-15. The data plot appeared more reliable than the uncorrected plot in that the trend showed a straight line that tended toward a residual drawdown of zero at a t/t' ratio of 1.0 as is theoretically expected. Using the saturated thickness of 156.6 ft, the computed hydraulic conductivity was 2.2 gpd/ft², or 0.29 ft/d.

C-8.2 Well R-25b Specific Capacity Data

Specific capacity data were used along with well geometry to estimate a lower-bound hydraulic conductivity value for the permeable zone penetrated by R-25b to provide a frame of reference for evaluating the above analyses.

At the end of the 24-h pumping test, the discharge rate was 0.58 gpm with a resulting drawdown of 14.06 ft for a specific capacity of 0.041 gpm/ft. In addition to specific capacity and pumping time, other input values used in the calculations included a range of storage coefficient values of 0.01 to 0.10, a borehole radius of 0.54 ft (inferred from the volume of filter pack required to backfill the screen zone), a screen length of 20.8 ft, and an assigned saturated thickness of 156.6 ft.

The observed drawdown was corrected for dewatering effects yielding a corrected drawdown of 8.83 ft. As discussed previously, for partially penetrating conditions, the dewatering correction algorithm likely results in an overcorrection of the drawdown. Thus, the true effective drawdown would be expected to fall between 8.83 and 14.06 ft. Therefore, the lower-bound hydraulic conductivity was computed using both drawdown values in an effort to bracket the possible range of lower-bound conductivity.

Applying the Brons and Marting method to these inputs yielded the lower-bound hydraulic conductivity values shown in Figure C-8.2-1. The actual drawdown produced lower-bound hydraulic conductivity estimates on the order of 0.24 ft/d while the corrected drawdown value yields lower bounds around 0.38 ft/d. The best estimate of lower-bound hydraulic conductivity would be expected to fall between these extremes. The pumping test analyses presented above suggested a formation hydraulic conductivity of around 0.3 ft/d. The lower-bound estimates were largely consistent with the pumping test values.

C-9.0 SUMMARY

A constant-rate pumping test was conducted at well R-25b. The test was performed to gain an understanding of the hydraulic characteristics of the screen zone and perched interval as well as to check for drawdown effects in nearby screen intervals.

Pumping R-25b induced slight drawdown in both screens 1 and 2 in R-25, 55 ft away.

The perched aquifer was interpreted as consisting of a 156.6-ft-thick interval extending from the static water level at R25 screen 1 (6779.3 ft amsl) to the base of R-25 screen 2 (6622.7 ft amsl). Water levels in R-25b and R-25 screens 1 and 2 showed steep downward gradients, suggesting significant vertical anisotropy. The anisotropy was judged to be more severe in the upper portion of the perched zone where heads between R-25b and R25 screen 1 were substantially different even though the elevation intervals spanned by the two screens overlap slightly. The vertical head differences also might be caused by preferential focused infiltration recharge of the perched zone in the vicinity of R-25b or by partial draining of the perched zone by construction defects in either R-25b or nearby dry perched zone well R-25c.

A comparison of barometric pressure and R-25b water level data showed close correspondence between the pressure curves, suggesting a barometric efficiency of near 100%.

The pumping test on R-25b was conducted using the dedicated Bennett pump; thus, no inflatable packer was used during the test. This, combined with the fact that the static water level was within the well screen, ensured that drainage of the screen and filter pack would occur causing significant storage effects. Indeed, storage effects persisted for several hours during pumping and recovery.

Storage effects and discharge rate variations precluded analysis of the pumping portion of the test. The late (post-storage) recovery data supported an analysis, yielding an estimated horizontal hydraulic conductivity of 0.29 ft/d. Hantush analysis of data from R-25 screen 2 produced horizontal hydraulic conductivity values averaging slightly more than 0.3 ft/d.

R-25b produced 0.58 gpm after 1440 min of pumping with 14.06 ft of drawdown for a specific capacity of 0.041 gpm/ft. The lower-bound hydraulic conductivity values computed from this information was around 0.24 ft/d. The drawdown in R-25b was corrected for dewatering effects, yielding a theoretical drawdown of 8.83 ft. The computation algorithm was expected to provide an overcorrection because it does not consider the effects of partial penetration. The lower-bound horizontal hydraulic conductivity computed from the corrected drawdown value was around 0.24 ft/d. The actual lower-bound hydraulic conductivity was expected to lie between these extremes, that is, between 0.24 and 0.38 ft/d. This result was consistent with the hydraulic conductivity values around 0.3 ft/d obtained from the pumping test analyses.

C-10.0 REFERENCES

The following list includes all documents cited in this appendix. Parenthetical information following each reference provides the author(s), publication date, and ER ID. This information is also included in text citations. ER IDs are assigned by the Environmental Programs Directorate's Records Processing Facility (RPF) and are used to locate the document at the RPF and, where applicable, in the master reference set.

Copies of the master reference set are maintained at the New Mexico Environment Department Hazardous Waste Bureau and the Directorate. The set was developed to ensure that the administrative authority has all material needed to review this document, and it is updated with every document submitted to the administrative authority. Documents previously submitted to the administrative authority are not included.

- Bradbury, K.R., and E.R. Rothschild, March-April 1985. "A Computerized Technique for Estimating the Hydraulic Conductivity of Aquifers from Specific Capacity Data," *Ground Water*, Vol. 23, No. 2, pp. 240-246. (Bradbury and Rothschild 1985, 098234)
- Brons, F., and V.E. Marting, 1961. "The Effect of Restricted Fluid Entry on Well Productivity," *Journal of Petroleum Technology*, Vol. 13, No. 2, pp. 172-174. (Brons and Marting 1961, 098235)
- Cooper, H.H., Jr., and C.E. Jacob, August 1946. "A Generalized Graphical Method for Evaluating Formation Constants and Summarizing Well-Field History," *American Geophysical Union Transactions*, Vol. 27, No. 4, pp. 526-534. (Cooper and Jacob 1946, 098236)
- Driscoll, F.G., 1986. Excerpted pages from *Groundwater and Wells*, 2nd Ed., Johnson Filtration Systems Inc., St. Paul, Minnesota. (Driscoll 1986, 104226)
- Hantush, M.S., July 1961. "Drawdown around a Partially Penetrating Well," *Journal of the Hydraulics Division, Proceedings of the American Society of Civil Engineers*, Vol. 87, No. HY 4, pp. 83-98. (Hantush 1961, 098237)
- Hantush, M.S., September 1961. "Aquifer Tests on Partially Penetrating Wells," *Journal of the Hydraulics Division, Proceedings of the American Society of Civil Engineers*, pp. 171-195. (Hantush 1961, 106003)
- Kruseman, G.P., N.A. de Ridder, and J.M. Verweij, 1991. Excerpted page from *Analysis and Evaluation of Pumping Test Data*, International Institute for Land Reclamation and Improvement, Netherlands. (Kruseman et al. 1991, 106681)
- Schafer, D.C., January-February 1978. "Casing Storage Can Affect Pumping Test Data," *The Johnson Drillers Journal*, pp. 1-6, Johnson Division, UOP, Inc., St. Paul, Minnesota. (Schafer 1978, 098240)
- Theis, C.V., 1934-1935. "The Relation Between the Lowering of the Piezometric Surface and the Rate and Duration of Discharge of a Well Using Ground-Water Storage," *American Geophysical Union Transactions*, Vol. 15-16, pp. 519-524. (Theis 1934-1935, 098241)
- Toll, N.J., and T.C. Rasmussen, January-February 2007. "Removal of Barometric Pressure Effects and Earth Tides from Observed Water Levels," *Ground Water*, Vol. 45, No. 1, pp. 101-105. (Toll and Rasmussen 2007, 104799)

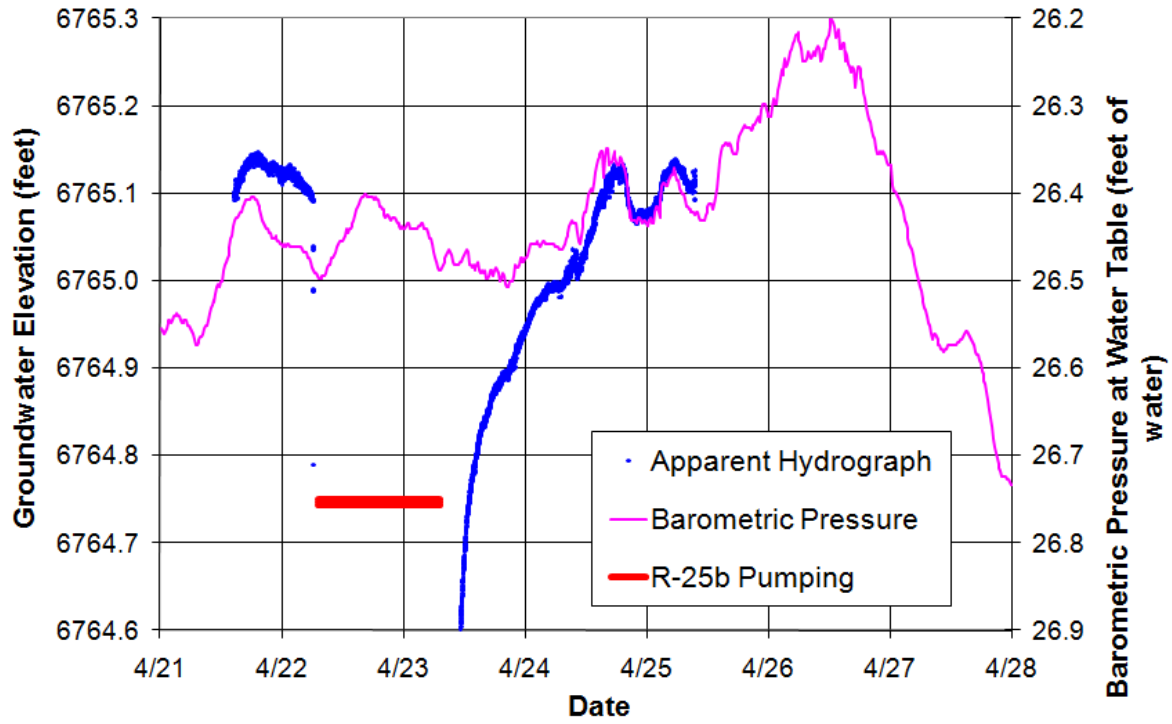


Figure C-7.0-1 Well R-25b hydrograph

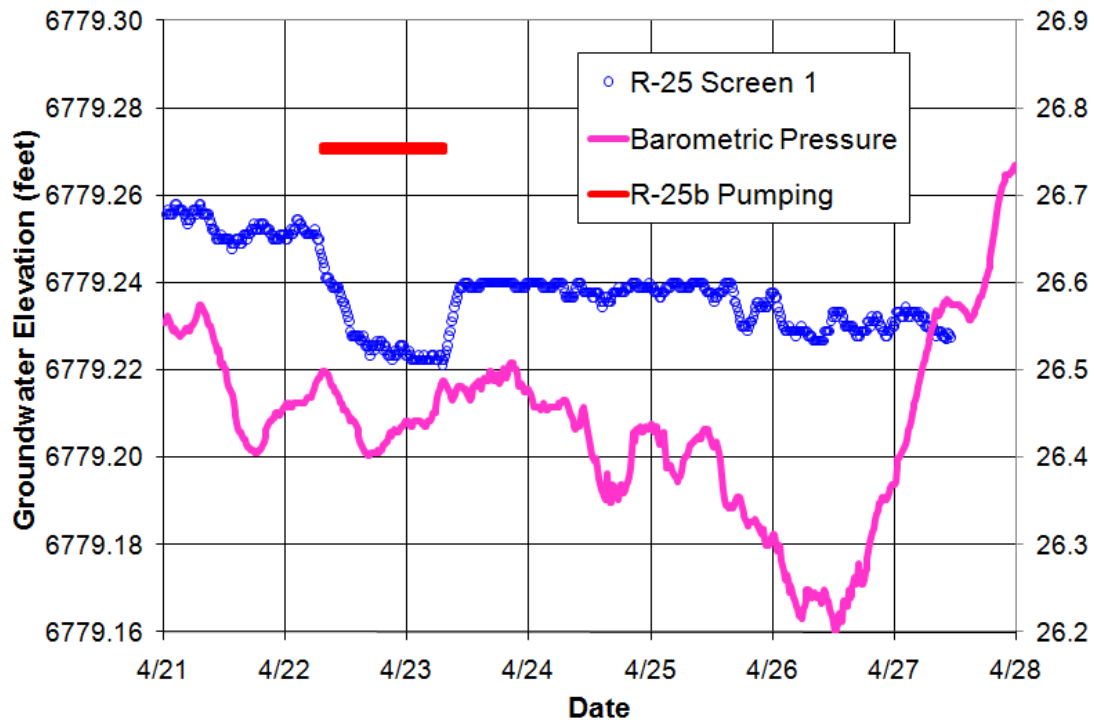


Figure C-7.0-2 Well R-25 screen 1 hydrograph

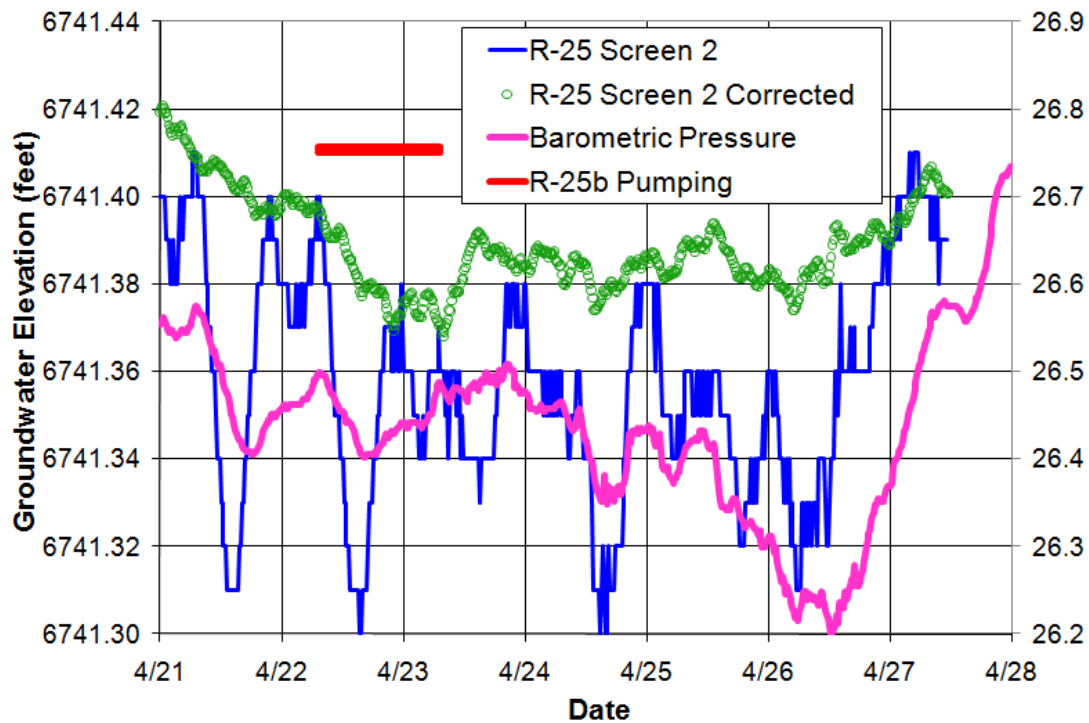


Figure C-7.0-3 Well R-25 screen 2 hydrograph

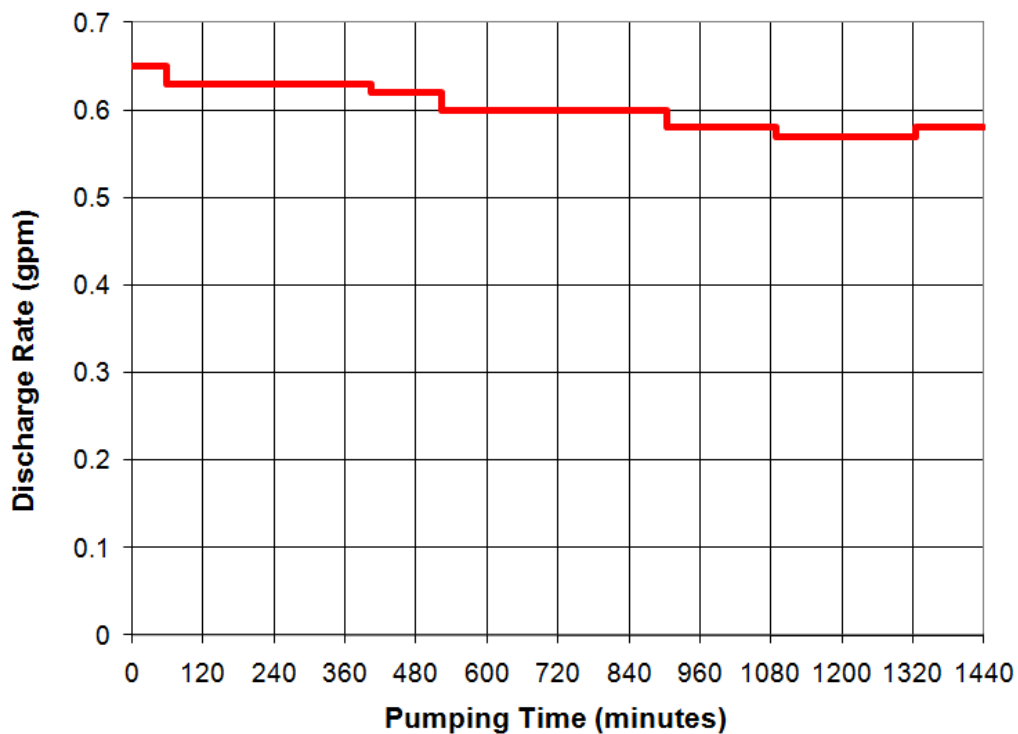


Figure C-8.1-1 Well R-25b discharge rates

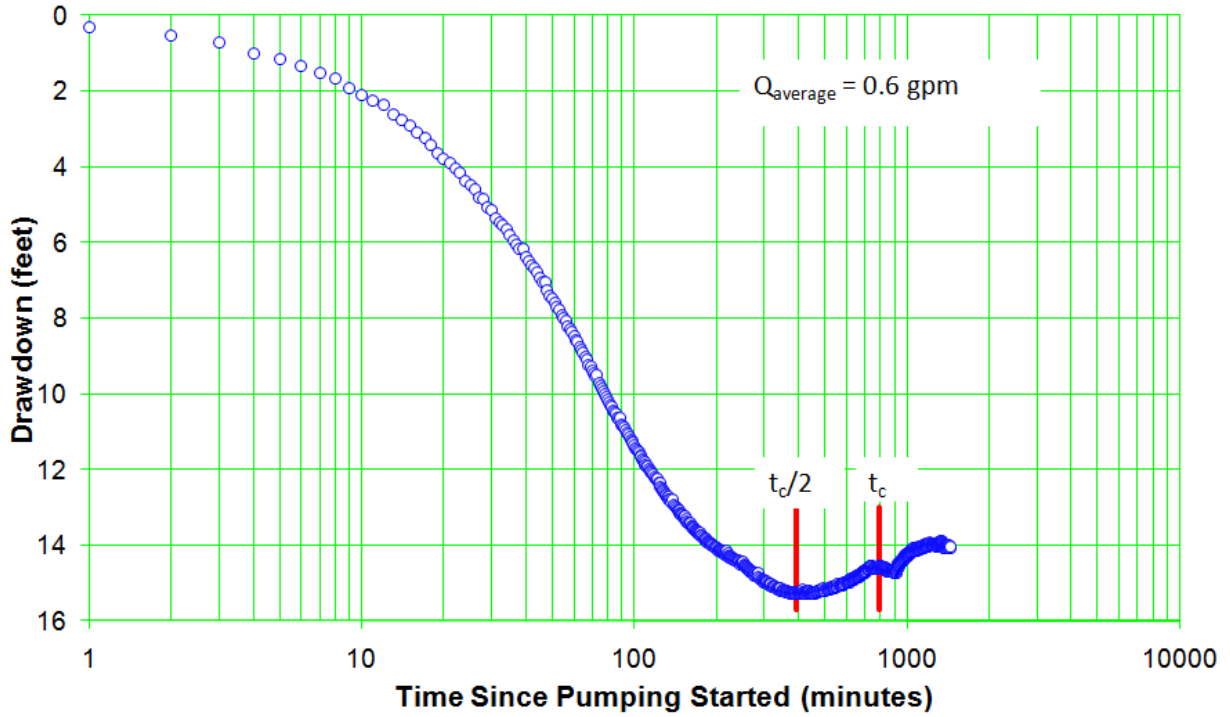


Figure C-8.1-2 Well R-25b drawdown

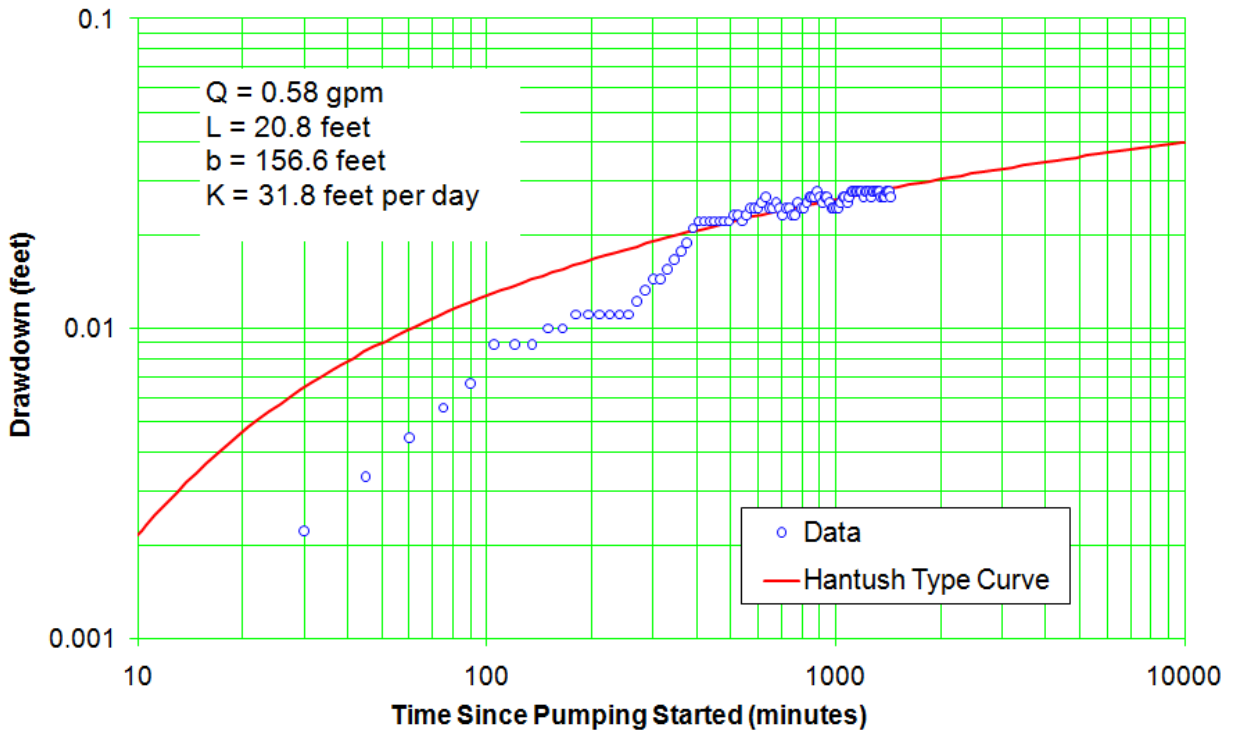


Figure C-8.1-3 Well R-25 screen 1 drawdown—Hantush solution for anisotropy of 0.00001

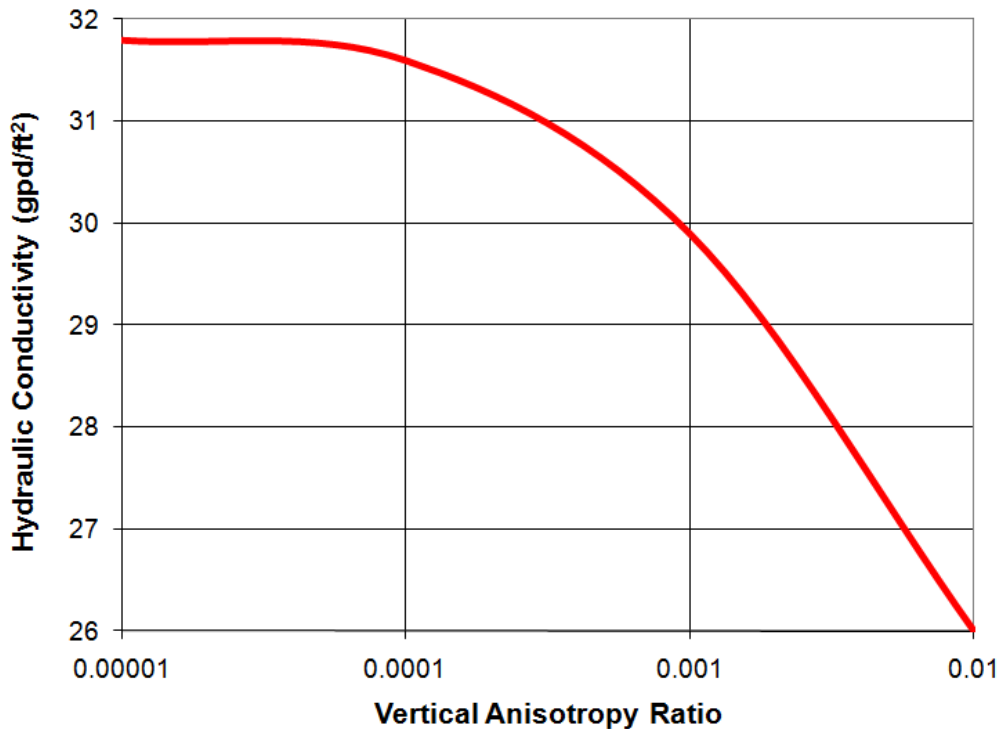


Figure C-8.1-4 Sensitivity analysis of the hydraulic conductivity and vertical anisotropy estimates based on Hantush analysis of well R-25 screen 1 data

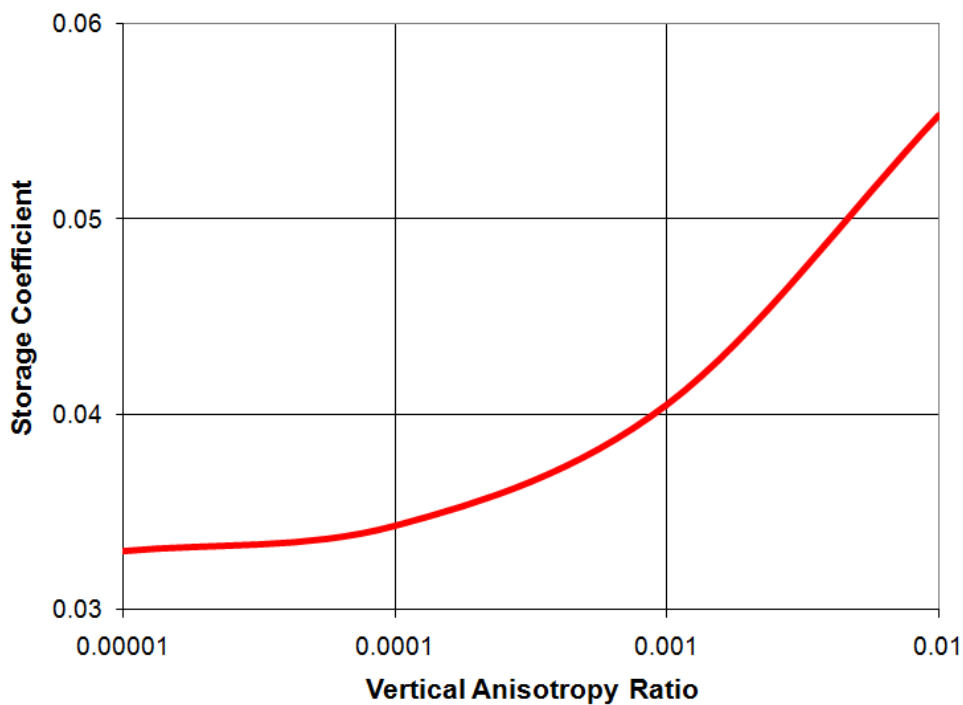


Figure C-8.1-5 Sensitivity analysis of the storage coefficient and vertical anisotropy estimates based on Hantush analysis of well R-25 screen 1 data

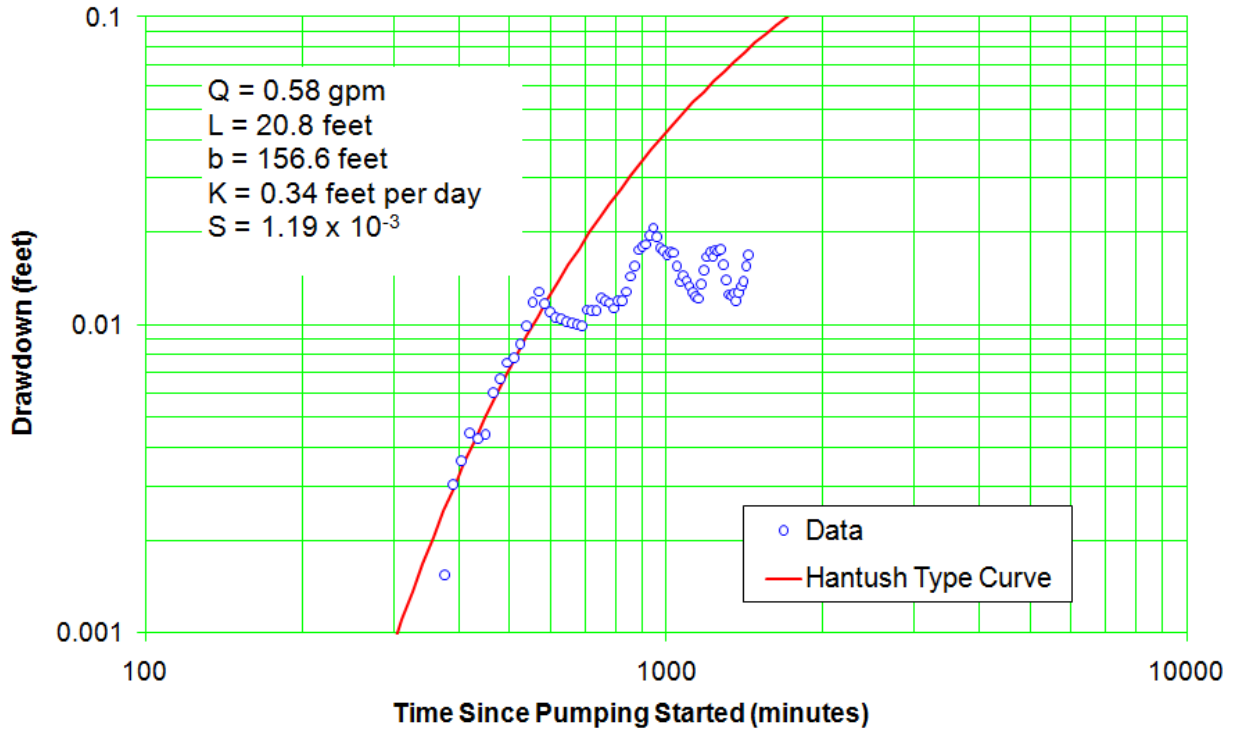


Figure C-8.1-6 Well R-25 screen 2 drawdown—Hantush solution for anisotropy of 0.1

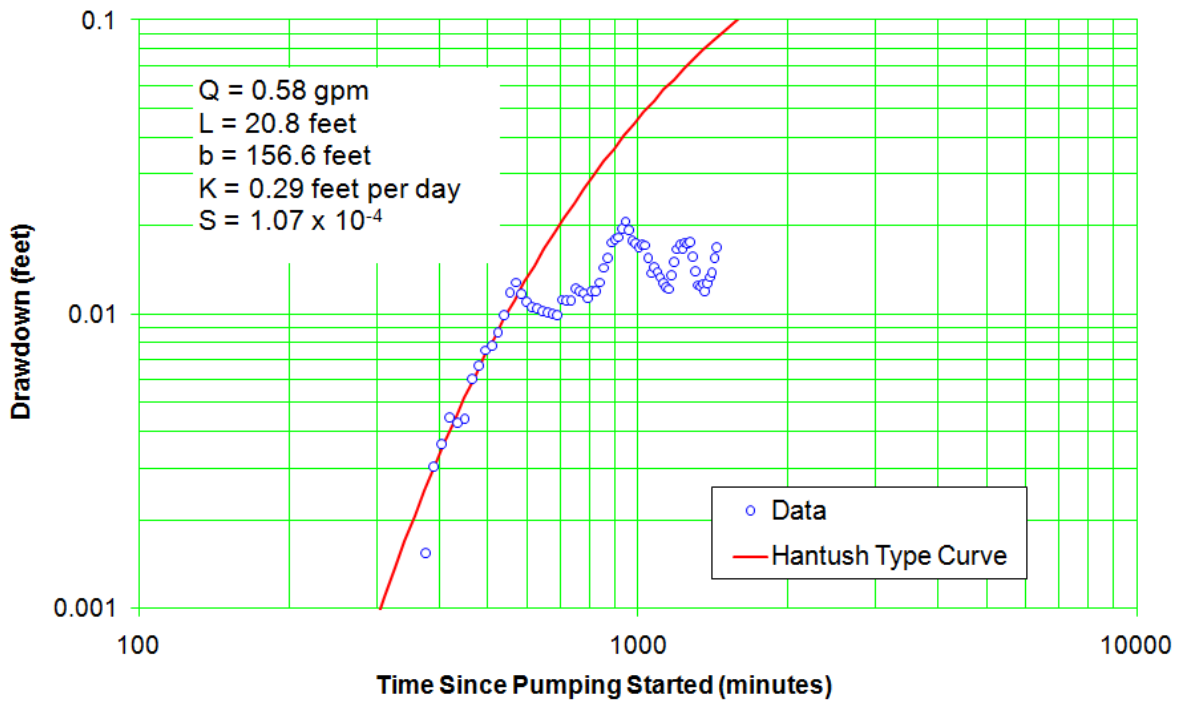


Figure C-8.1-7 Well R-25 screen 2 drawdown—Hantush solution for anisotropy of 0.01

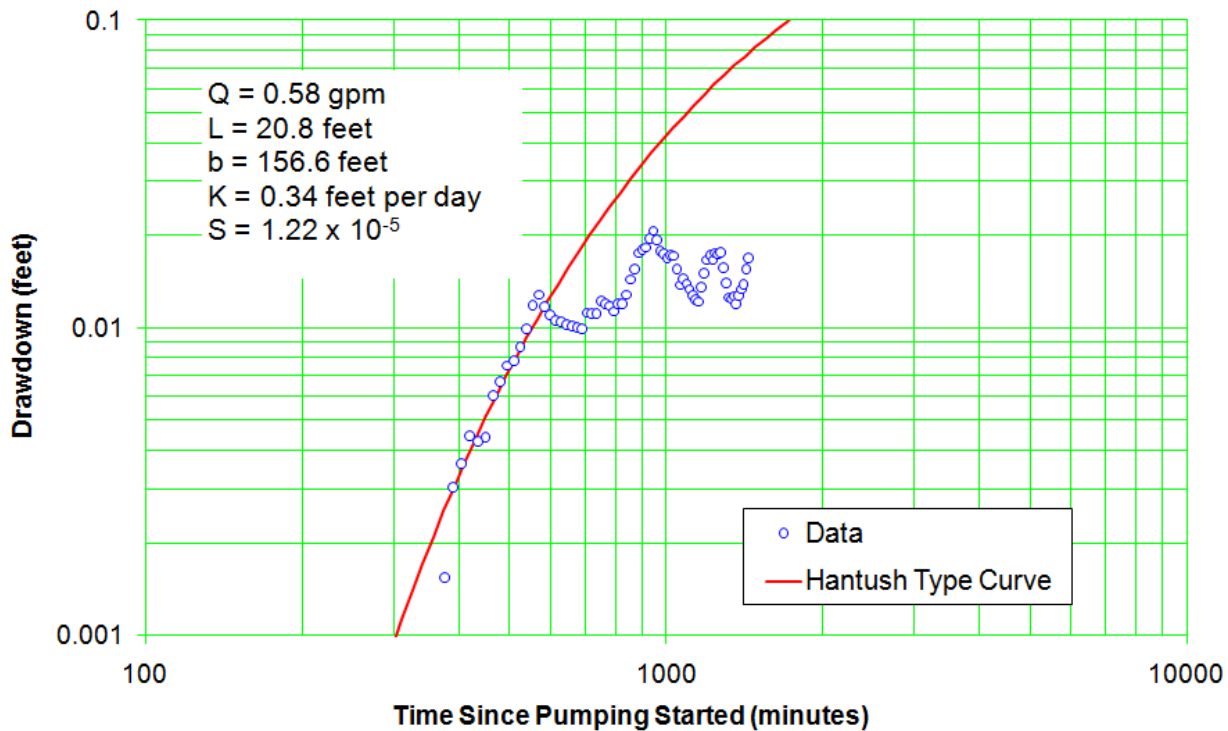


Figure C-8.1-8 Well R-25 screen 2 drawdown—Hantush solution for anisotropy of 0.001

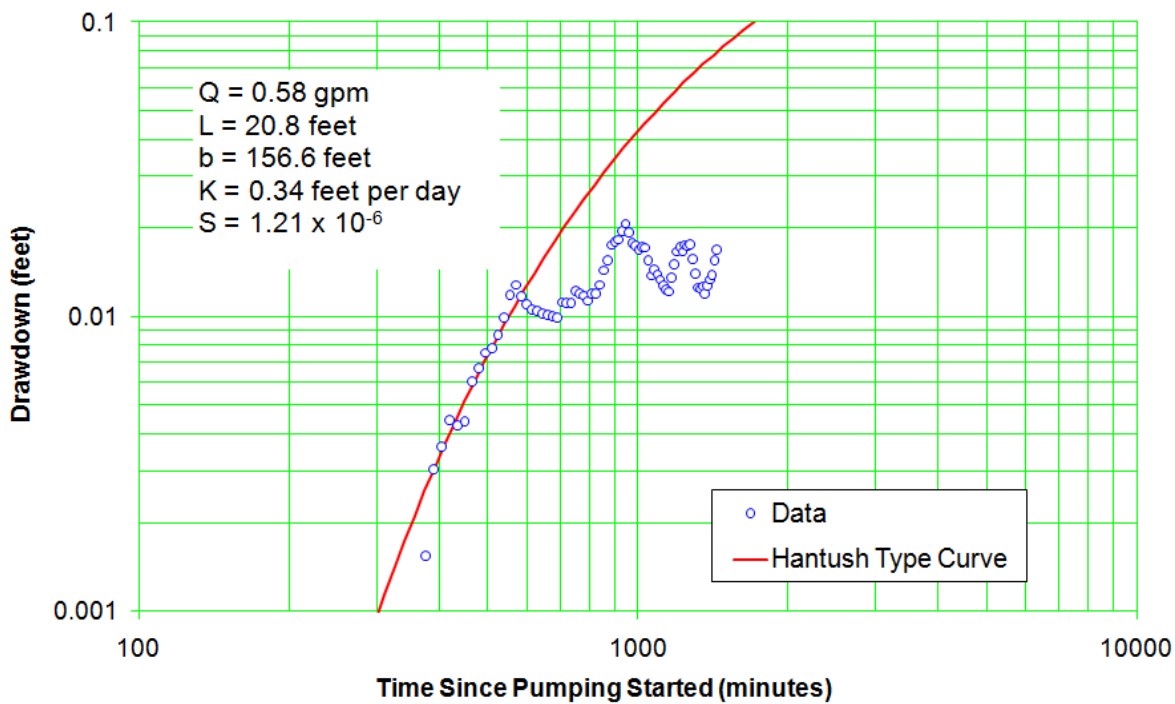


Figure C-8.1-9 Well R-25 screen 2 drawdown—Hantush solution for anisotropy of 0.0001

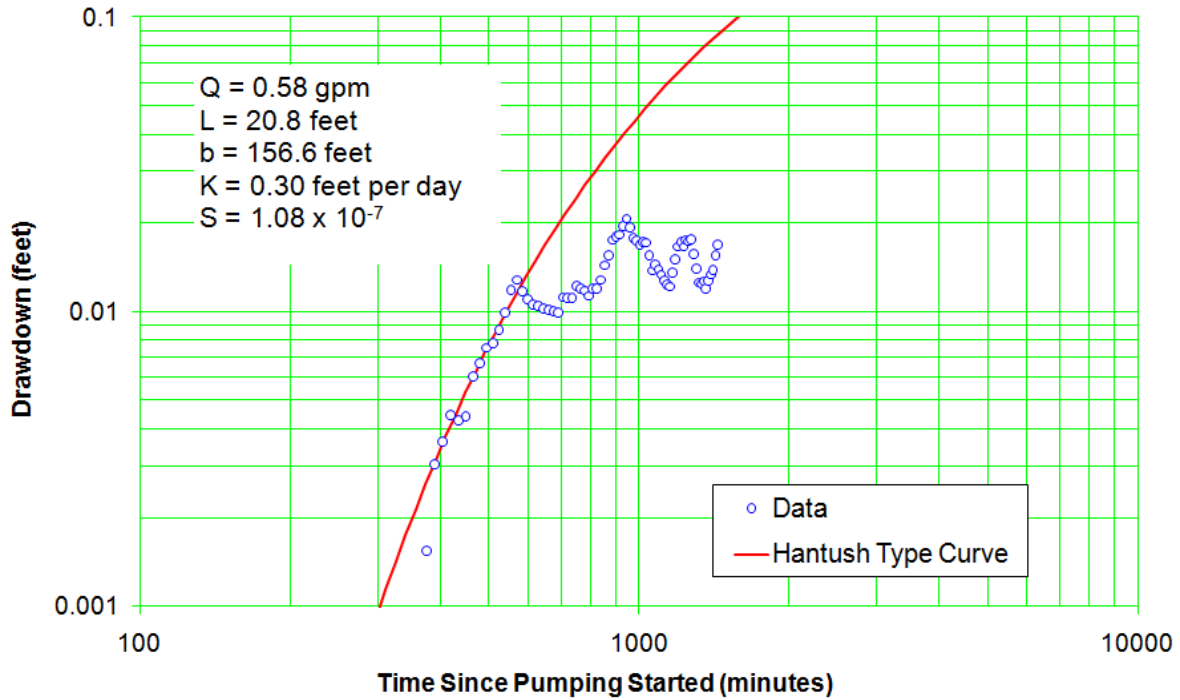


Figure C-8.1-10 Well R-25 screen 2 drawdown—Hantush solution for anisotropy of 0.00001

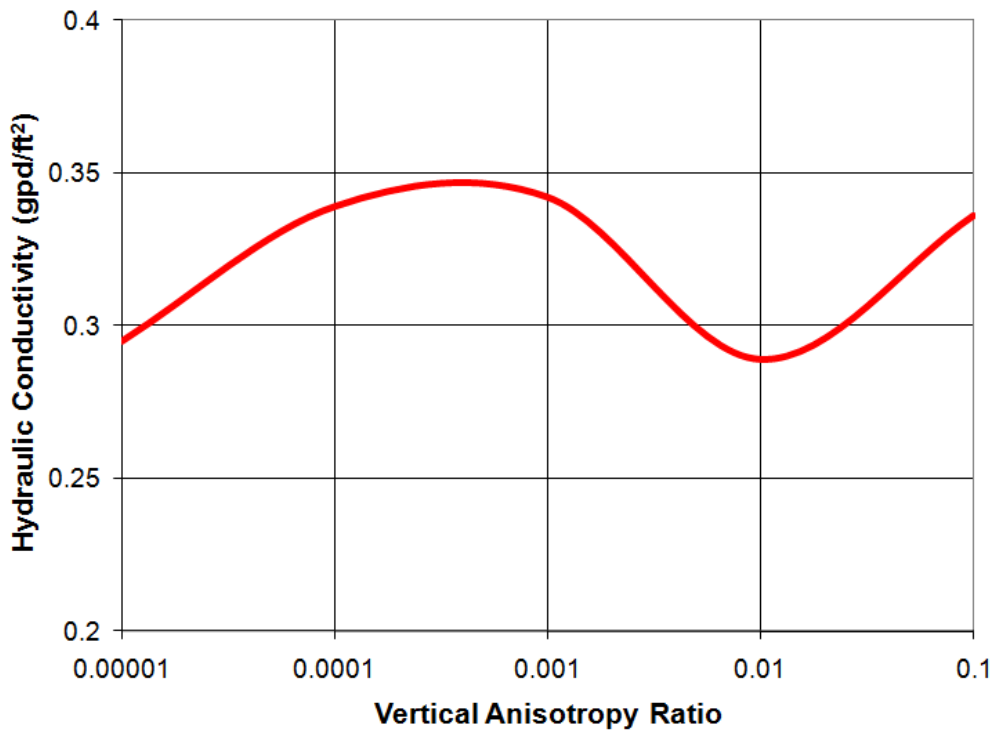


Figure C-8.1-11 Sensitivity analysis of the hydraulic conductivity and vertical anisotropy estimates based on Hantush analysis of Well R-25 screen 2 data

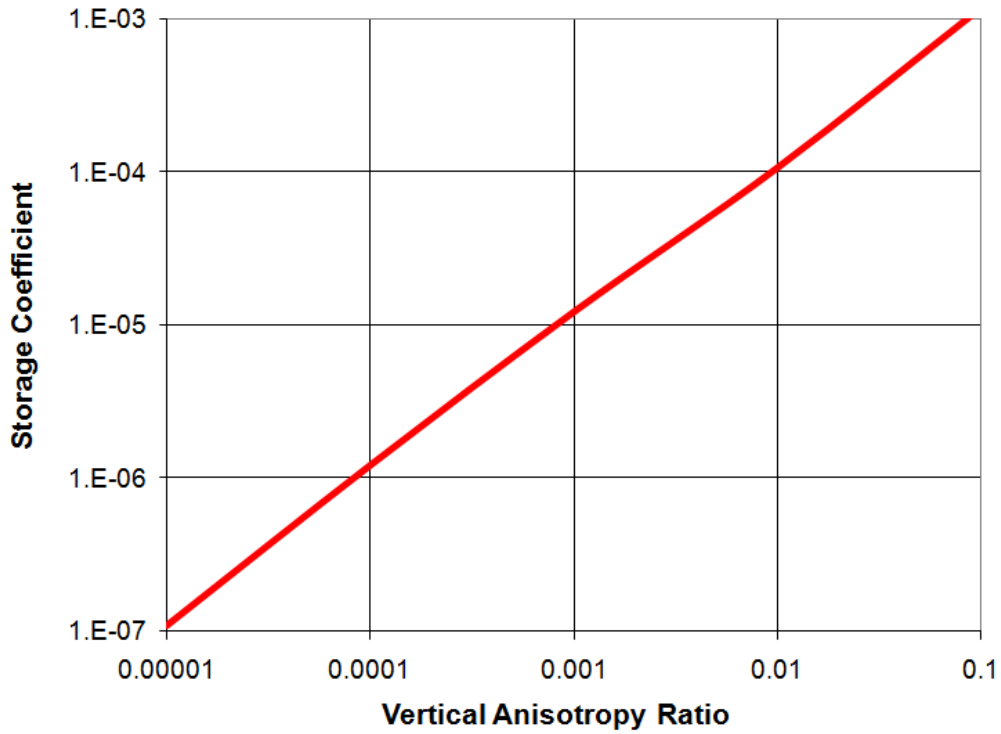


Figure C-8.1-12 Sensitivity analysis of the storage coefficient and vertical anisotropy estimates based on Hantush analysis of well R-25 screen 2 data

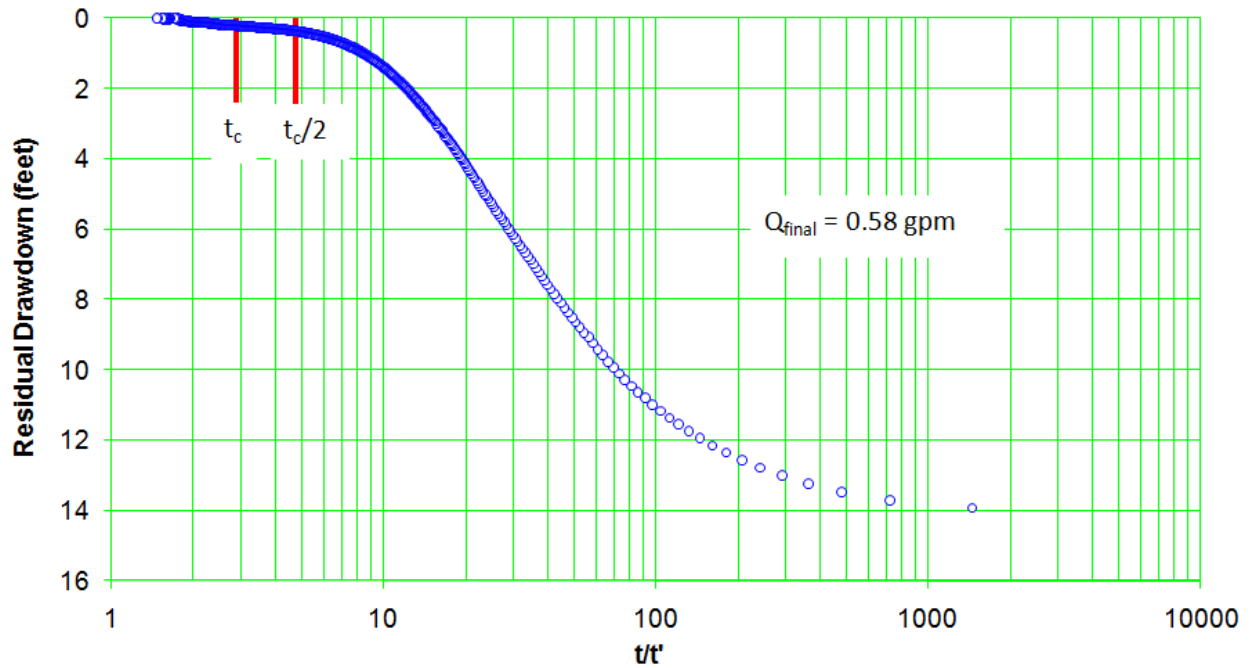


Figure C-8.1-13 Well R-25b recovery

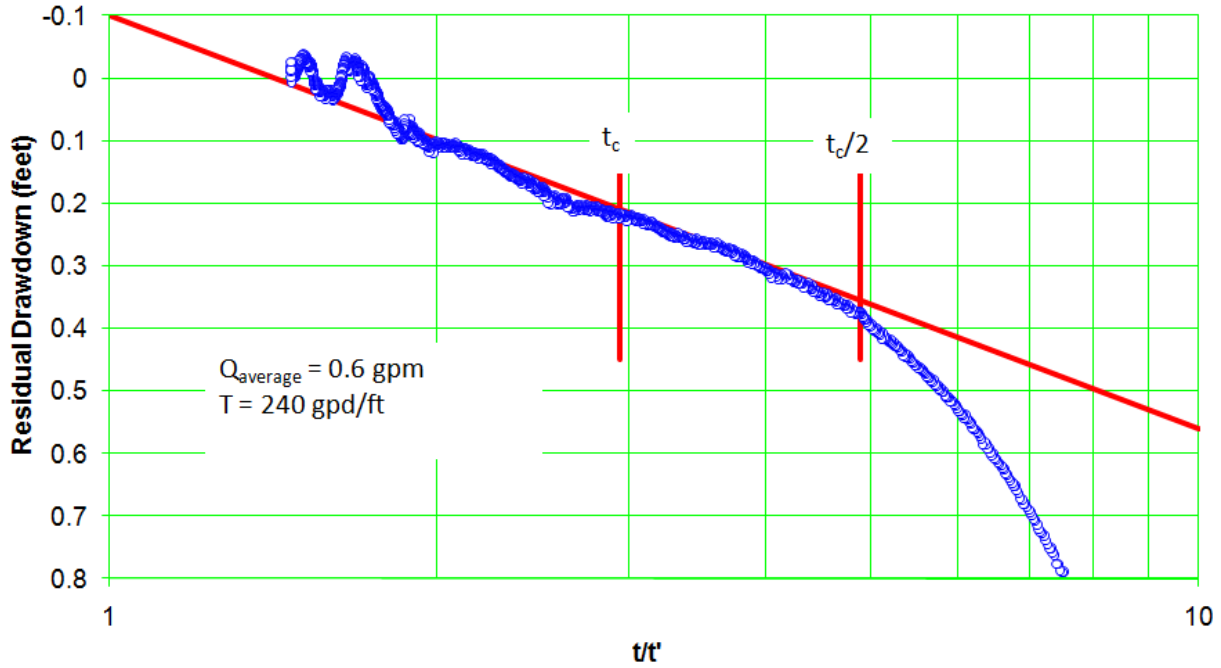


Figure C-8.1-14 Well R-25b recovery—expanded scale

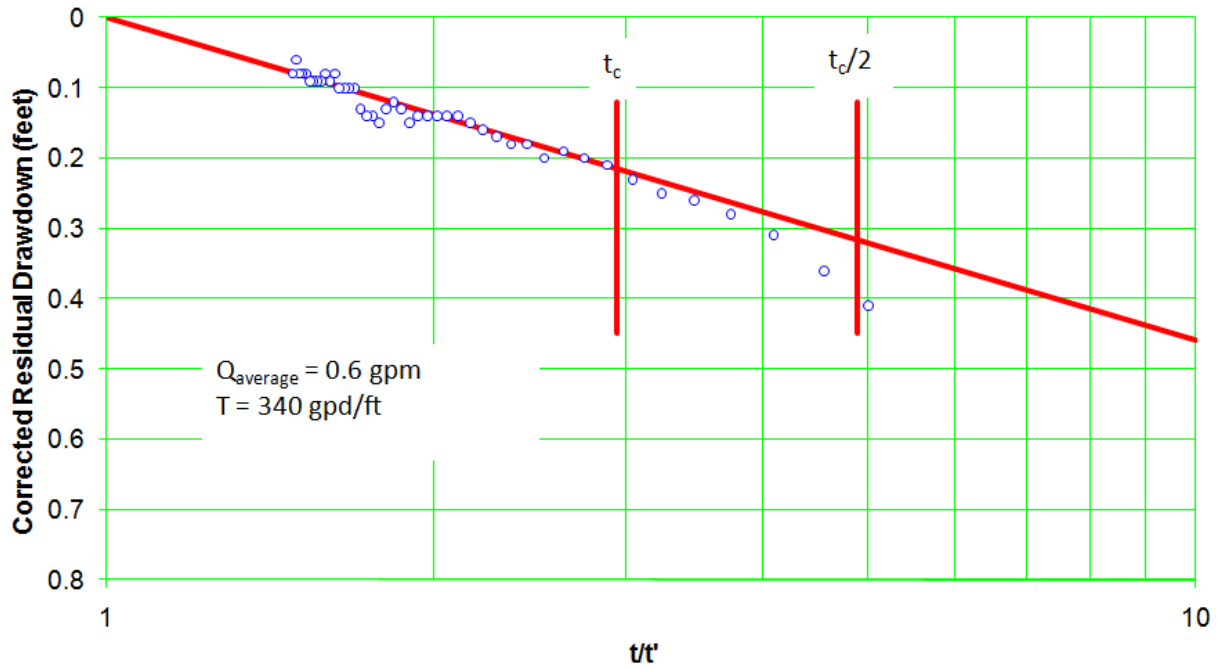


Figure C-8.1-15 Well R-25b corrected recovery

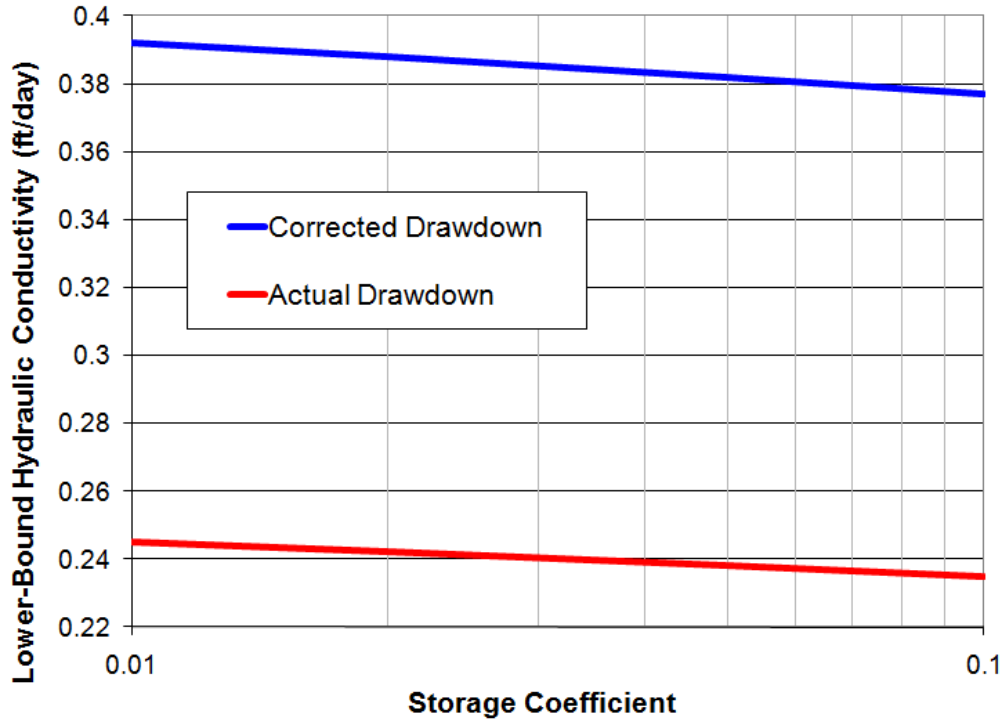


Figure C-8.2-1 Lower-bound hydraulic conductivity estimates

Appendix D

Groundwater Treatment

D-1.0 PURPOSE

Following the installation and development of groundwater monitoring well CdV-16-4ip, a conceptual design was developed for management of the development and pump test water. A treatment system was necessary to reduce concentrations of RDX (hexahydro-1,3,5-trinitro-1,3,5-triazine) to allow land application of the effluent. Sufficient storage capacity of raw and treated groundwater was provided to allow flexibility of treatment system operation and land application. Operation of the system was based in part on rapid-turnaround analysis of treated water samples, documenting the effectiveness of system operation.

D-1.1 Treatment System

A review of historical data for nearby wells and the results of analyses of well development water indicated that RDX was the only contaminant that would require treatment before land application and was the only constituent of concern for system design. The following assumptions were made in the development of the design basis:

- The removal capacity of the treatment system was based on an influent concentration of 320 µg/L (the upper screen development water concentration of 265 µg/L plus a 20% contingency) and an effluent concentration of 3 µg/L (50% of the land application limitation), requiring approximately 99% removal. This removal rate was to be met at a maximum flow rate of 25 gallons per minute (gpm).
- Carbon usage was estimated based on pumping of the upper screen at 15 gpm for 10 d, and an influent concentration of 265 µg/L, plus pumping the lower screen at 10 gpm for 5 d and an influent RDX concentration of 205 µg/L.
- Granular activated carbon (GAC) was selected as the adsorption media, based on the successful application of this technology in similar situations, both at Los Alamos National Laboratory (LANL) and other sites involved in cleanup of explosives-affected groundwater.

A minimum of two treatment units were required, to be supplied in series, fed via a duplex set of influent pumps of sufficient capacity to direct GAC-treated effluent from the second carbon unit to an effluent holding tank. Sampling ports were required before, between, and after each unit. Figure D-1.1-1 illustrates the required components of the treatment system.

Based on the performance requirements for the treatment system, the subcontractor provided the treatment system for use during the pump test. A “pre-filter” was provided by the subcontractor to remove suspended solids. As a back-up measure, a third carbon unit was provided for use if necessary during the test.

D-1.2 Operation Data

The treatment system was generally operated continuously during the pump tests of the upper and lower screens. The operators adjusted the treatment rate to approximate the flow from the well, minimizing the storage requirements yet ensuring there would always be flow through the system to avoid freezing. Detailed operation logs were kept during the test, documenting the flow through the system. Well samples and samples of the effluent from each carbon unit were collected twice daily and analyzed in an on-site LANL analytical laboratory.

The volume of groundwater treated in 12-h intervals was tabulated for comparison to the influent RDX concentrations observed in water pumped from the well zones during the pump tests and are included in Appendix A (on CD). Treated effluent from the first and second units was always below the detection limits of the analytical method (2 to 5 µg/L). For the purposes of this review, all of the RDX reported in the well water was assumed to be removed (ignoring the small amount that may have been present in the effluent below the limits of detection).

D-2.0 SUMMARY

Carbon treatment was successfully employed during the pumping test to treat groundwater from both the upper and lower screens in well CdV-16-4ip. The influent RDX concentration averaged 185 µg/L during the testing of the upper screen. At an average flow rate of just under 10 gpm, approximately 0.3 lb of RDX was removed. The influent concentration of RDX in the lower screen averaged just 24 µg/L, which was lower than expected. The average flow rate was just over 6 gpm; over 10 d, only an additional 0.02 lb of RDX was removed.

A plot of the influent RDX concentration over time is included with the data tabulation in Appendix A and indicates that influent concentration remained fairly constant or increased slightly over the course of the pumping of each screen.

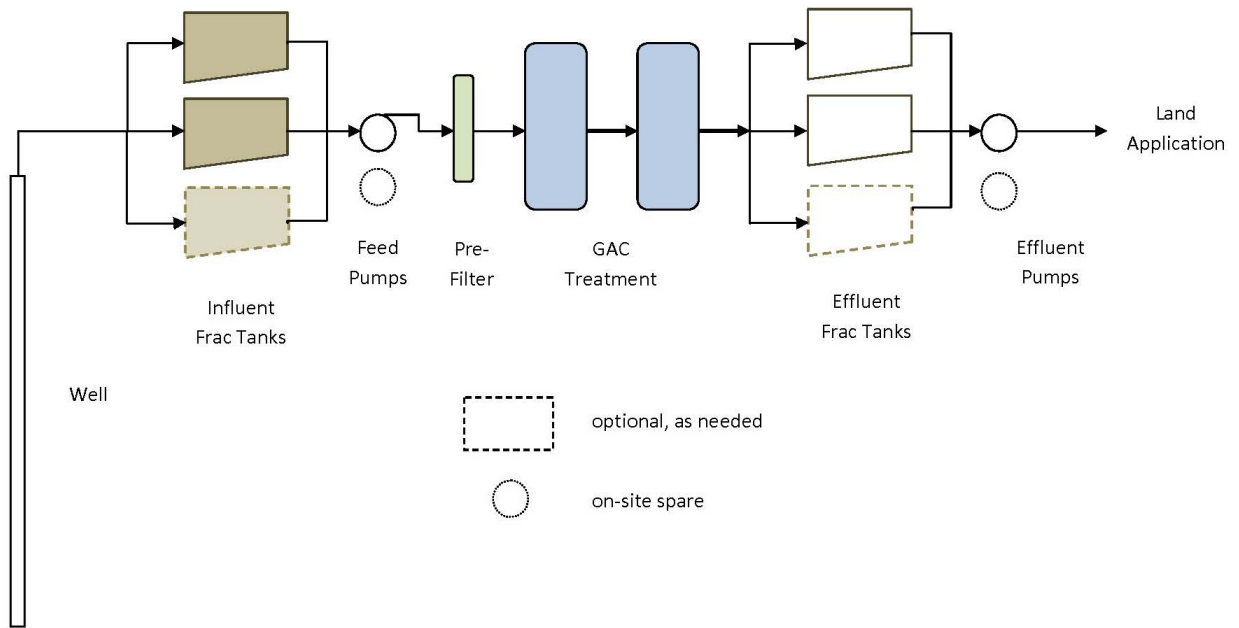


Figure D-1.1-1 Components of the groundwater treatment system

